The Dissertation Committee for Khalid Mohammad Omer Certifies that this is the approved version of the following dissertation:

The Electrogenerated Chemiluminescence of Highly Fluorescent Organic Chromophores and Nanoparticles

Committee:

Allen J. Bard, Supervisor

Keith J. Stevenson

Bradley J. Holliday

Katherine A. Willets

Arumugam Manthiram

The Electrogenerated Chemiluminescence of Highly Fluorescent Organic Chromophores and Nanoparticles

by

Khalid Mohammad Omer, B.S.; M.S.

Dissertation

Presented to the Faculty of the Graduate School of

The University of Texas at Austin

in Partial Fulfillment

of the Requirements

for the Degree of

Doctor of Philosophy

The University of Texas at Austin

December, 2009

Dedication

To my mom,
my sisters, my brothers,
and my wife.

Acknowledgements

I would like to thank my advisor, Professor Allen J. Bard, for his advice and intellectual guidance throughout my research work. It is my pleasure that he allowed me to work with him.

Thanks also to Angie Nelson for her help during writing this dissertation and articles and Dr. Matthew Sartin for helping me in starting my research project.

I would like also to thank Sung-Yu Ku, Ken-Tsung Wong for synthesizing Green ECL emitters and blue emitters, Alexander L. Kanibolotsky, Peter J. Skabara and Igor F. Perepichka for synthesizing star-shaped oligofluorene.

Thanks to my family for encouraging me, and my lab-mates and friends, past and present, for many fond memories.

The Electrogenerated Chemiluminescence of Highly Fluorescent Organic Chromophores and Nanoparticles

Publication No._____

Khalid Mohammad Omer, Ph.D.

The University of Texas at Austin, 2009

Supervisor: Allen J. Bard

Electrogenerated chemiluminescence (ECL) of new, highly fluorescent molecules was studied. Six novel, highly fluorescent, green emitters were synthesized by incorporating an acceptor group like 2,1,3-Benzothiadiazole between different donor groups. The structural effects on the electrochemical, spectroscopic, and ECL behavior are shown in detail. Stable electrochemistry and high PL quantum yield were observed. Most of the ECL was visible by the naked eye. Well-known, fluorescent, polyaromatic hydrocarbons (PAH), like 9,10-diphenylanthracene derivatives, pyrene, and anthracene were incorporated between two bulky fluorene derivative groups. The fluorene substitutions block the active positions of the PAH cores, permitting the formation of

stable radical ions upon electrochemical oxidation or reduction. Such a tailoring led to increase electrochemical reversibility and tuning of the ECL wavelength. Fluorene-based DPA (**FDF)** is characterized by a highly efficient and stable blue-cyan color. Another interesting type of molecules was star-shaped structures. The effects of structure on the electrochemistry and spectroscopy of a series of star-shaped, rigid molecules was examined. **T1-T4** is composed of oligofluorene arms with truxene as a central core basically there were weak donor and weak acceptors. The ECL quantum efficiency was near 80% for the long-arm **T4**. One of the interesting goals in ECL is to find ECL emitters in aqueous media. Organic nanoparticles (ONPs) were chosen to achieve this goal. An organic nanoparticle (ONPs) is still challenging area in nanoscience. The key factor of such a challenge comes from the difficulty to control the size and shape of the prepared nanoparticles. ONPs of common hydrocarbon ECL emitters like rubrene and 9,10-diphenylanthracene (DPA) were prepared in aqueous solution using a reprecipitation method. ECL of rubrene NPs was observed when tripropylamine (TPrA) was used as a coreactant, and weaker ECL of DPA NPs was observed when the oxalate ion was used as a coreactant. The ECL of ONPs in aqueous media may open a new field in ECL, allowing the exploration of more phenomena in organic nanoscience. Organic nanoparticle ECL (especially if one able to make small size to be diffused easily) has potential application as a tag for the analysis of biologically interesting molecules.

Table of Contents

List of Tables

List of Figures

List of Illustrations

Chapter 1: Electrogenerated Chemiluminescence

1.1 BACKGROUND

Electrogenerated Chemiluminescence is the emission of light due to electron transfer at the vicinity of the electrode.[1] For example applying a positive and negative voltage on the electrode (either metallic, semiconductor) immersed in the solution containing 9, 10 diphenylanthracene in acetonitrile produce strong blue light due to annihilation of the radical cation and anion formed with each pulse and making excited state then producing characteristic light when it comes back to ground state. This light is called electrogenerated chemiluminescence or some time in literature is called electrochemiluminescence.

The history of ECL started at the mid-1960s when Hercules at MIT, Bard at University of Texas at Austin and Chandross at Bell Laboratories, NJ reported independently the phenomenon and explained the basic principles.[2] Since then, many articles, patents, review articles, book chapters have been published from very fundamental to the applied.[1]

ECL has been used for many real applications: like in immunoassay and DNA analysis,[3] food and water analysis with a very lower limit of detection which still make people to search for new ECL label with better sensitivity and higher selectivity.[1a]

Since ECL deals with the emission of the light due to electrically generated excited species, in other words this marriage between Electrochemistry and Spectroscopy

offers some main advantages over both spectroscopy alone and electrochemistry alone: like; there is no light source in ECL compared to fluorescence techniques, so there is no light background problem. High selectivity of ECL labels makes the interference problems very small.[1a]

1.2 BASIC PRINCIPLES OF ECL

1.2.1 Ion annihilation

The simple form of ECL involves the generation of the light via the annihilation of the cations and anions on the surface of the electrodes according to the following equations:

$$A - e \rightarrow A^{\bullet +} \quad \text{(cation radical formation)} \quad (1.1)$$

$$A + e \rightarrow A^{\bullet -} \quad \text{(anion radical formation)} \quad (1.2)$$

$$A^{\bullet +} + A^{\bullet -} \rightarrow A^* + A \quad \text{(annihilation)} \quad (1.3)$$

$$A^* \rightarrow A + h\nu \quad \text{(ECL emission)} \quad (1.4)$$

As clear from equations 1.1 to 1.4, oxidation and reduction makes cation ($A^{\bullet +}$) and anion ($A^{\bullet -}$), then the opposite radicals annihilate to make excited state species (A*). The stability and efficiency of the ECL emission is directly depends upon the stability of the both types of radicals due to the time scale of the alternating of the potential of the electrode. High photoluminescence quantum (Φ_{PL}) is another requirement.

The excited state formed as a result of the annihilation reaction depends mainly on the amount of the energy available in the annihilation reaction. Direct population to excited state can only happen if the energy of ion annihilation is greater than the electronic transition energy. If the energy available in ion annihilation, the product R* can be either in lowest excited singlet state ($^1R^*$) or in the lowest excited triplet state ($^3R^*$). The well known equation is ($-\Delta H_{ann} = E^o_{ox} - E^o_{red} - T\Delta S$), where ΔH is the enthalpy of annihilation $E^o_{ox,}$ E^o_{red} are thermodynamic formal potentials of the oxidation and reduction of the (A), $T\Delta S \sim 0.1$ eV.

If $-\Delta H_{ann} > Es$ (energy required to make lowest excited singlet state); then it is possible to directly populate the excited singlet state from annihilation ($^1A^*$), then the route is so called S-route or energy sufficient system. If $Et < -\Delta H_{ann} < Es$ (Et: energy required to make triplet excited state) then the annihilation cannot directly populate the singlet excited state, but emission still is possible via triplet state formation and then triplet triplet annihilation, which is called T-route, as these equations below:

T-route ECL:

$A^{\bullet+} + A^{\bullet-} \rightarrow {}^3A^* + A$ (triplet state formation) (1.5)

${}^3A^* + {}^3A^* \rightarrow {}^1A^* + A$ (triplet triplet annihilation) (1.6)

${}^1A^* \rightarrow A + h\nu$ (ECL emission) (1.7)

The common example of S-route is emission of 9, 10 diphenyl anthracene (known as DPA).[4]

The example of T-route (i.e energy deficient system) is TMPD / DPA or TMPD/An.; (TMPD: N, N,N',N'- tetramethyl *p*-phenylenediamine), An: Anthracene.[5]

1.2.2. Coreactant ECL

If one cannot use one side of the potential scan, either negative side or positive side, due to either instability of the cation or anion or due to the limitation of the potential window, then; coreactant is useful.

A coreactant is a species that upon oxidation or reduction produces an intermediate that can react with an ECL emitter to produce excited states. Usually, this occurs upon bond cleavage of the coreactant to form strong oxidizing agent or reducing agent.

The first coreactant which was oxalate ion and was discovered by Bard and Rubinstein in which after electrooxidizing it produces strong reducing agent $CO_2^{\bullet -}$, that can reduce the ECL emitter (either R or $R^{\bullet +}$) to form excited state. [6]

$$C_2O_4^{2-} - e \rightarrow C_2O_4^{\bullet -} \rightarrow CO_2^{\bullet -} + CO_2 \qquad (1.8)$$

$CO_2^{\bullet -}$ is a strong reducing agent that may react with cation radical to form excited state.

$$A^{\bullet +} + CO_2^{\bullet -} \rightarrow A^* + CO_2 \qquad (1.9)$$

The other common coreactants are tri-n-propyl amine (TPrA),[7] persulfate,[8] benzoyl peroxide (BPO)[9].

The most common system in coreactant ECL is using TPrA $(CH_3CH_2CH_2)_3N$ with $[Ru(bpy)_3]^{2+}$, which is now commercially available system for the immunoassay and DNA analysis. The mechanism is as following:[1]

$$Ru(bpy)_3^{2+} - e \rightarrow Ru(bpy)_3^{3+} \quad (1.10)$$

$$TPrAH - e \rightarrow TPrAH^{\bullet +} \rightarrow TPrA^{\bullet} + H^{+} \quad (1.11)$$

$$Ru(bpy)_3^{3+} + TPrA^{\bullet} \rightarrow Ru(bpy)_3^{*2+} + Products \quad (1.12)$$

$$Ru(bpy)_3^{*2+} \rightarrow Ru(bpy)_3^{2+} + h\nu \quad (1.13)$$

TPrA after oxidizing, produce strong reducing agent TPrA•, (Ep/TPrA• = –1.7)[10].

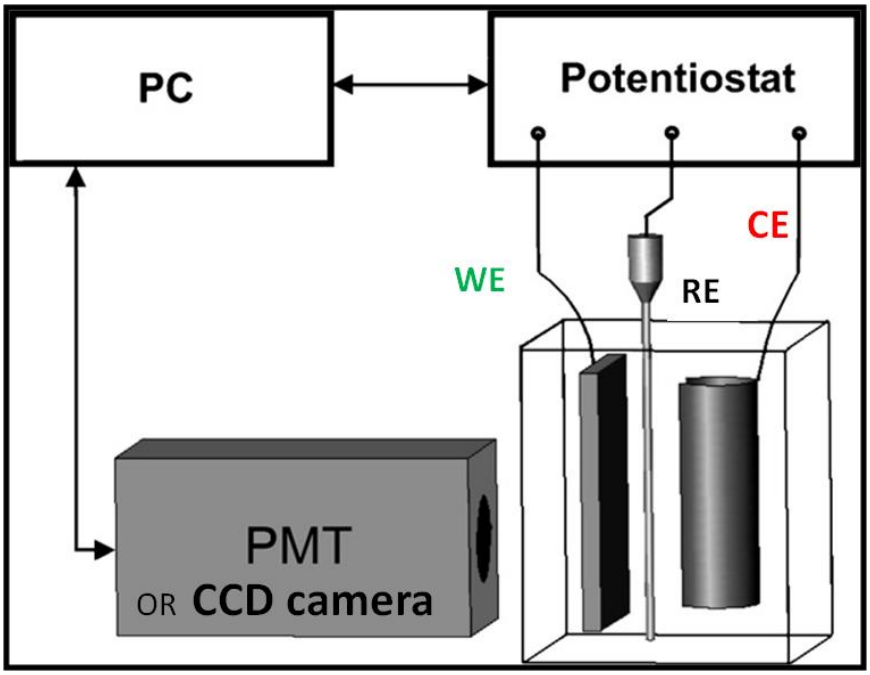

Figure 1.1: Diagram of the ECL set-up. The electrochemical cell consists of three electrodes, working electrode (WE), Counter electrode (CE) and reference electrode (RE) immersed in the solution containing the ECL emitter, solvent and 0.1 M Supporting electrolyte. The WE is bent to face the photodetector either CCD camera or photomultiplier tube (PMT).

1.3 EXCIMER

It is the electronically excited dimeric species, which is immediately dissociated after its emission. The usual characteristics of excimer emission are the broad structureless emission band appearing at the longer wavelength side of the monomeric fluorescence and it is concentration dependent, i.e. increasing emission intensity with increasing concentration.

$$A^* + A \rightarrow A_2^* \quad (1.14)$$

$$A_2^* \rightarrow 2A + h\nu \quad (1.15)$$

In Photoluminescence, excimer is formed due to association of the excited state (A_2^*) with corresponding to the ground state. In ECL, it is believed to be from the close proximity of the two species at the time of annihilation.[11] Like in 9,10-dimethylanthracene, phenanthrene, perylene, and 3,4-

benzopyrene, the suggested equation is:

$$A^{\bullet+} + A^{\bullet-} \rightarrow A_2^* \quad (1.16)$$

However, triplet triplet annihilation for energy defeceint system may lead to the formation of excimer.[12] Like annihilation of pyerene radical with TMPD radiacal, as follow:

$$Py^{\bullet-} + TMPD^{\bullet+} \rightarrow {}^3Py^* + TMPD \quad (1.17)$$

$$^3Py^* + {}^3Py^* \rightarrow Py_2^* \quad (1.18)$$

In general, and in many cases, long wavelength ECL could be ascribed to excimer, while this long wave ECL does not necessarily mean excimer, because the

electrochemical involved with ECL contributes to formation of some of by-products due to the instability of either cation or anion or both. To test the stability, cyclic voltammetry is used as a typical electrochemical method to gauge the stability of the radicals formed. the emissive byproducts formed could be the reason for long wavelength ECL. However, to test this long wavelength, and to assign whether is from excimer or no, Coreactant ECL could be used, in which in coreactnat experiment, ion pair annihilation will be very low, so the long wavelength excimer should absent from the ECL spectrum.

1.4 ORGANIC NANOPARTICLES (ONPS)

Metallic and semiconductor nanoparticles have been the subject of much research due to their unique properties like the quantum size effect.[13] Much less attention is paid to organic nanoparticles (ONPs) mainly because of lacking of quantum effect and difficulty to prepare and control the size of the particles. However, it is expected that organic nanoparticles (ONPs) hold brighter future due to the ease of tailoring the organic molecules and flexibility of the organic materials.[14]

In fact, researches on ONPs are in the initial stage and literature still is poor, so basic principles of ONPs are not well established yet.

The chemical growth of bulk or nanometer-sized materials inevitably involves the process of precipitation of a solid phase from solution. The precipitation process basically consists of a nucleation step followed by particle growth stages.[15]

Organic nanoparticles were prepared in aqueous solution using reprecipitation method, [16] sol-gel phase transition,[17] stratification deposition in a vacuum chamber, [18] and laser ablation method. [19]

The reprecipitation method includes injecting of small volume (~100 μL) of the compound from a "good solvent" (highly soluble) to high volume (~10 mL) of the "poor solvent" (less or insoluble) with continuous stirring.

The reprecipitation relies on the sudden change in solubility of the molecule, in which a solid state compound is dissolved completely in a "good solvent" like THF, and

then rapidly injected into the solvent which the materials solubility is very "poor" but is miscible with the good solvent.

Good solvent disperses the molecules, but poor solvent makes the molecules to aggregate (via nucleation and particle growth). The particle formed this way might be stable over period of seconds to days to months. Surfactants help to stabilize the particles and make them smaller.

The particle formation at the injection method in the very beginning moments is not easy to characterize well, due to the small distance and time scales. The initial steps of nucleation are the key aspects of these processes which still is not well understood, making the particle size using reprecipitation uncontrollable.[16]

The size of the formed particles is limited by many factors, like; solubility of the compounds in both solvents, temperature, stirring rate, presence of stabilizer (surfactants)....etc.

ECL of ONPs has been reported recently by our group.[20] The compound used is the water-insoluble derivative of tris(bipyridine) Ru(II), $[Ru(bpy)_2(4,4'-(CH_3(CH_2)_{14}COO)_2\text{-bpy})](ClO_4)_2$ which makes nanobelt after reprecipitation, and ECL of single nanocrystals have been observed. ONPs of Rubrene and DPA the two common ECL emitters were prepared in water and their ECL observed. It was observed that Rubrene makes nanoparicles (~50 nm), while DPA at the early stages makes nanorods and then after week make nanowire.

Although preparation, spectroscopy, electrochemistry and ECL of ONPs are in the early stages, such findings in ECL hold future application to be used as a tag for detecting and determination of biological interesting molecules.

ECL is one the most highly sensitive and selective tool for real analysis. However the task of ECL researchers is to find highly efficient ECL emitter, different colors to cover broad spectrum of emitters. Exploring ECL of ONP can be another realm to overcome solubility of the insoluble ECL emitters in aqueous media to make ECL more practical for analysis various biological interesting molecules with physiological media.

1.5 REMARKS

ECL became one of the most selective and sensitive methods for analytical purposes. In a application view, ECL has been used for DNA and immunoassay,[21] food and water analysis, HPLC detection,[22] and sensor.[23] Therefore, it is important to find out new ECL emitters with different emission wavelength, rather than common red and blue emitter (Chapter 3) and also trying to increase the electrochemical stability of radical cation and anion of well-known ECL emitters like DPA, pyrene, anthracene (Chapter 4). New organic class in ECL realm, which is star-shaped oligofluorene arms with truxene core has been studied (Chapter 5). In trying to overcome the non aqueous problem and to be close to physiological pHs, Organic nanoparticles have been prepared in water solution to observe ECL (Chapter 6). Organic compounds like Rubrene and DPA molecules were tested. Organic nanoparticle research is still in progress, and it has potential to be an alternative method to use variety of ECL emitters as a nanoparticles in aqueous solution with high sensitivity and low cost.

1.6 REFERENCES

[1] For review on ECL: (a) ElectrogeneratedChemiluminescence; Bard, A. J.; Ed.; MarcelDekker, Inc.: New York, 2004. (b) Miao, W. *Chem. ReV*. **2008**, *108*, 2506. (c) Richter, M. M. *Chem. ReV*. **2004**, *104*, 3003. (d) Knight, A. W.; Greenway, G. M. *Analyst* **1994**, *119*, 879. (e) Bard, A. J.; Debad, J. D.; Leland, J. K.; Sigal, G. B.; Wilbur,J. L.; Wohlstadter, J. N. In Encyclopedia ofAnalytical Chemistry:Applications, Theory and Instrumentation; Meyers, R. A., Ed.; John Wiley & Sons: New York, **2000**; Vol. 11, p 9842.

[2] (a) Hercules, D. M. *Science* **1964**, *145*, 808.; (b) Santhanam, K. S. V.; Bard, A. J. *J. Am. Chem. Soc*. **1965**, *87*, 139. (c) Visco, R. E.; Chandross, E. A. *J. Am. Chem. Soc.* **1964**, *86,* 5350.

[3] Bard, A. J.; Debad, J. D.; Leland, J. K.; Sigal, G. B.; Wilbur, J. L.; Wohlstadter, J. N. Encyclopedia of Analytical Chemistry; Meyers, R. A., Ed.; Wiley: Chichester, U.K., **2000**; pp 9842.

[4] (a) Faulkner, L. R.; Tachikawa, H.; Bard, A. J. *J. Am. Chem. Soc*. **1972**, *94*, 691. (b) Beideman, F. E.; Hercules, D. M. *J. Phys. Chem*. **1979**, *83*, 2203.

[5] (a) Faulkner, L. R.; Bard, A. J. *J. Am. Chem. Soc*. **1969**, *91*, 209. (b) Faulkner, L. R.; Tachikawa, H.; Bard, A. J. *J. Am. Chem. Soc*. **1972**,*94*, 691.

[6] Rubinstein, I.; Bard, A. J. *J. Am. Chem. Soc*. **1981**, *103*, 512.

[7] Leland, J.; Powell, M. *J. Electrochem. Soc.* **1990**, *137*, 3127.

[8] White, H.; Bard, A. *J. Am. Chem. Soc.* **1982**, *104*, 6892.

[9] Chandross, E.; Sonntag, F. *J. Am. Chem. Soc.* **1966**, *88*, 1089.

[10] Lai, R. Y.; Bard, A. J. *J. Phys. Chem. A* **2003**, *107*, 3335.

[11] Chandoross E.; Longworth, J.; Visco, R. *J. Am. Chem. Soc.* **1965**, *87*, 3259.

[12] Maloy, J.; Bard, A. *J. Am. Chem. Soc.* **1971**, *93*, 5968.

[13] (a) Brus, L. E. *J. Chem. Phys*. **1984**, *80*, 4403. (b) Alivisatos, A. P. *Science* **1996**, *271*, 933. (c) Empedocles, S. A.; Bawendi, M. G. *Science* **1997**, *278*, 2114.

[14] An, B.-K.; Kown, S.-K.; Jung, S.-D.; Park, S.-Y. *J. Am. Chem.Soc*. **2002**, *124*, 14410.

[15] Burda, C.; Chen, X.; Narayanan, R.; El-Sayed, M. A. *Chem. Rev*. **2005**, *105*, 1025.

[16] (a) Kasai, H.; Oikawa, H.; Okada, S.; Nakanishi, H. *Bull. Chem. Soc. Jpn*.**1998**, *71*, 2597. (b) Horn, D.; Rieger, *J. Angew.Chem., Int. Ed***. 2001**, *40*, 4330.

[17] Ibanez, A.; Maximov, S.; Guiu, A.; Chaillout, C.; Baldeck, P. L . *Adv. Mater*. **1998,** *10*,1540.

[18] Seko, T.; Ogura, K.; Kawakami, Y.; Sugino, H.; Toyotama, H.; Tanaka, *J.Chem. Phys. Lett*. **1998,** *291*, 438.

[19] (a) Tamaki, Y.; Asahi, T.; Masuhara, H. *Applied Surface Science.* **2000**, *168*, 85. (b) Tamaki, Y.; Asahi, T.; Masuhara, H. *Jpn. J. Appl. Phys*. **2003**, *42*, 2725. (c) Kita, S.; Masuo, S.; Machida, S.; Itaya, A. *Jpn. J. Appl. Phys*. **2006**, *45,* 6501.

[20] (a) Omer, K. M.; Bard, A. J. *J. Phys. Chem. C* **2009***, 113*, 11575. (b) Yu, J.; Fan, F-R F. Pan, S.; Lynch, V.M.; Omer, K. M.. Bard, A.J. *J. Am. Chem. Soc.* **2008**, *130,* 7196.

[21] DiCesare, J.; Grossman, B.; Katz, E.; Picozza, E.; Ragusa, R.; Woundenberg, T. Biotechniques 1993, 15, 152.

[22] (a) Uchikura, K.; Kirisawa, M. Anal.Sci. 1991, 7, 971. (b) Skotty, D. R.; Lee, W. Y.; Nieman, T. A. Anal. Chem. 1996, 68, 1530.

23 (a) Yokoyama, K.; Sasaki, S.; Ikebukuro, K.; Takeuchi, T.; Karube, I.; Tokitsu, Y.; Masuda, Y. Talanta 1994, 31, 1035. (b) Jameison, F.; Sanchez, R. I.; Dong, L.; Leland J. K.; Yost, D.; Martin, M. T. Anal. Chem. 1996, 68, 1298.

Chapter 2: Experimental Section

2.1 ELECTRODES AND ELECTROCHEMICAL CELLS:

The electrochemical cell consisted of a working electrode with a ~1 mm diameter inlaid platinum disk, a Ag wire quasireference electrode in non-aqueous solution (referenced after each series of experiments against the ferrocene/ferrocenium couple to obtain the potentials vs. SCE) and Ag/AgCl used in aqueous solution, and a Pt wire counter electrode. For ECL, the working electrode was a 2 mm inlaid J-type (bent to face the detector) platinum disk, see Illustration 2.1. For transient ECL experiment (i-t-ECL), the whole electrochemical cell was covered with a black tape to prevent detecting any light emitting from the counter electrode, a very small hole is left open to face the working electrode to the detector.

***For cleaning of the electrodes*:** The working electrode was polished on a polish cloth with 1 μm alumina (Buehler, Ltd., IL), then 0.3 μm, and 0.05 μm, followed by sonication in DI water and ethanol for 5 min each. Counter electrode (Platinum coil) and quasi reference electrode (Ag wire) were cleaned with acetone and ethanol. In case of ITO, the 1×1 cm^2 piece of ITO (Delta technologies Inc, Rs ~ 15- 20 nm) was put and sonicated for 20 minutes in acetone, dichloroethylene, ethanol and then dried with nitrogen gas.

Glassware (if non aqueous media were intended) were washed with Acetone then aqueous solution of detergents and putting in oven until become totally dry, then transferring to glove box when they are hot. While, for aqueous media, the glassware were cleaned with detergents and rinsed with deionized water.

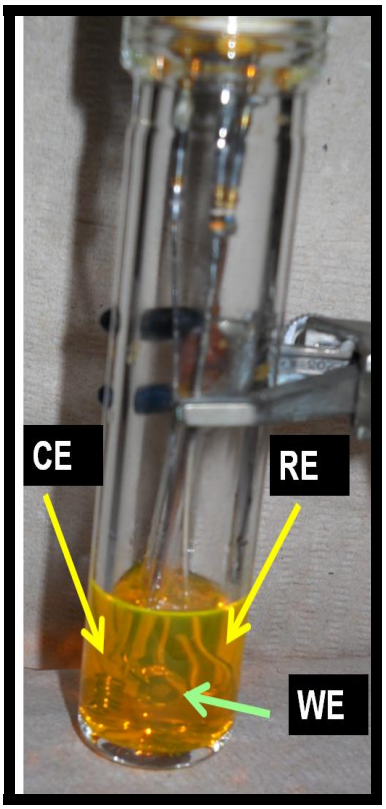

Illustration 2.1 Picture of the electrochemical cell consists of three electrodes, working electrode (WE), Counter electrode (CE) and reference electrode (RE) immersed in the solution containing the ECL emitter, solvent and 0.1 M Supporting electrolyte. The WE is bent to face the photodetector either CCD camera or photomultiplier tube (PMT).

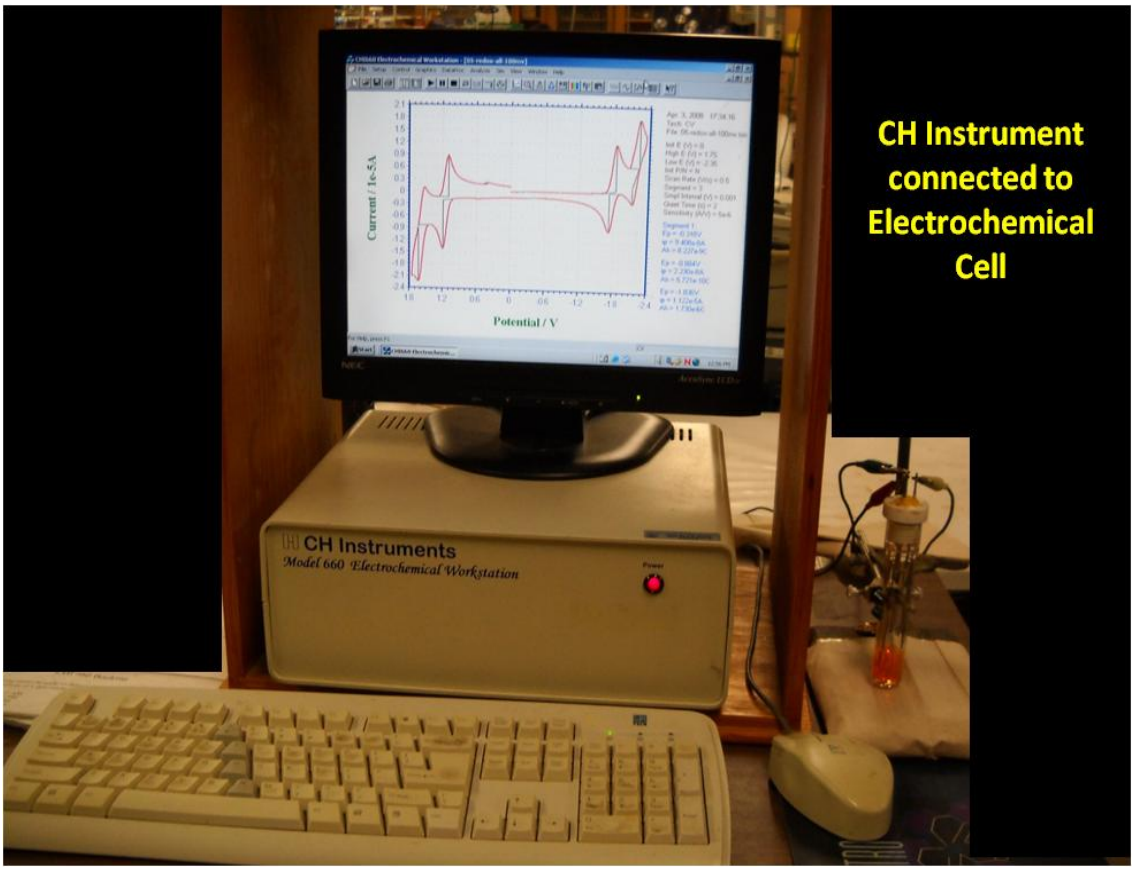

Illustration 2.2 Photograph showing electrochemical workstation model 660 (CH Instruments, Austin, TX) connected to the home made electrochemical cell.

2.2 INSTRUMENTS AND APPARATUS:

Cyclic voltammograms (CVs) were recorded on a model 660 electrochemical workstation (CH Instruments, Austin, TX) look at (Illustration 2.2). Faradaic current and ECL transients were simultaneously recorded using an Autolab electrochemical workstation (Eco Chemie, The Netherlands) coupled with a photomultiplier tube (PMT, Hammamatsu R4220p, Japan) held at −750 V with a high-voltage power supply (Kepco, Flushing, NY). The photocurrent produced at the PMT was converted to a voltage signal with an electrometer/high resistance system (Keithley, Cleveland, OH) and fed into the external input channel of an analog-to-digital converter (ADC) of the Autolab. The ECL spectra were taken using a calibrated charge coupled device (CCD) camera (Princeton Instruments, SPEC-32). Absorption spectra were recorded with a Milton Roy Spectronic 3000 array spectrophotometer. Fluorescence spectra were acquired on a QuantaMaster spectrofluorimeter (Photon Technology International, Birmingham, NJ). DigiSim 3.03 (Bioanalytical Systems, Inc., West Lafayette, IN) was used to simulate the cyclic voltammograms.

Scanning electron microscopy (SEM) was performed with a LEO 1450VP microscope at an accelerating voltage of 20 kV and linked with an Oxford Instruments X-ray analysis system. Transmission electron microscopy (TEM) analysis and selected area electron diffraction (SAED) were conducted using a JEOL 2100F microscope at an accelerating voltage of 200 kV. Fluorescence imaging was carried out with an inverted

optical microscope (Model TE 300, Nikon) and images of the emission were taken with a Model 7404-0001, Roper Scientific Inc. camera.

Dynamic light scattering measurement were performed on 90Plus/BI-MAS Particle Size Analyzer (Brookhaven Instruments Corporation, Holtsville, NY), The technique employed - photon correlation spectroscopy (PCS) of quasi-elastically scattered light (QELS) - is based on correlating the fluctuations about the average, scattered, laser light intensity.

2.3 CHEMICALS:

Anhydrous acetonitrile (MeCN, 99.93%, in a sure-sealed bottle), anhydrous benzene (Bz, 99.8% in a sure-sealed bottle), tetrahydrofuran (THF, anhydrous 99.9%), N,N-dimethylformamide (DMF, anhydrous 99.8%) were obtained from Aldrich. Tetra-*n*-butylammonium hexafluorophosphate (n-Bu_4NPF_6) was used as received from Fluka and benzoyl peroxide (BPO) (reagent grade, 97%) from Aldrich. All solutions were prepared in a glove box (Vacuum Atmospheres Corp.) and placed in airtight vessels for electrochemical and ECL measurements outside of the glove box. Tetra-n-butylammonium oxalate (TBAOX) was prepared by mixing oxalic acid (EM Science) and tetra-n-butylammonium hydroxide in methanol (Fluka) in a mole ratio of 1:2 followed by evaporation and drying in a rotary evaporator. All solutions were prepared in the dry box in an airtight cell for measurements completed outside the dry box. Tripropylamine (TPrA) was purchased from Sigma-Aldrich and used as was delivered it.

2.5 PREPARATION OF NANOPARTICLES

The reprecipitation method was used for synthesis of well-dispersed ONPs in aqueous solution.[1] The rubrene NPs were synthesized by dissolving the rubrene at a 5 mM concentration in THF and quickly injecting 100 μL of this solution into 10 mL of deionized water under an argon atmosphere with vigorous stirring at room temperature (Illustration 2.3). The resulting NP solution, after filtering through a 0.22 μm pore-size

filter (Millex GP, PES membrane), had a clear pale red color. The same procedure was followed for the preparation of DPA NPs by using MeCN, DMF or THF as the solvent.

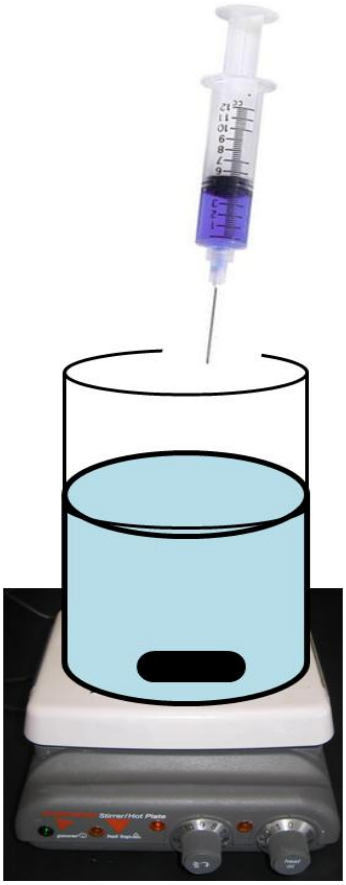

Illustration 2.3 Injection of the compound from the (good solvent, in syringe) to (Poor solvent, in the beaker) as quickly as possible and with continuous stirring.

2.6 REFERENCES

[1] (a) Mori , J.; Miyashita, Y.; Oliveira,D.; Kasai, H.; Oikawa, H.; Nakanishi, H. *Journal of Crystal Growth* , **2009**, *311*, 553 (b) Wu, C.; Peng, H.; Jiang,Y.; McNeill**,** J**.** *J. Phys. Chem. B* **2006,** *110,* 14148 (c) Kaneko, K.; Shimada, S.; Onodera, T.; Kimura, T.; Matsuda, H.; Okada S.; Kasa, H.; Oikawa, H.; Kakudate, Y.; Nakanishi, H, *Jpn. J. Appl. Phys*, **2007**, *46*, 6893, (d) Kasai, H.; Nalwa, H. S.; Oikawa, H.; Okada, S.; Matsuda, H.; Minami, N.; Kakuta, A.; Ono, K.; Mukoh,A.; Nakanishi, H.; *Jpn. J. Appl. Phys*, **1992**, *31*, 1132 (e) Kasai, H.; Oikawa, H.; Okada, S.; and Nakanishi, H.; *Bull.chem. Soc. Jpn*, **1998**, *71*, 2597.

Chapter 3: Green Electrogenerated Chemiluminescence of Highly Fluorescent Benzothiadiazole and Fluorene Derivatives

3.1 INTRODUCTION

In this chapter we report the synthesis, electrochemical, and photophysical characterization, as well as the electrogenerated chemiluminescence (ECL) of a series of novel, low-molecular weight, highly fluorescent 2,1,3-benzothiadiazole derivatives, Scheme 3.1.

ECL is a unique type of luminescence in which the electron transfer between electrogenerated ion radicals produces an electronically excited product in the vicinity of the electrode, with the emission of light.[1]

ECL and electrochemistry are versatile and sensitive tools that can be used to obtain valuable information about radical ion formation and stability and about often subtle interactions within molecules. Such information is of use in the design of organic light emitting devices (OLEDs), where charge creation, migration, and recombination, are determined by analogous charged states in the active organic layer.[2] Another use of ECL, involves development of new ECL emitters for labels at different wavelengths for bioanalytical applications, i.e. finding ECL emitters of different wavelengths than the currently used species.

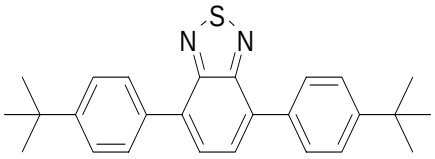

BH0

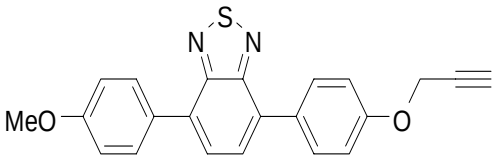

BH1

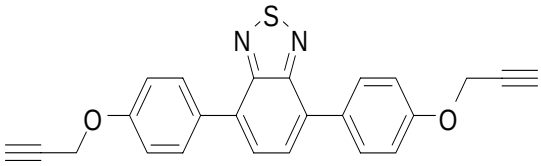

BH2

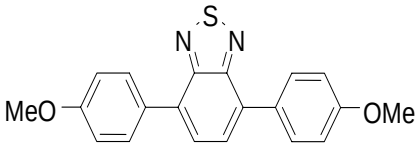

BH3

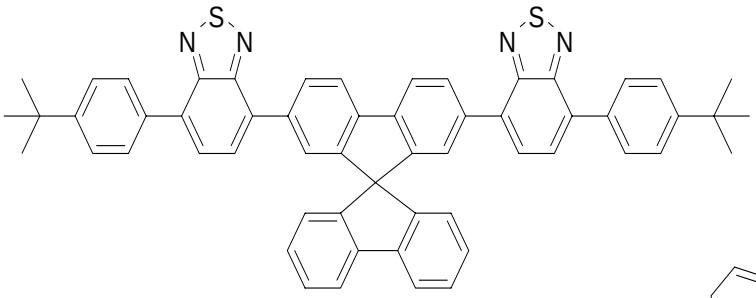

AB2

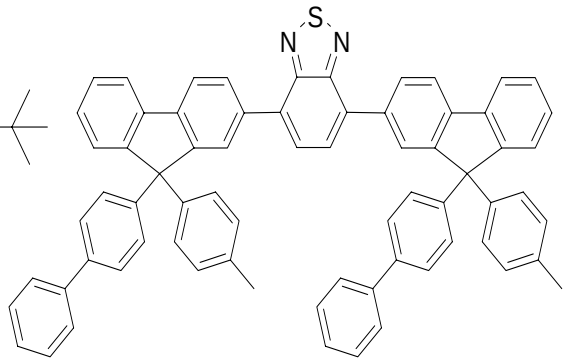

C01

Scheme 3.1 The novel Green PL emitters.

Fluorene-based materials, such as terfluorenes,[3] oligofluorene,[4] and polyfluorenes,[5] have emerged as promising candidates for OLEDs due to their high photoluminescence (PL) and electroluminescence (EL) efficiencies, good thermal stability, and color tunability across the full visible range. Tuning of the emission can be achieved by adding more units of conjugation or modulation of the donor and acceptor strength in bipolar compounds.[6] Generally, fluorene derivatives emit blue light due to their large energy gap. By introducing a unit with a narrower energy gap, like the electron-deficient 2,1,3-benzothiadiazole group into the fluorene backbone, the emission color can be tuned to the green region.[7] Therefore, the ability to tune the luminescence of these systems also makes them of interest for developing new, multicolor, light-emitting materials which are needed for full color displays and also to achieve multiple wavelength ECL labels.

We previously reported the electrochemical behavior and ECL of *ter*-9,9-diarylflourenes,[8] spirobifluorene-bridged bipolar systems with stable radical ions,[9] star-shaped truxene core-oligofluorene,[10] and *N*-phenylcarbazole bridged dispirobifluorene.[11]

ECL involves electron transfer between electrochemically generated species, often radical ions, which results in an excited species that emits light.[1] The simplest ECL process is the radical ion annihilation reaction, which can be represented as follows:

$$A + e^- \longrightarrow A^{\bullet -} \quad \text{(formation of radical anion)} \qquad (3.1)$$

$$A - e^- \longrightarrow A^{\bullet +} \quad \text{(formation of radical cation)} \qquad (3.2)$$

$$A^{\bullet -} + A^{\bullet +} \longrightarrow {}^1A^* + A \quad \text{(excited state formation)} \qquad (3.3)$$

$${}^1A^* \longrightarrow A + h\nu \quad \text{(ECL emission)} \qquad (3.4)$$

The energy available for excited state generation is approximately equal to the enthalpy of annihilation: $-\Delta H^{o} = -\Delta G^{o} - T\Delta S^{o}$. If $-\Delta H^{o}$ is greater than the energy of an excited state, E_s (singlet) or E_T (triplet), a molecule can achieve that state upon radical ion annihilation. If the singlet state is directly populated, then the ECL mechanism is referred to as S- route ECL. If the triplet state is populated, triplet-triplet annihilation can occur to create a singlet state in what is known as T-route ECL.[12,1a]

If either the cation radical or anion radical is unstable (e.g. if the radical cation or anion is unstable or cannot be generated prior to the oxidation or reduction of solvent or supporting electrolyte), then ECL can often be generated by use of a coreactant, which can form either a strong reducing agent when oxidized (as oxalate or triproplyamine) or a strong oxidizing agent when reduced (as persulfate or benzoyl peroxide). For example, the oxidation wave of **BH0** is not chemically reversible at scan rates of 100 mV/s (i.e. the cation radical is not stable), so benzoyl peroxide (BPO) was used as a coreactant for ECL studies of this species. BPO forms a strong oxidizing agent (E^{oxd} = +1.5 V vs SCE).[13,1a] and leads to the singlet excited state of **BH0** (D*) as follows:

$$BPO + e^{-} \longrightarrow BPO^{\bullet -} \qquad (3.5)$$

$$BPO^{\bullet -} \longrightarrow BPO^{-} + BPO^{\bullet} \qquad (3.6)$$

$$BPO^{\bullet} + A^{\bullet -} \longrightarrow BPO^{-} + A^{*} \qquad (3.7)$$

Here we describe the synthesis, electrochemistry, spectroscopy, and ECL of a series of benzothiadiazole and fluorene derivatives. The electrochemical reduction, oxidation, and radical ion annihilation ECL of the benzothiadiazole derivatives (**BH0-BH3**) and fluorene derivatives (**AB2** and **C01**) are described below. Photophysical measurements were carried out and a comparison of their ECL spectra and PL is discussed.

3.2 SYNTHESIS OF GREEN EMITTERS

3.2.1 Synthesis of benzothiadiazole derivatives

The detailed synthesis is shown in the Chapter 2. Scheme 3.2 shows the synthesis of **BH0** by Suzuki coupling of dibromobenzothiadiazole with 4-*tert*-butylphenylboronic ester in the presence of a catalytic amount of $Pd(PPh_3)_4$ and P^tBu_3, leading to **BH0** in an isolated yield of 80% after purification through recrystallization.

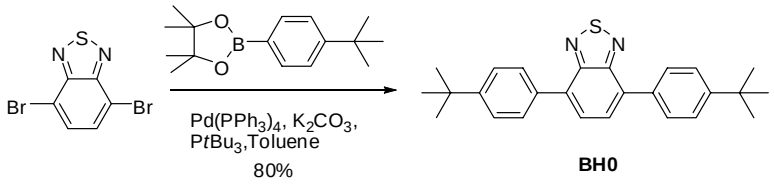

Scheme 3.2. The synthetic route for **BH0**

Scheme 3.3 depicts the synthetic routes for **BH1**, **BH2**, and **BH3**.[14] A Suzuki coupling reaction of 4,7-dibromo-benzo[1,2,5]thiadiazole with 4-methoxyphenylboronic acid in the presence of a catalytic amount of $Pd(PPh_3)_4$ and P^tBu_3 gave **BH3** in an isolated yield of 90% after purification through recrystallization. Subsequent selective

mono-deprotection or di-deprotection of **BH3** afforded **B1** and **B2** by means of excess amounts of HBr (33 % in HOAc). Then, treatment of **B1** and **B2** with excess amounts of propagyl bromide, K_2CO_3 and a catalytic amount of KI (10 mol%) in acetonitrile at 60 ^oC for 5 h led to the desired compound **BH1** and **BH2** in a good yield of 80% and 99%, respectively.

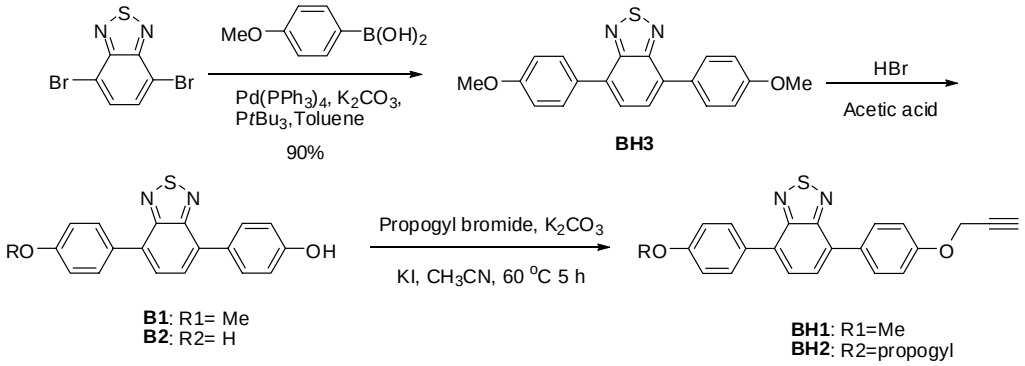

Scheme 3.3. The synthetic routes for **BH1**, **BH2**, and **BH3**

3.2.2 Synthesis of AB2

AB2, which consisted of a spirobifluorene core, benzothiadiazole moieties, and *tert*-butylbenzene, was synthesized from 4,7-dibromo-benzo[1,2,5]thiadiazole and 9,9'-spirobifluorene 2,7-diboronic ester (**1**) through a Suzuki coupling reaction. Scheme 3.4 depicts the synthetic route of **AB2** from compound **1**. Selective Suzuki coupling of the diboronate **1** with a large amount (6 equivalents) of dibromo-benzothiadiazole afforded the dibromo **2** in 30% yields. Then Suzuki coupling of the dibromo **2** with 4-*tert*-butylphenylboronic ester afforded **AB2** in 45% yield.

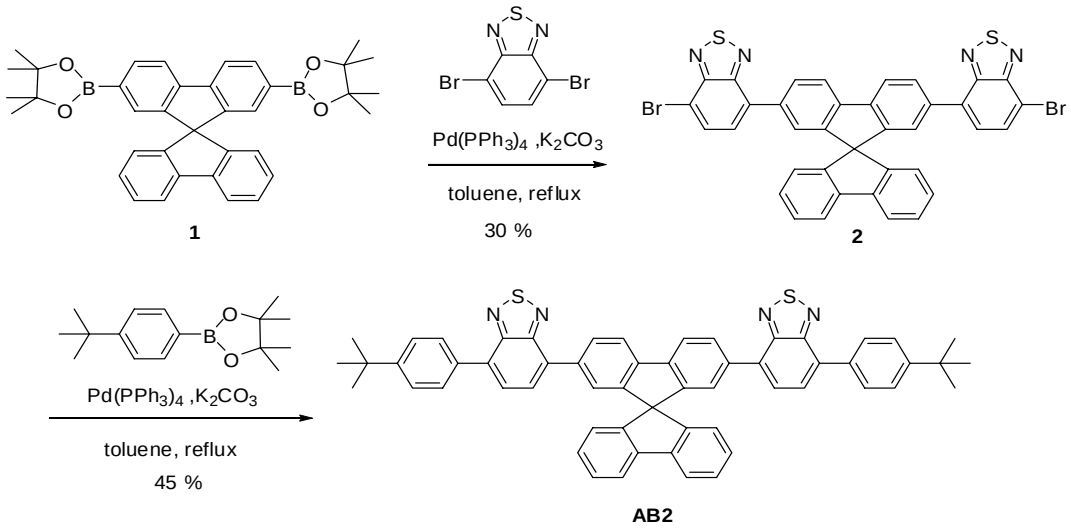

Scheme 3.4 The synthetic route of **AB2**

C01 was previously used as an efficient green emitter in organic light-emitting diode.[15]

3.4 RESULT AND DISCUSSION

3.4.1 Electrochemistry

Oxidation and reduction potentials provide information concerning the relative energetic positions of the frontier orbitals. Cyclic voltammetry was used to probe the electrochemistry of the compounds, assess the stability of the radical ions in the solution, and to find the energy of the radical ion annihilation in ECL. CVs of these compounds are shown in Figure 3.1 and the electrochemical results are summarized in Table 3.1.

3.4.1.1 Benzothiadiazole derivatives (BH0, BH1, BH2 and BH3)

Oxidation. These four compounds differ only in the substituents on each phenyl and generally show similar behavior. The electrochemical results are summarized in Table 3.1. Upon scanning to positive potentials, all show two consecutive, closely-spaced, one-electron transfer peaks. These peaks correspond to the formation of the radical cation and dication, since the consecutive peaks have similar peak currents, ~ 5 μA. The first oxidation waves for **BH1**, **BH2** and **BH3** were chemically reversible at scan rates as low as 50 mV/s, showing that the radical cations were stable in the time scale of the experiment. The peak separation for reversible oxidation peaks were ~ 70 mV, slightly larger than the expected value for nernstian behavior for a one electron transfer reversible peak, about 59 mV. However, the internal reference, ferrocene, which is known to produce a nernstian one electron wave, gave the same peak potential separation under the same conditions, which is usual for aprotic media where the ohmic drop can be

high (~ 1 kΩ) without positive feedback. Scan rate studies showed that the anodic and cathodic peak currents (i_{pa}, i_{pc}) of the first oxidation wave were proportional to the square root of the scan rate ($\nu^{1/2}$). Additionally, the peak current ratio (i_{pa}/i_{pc}) was approximately unity down to a scan rate of 50 mV/s, indicating the absence of a following chemical reaction. This suggests that the first oxidation to the stable cation radical is near nernstian for **BH1-3**.

The second oxidation wave is only slightly chemically reversible. Taking **BH3** as an example, we could simulate the observed behavior by an EC mechanism, with a homogenous forward rate constant, k_f = 10 s^{-1}, K_{eq} = 0.6, and a heterogeneous rate constant, k^o of about 5 $\times 10^{-3}$ cm^2/s. Figure 3.2 and Figure 3.5 show the simulation of both oxidation waves and the reduction side of **BH3** at several scan rates.

The oxidized forms of **BH0** are less stable, since it shows two sequential chemically quasireversible peaks at 1.64 and 1.83 V. As shown in Table 3.1, the trend in the potentials for oxidation of the first wave is **BH3 < BH1 < BH2 < BH0**. **BH3** with two methoxy groups, which are strong electron donors, is easiest to oxidize followed by **BH1** with one methoxy group. The absence of stabilizing or bulky substituents in **BH0** makes the oxidation more difficult with lesser stability for the radical cation. In fact, because of instability of the cation radical the wave is shifted to less positive potentials with respect to the thermodynamic $E_{1/2}$, which is thus somewhat more positive than the value shown (Table 3.1).

BH0 oxidation is distinguishable from that of the other **BHs**. The oxidation waves are less chemically reversible at v = 50 mV/s. Equal anodic peak currents indicate the same number of electrons participate in each oxidation step. However the first oxidation, which was irreversible at scan rate v = 50 mV/s, became reversible at v > 500 mV/s, indicating that a homogeneous chemical reaction follows the heterogeneous electron transfer. Simulation of oxidation wave of **BH0** is shown (Figure 3.3). The best fit was an EC mechanism, i.e. a chemical reaction following an electrochemical electron transfer with a heterogeneous rate constant k_o= 0.025 cm/s, and a homogenous forward rate constant (k_f = 3.6 s^{-1}, k_{eq} = 0.5).

Reduction. In scanning negatively, all **BHs** show two reversible reduction waves, as tabulated in Table 3.1, and shown in Figure 3.1. A CV of 2,1,3-benzothiadiazole, the central group, taken under the same conditions, Figure 3.4 showed a single reversible reduction peak at –1.47 V vs. SCE. 2,1,3-benzothiadiazole is a well-known heteroatomic compound with a high electron-accepting part because it has two electron-withdrawing imine groups (C=N).[16] Thus, this peak for the **BH0 to BH3** can be attributed to the benzothiadiazole group. The fact that all four compounds show essentially the same potential for reduction demonstrates that there is little effect from the electron donating substituents.

In addition to the benzothiadiazole peak, all **BHs** show another one-electron reduction peak, which probably corresponds to a second electrochemical reduction of the same benzothiadiazole group for all **BHs** at around –2.18 V vs. SCE. The absence of this

peak in unsubstituted benzothiadiazole and the presence in the **BH** series might be due to slightly better electron delocalization in the phenyl groups.

3.4.1.2 Fluorene derivatives (C01 and AB2)

AB2 involves the coupling of two benzothiadiazole groups through a spirodifluorene while **CO1** involves two spirodifluorenes coupled through a benzothiadiazole group.

Oxidation. A scan towards positive potentials for a **C01** solution shows two sequential reversible waves at 1.46 V and 1.61 V vs. SCE respectively, Figure 3.1. Both have equal peak currents ~ 5 μA, consistent with one-electron transfers for the electrochemical oxidation processes. The first peak is chemically reversible down to 50 mV/s, demonstrating a fairly stable cation radical.

The oxidation of **AB2** shows similar behavior as **C01**, with two consecutive, reversible peaks 30 mV less positive than those of **C01** for the first oxidation peaks, (1.43 and 1.56 V vs SCE). The small difference is attributed to the greater delocalization in the positive **AB2** cation than the **C01** cation. This delocalization is slightly greater for the **AB2** dication, with a shift of 50 mV compared to the dication of **C01**. These differences imply that the HOMO energy is raised slightly from **C01** to **AB2**.

Reduction. C01 reduction produces two reversible peaks at −1.39 and −1.93 V. Both reductions are expected to occur at the benzothiadiazole group, which is a good acceptor, as discussed previously. Unsubstituted benzothiadiazole does not exhibit a second reduction peak. Here, the second reduction peak of **C01**, is less negative than

BH0 by 250 mV. This potential shift indicates greater delocalization onto the two fluorene moieties. In **AB2**, the potential difference is 130 mV because **AB2** possesses only a single fluorene moiety. The first **AB2** reduction peak occurs at –1.44 V and represents a two-electron transfer (i_{pc} = 10 μA, compared with i_{pc} = 5 μA for the first **C01** reduction and the other peaks), indicating minimal conjugation (electronic communication) through the fluorene moiety so that both benzothiadiazole moieties are reduced at the same potential. However, the second and third reduction of **AB2** shows a small splitting of about 150 mV, indicating that in contrast to the dianion radical, the benzothiadiazole radical trianion is delocalized across the spirobifluorene moiety. The two processes do not occur at the same potential because the electrostatic repulsion from the second reduction (–2.05 V) shifts the third to more negative potentials (–2.20 V).

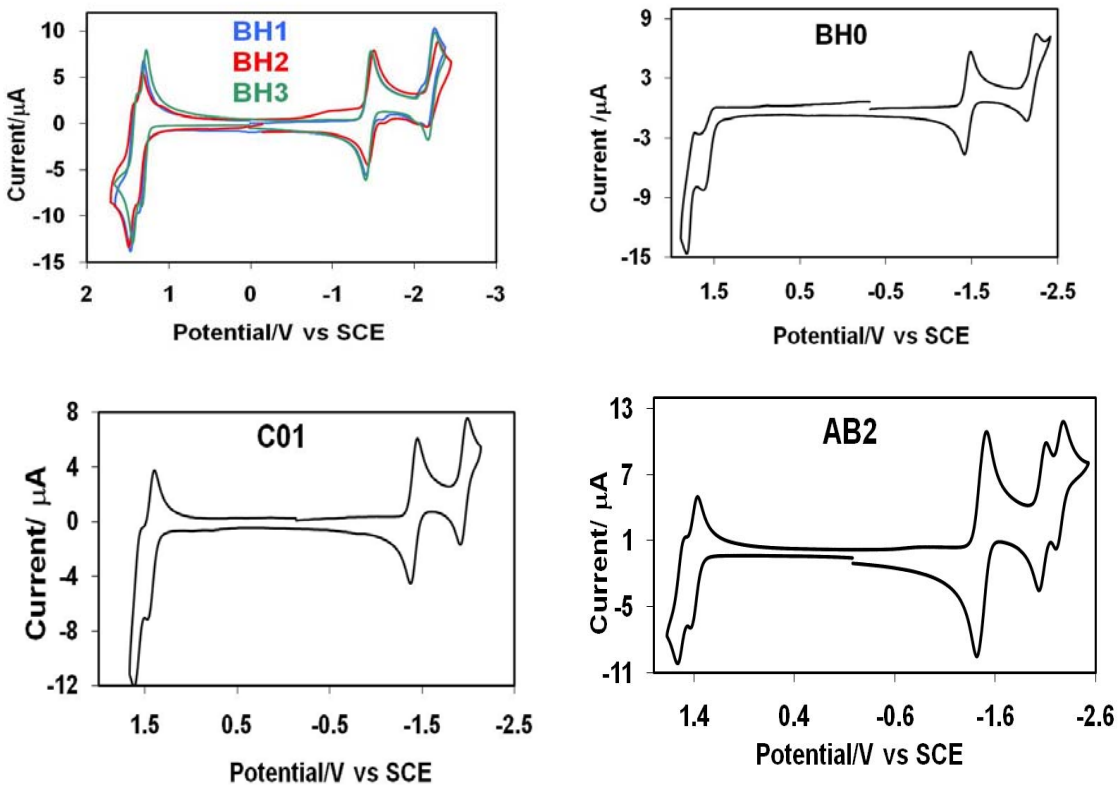

Figure 3.1 Cyclic voltammograms for the compounds, supporting electrolyte 0.1 M Bu_4NPF_6: 1 mM (**BH0**, **BH1**, **BH2**, **BH3)** in MeCN, 1 mM (**C01, AB2)** in 1:1 MeCN:Bz . Scan rate: 100 mV/s, WE:Pt disk electrode (~1 mm diameter), CE:Pt coiled electrode.

Table 3.1. Electrochemical data

Cpd[a]	Oxidation waves, V vs SCE		Reduction waves, V vs SCE			D ($\times 10^{-6}$) cm^2/s	E_g(eV)[b]	E_{HOMO}(eV)[c]	$E_{(LUMO)}$ (eV)[d]
	$E_{1/2}^{oxd1}$	$E_{1/2}^{oxd2}$	$E_{1/2}^{red1}$	$E_{1/2}^{red2}$	$E_{1/2}^{red3}$				
BH0	1.64(E_p)	1.83(E_p)	–1.40	–2.18	–	9	3.04	–6.02	–2.93
BH1	1.37	1.49	–1.40	–2.18	–	9	2.77	–5.75	–2.93
BH2	1.42	1.54	–1.38	–2.18	–	9	2.80	–5.79	–2.92
BH3	1.33	1.45	–1.42	–2.21	–	9	2.75	–5.71	–2.92
C01	1.46	1.61	–1.39	–1.93	–	7.5	2.85	–5.84	–2.89
AB2	1.43	1.56	–1.44	–2.05	–2.20	7	2.87	–5.81	–2.88

[a] Concentrations, 1 mM. [b] From the CV. [c] The HOMO values are calculated based on the value of –4.8 eV for ferrocene with respect to the vacuum[17,9a]. [d] From first reduction wave. *Ep* is peak potential.

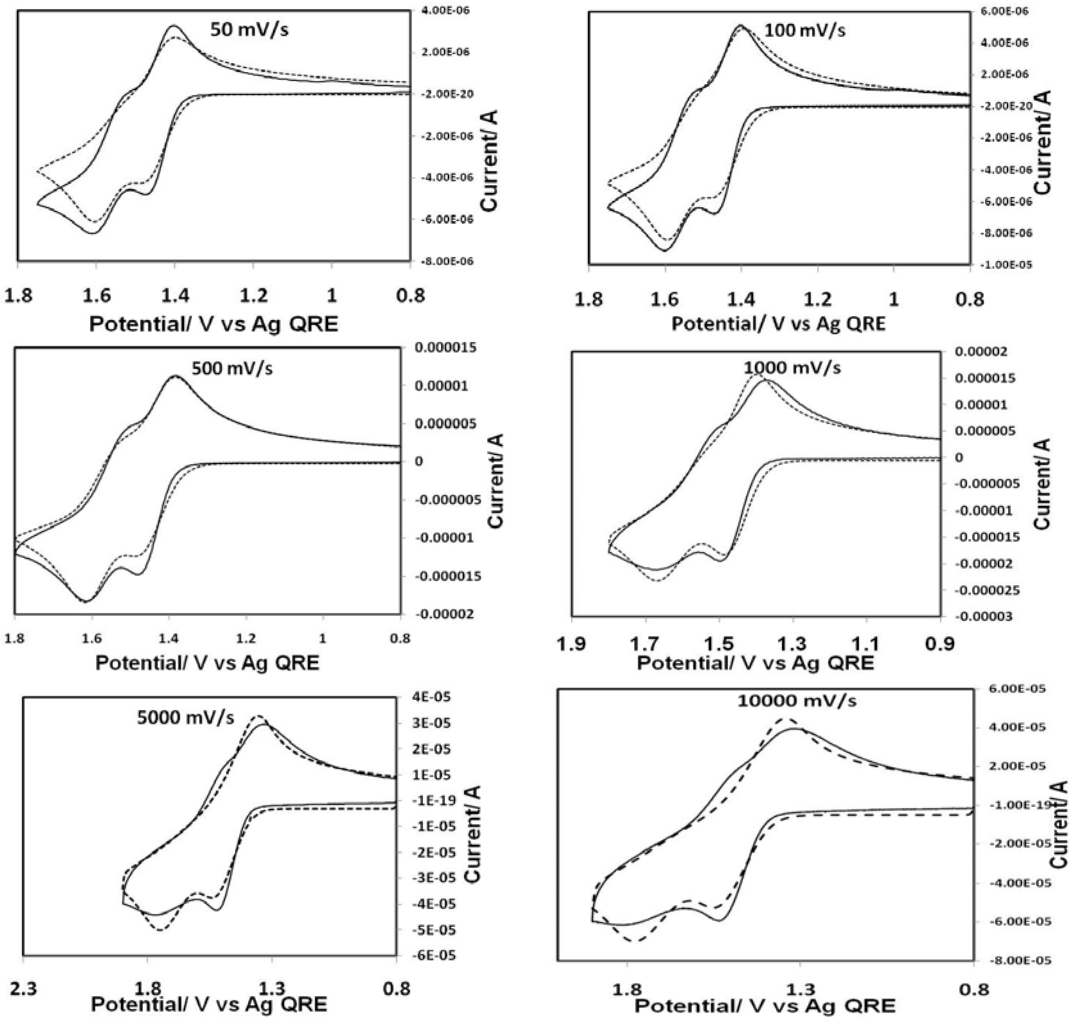

Figure 3.2 Simulation of oxidation 1 mM **BH3**, the simulation corrected for resistance and capacitance, experimental (solid line), Simulation (dotted line). The first wave is completely reversible with one electron transfer ($k^o = 1\times10^4$ cm/s), the second wave one-electron transfer of EC mechanism. Ru = 1.2 kΩ, Cd= 10 nF, α =0.5, D = 9×10^{-6} cm^2/s.

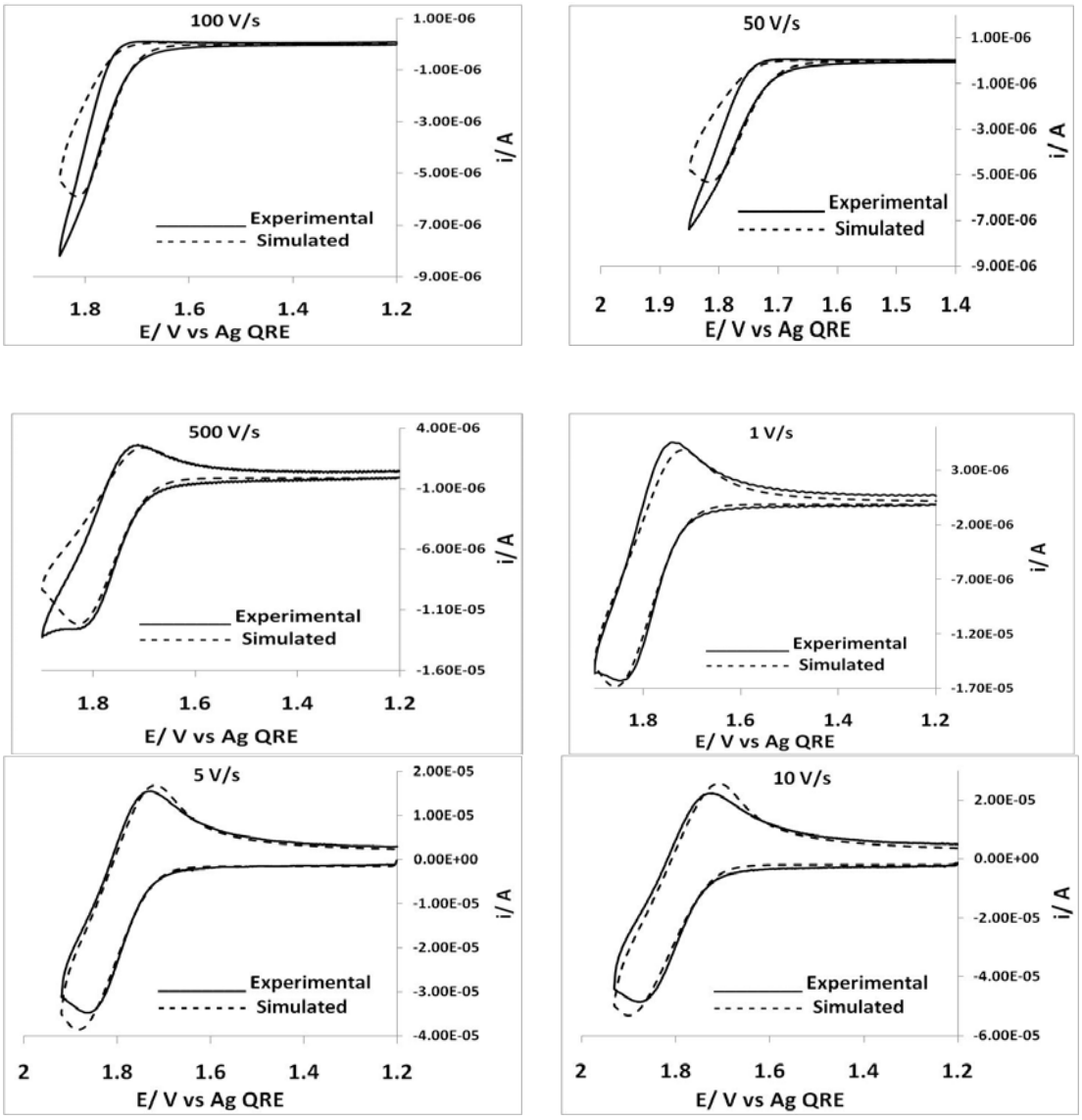

Figure 3.3. Simulation of first oxidation wave of 1 mM **BH0**, the simulation corrected for resistance and capacitance, experimental (solid line), simulation (dotted line). The simulation mechanism was EC model with one-electron transfer (k^o = 0.025 cm/s), with a homogenous forward rate constant = 3.6 S^{-}, keq= 0.57. Ru = 1.2 kΩ, Cd= 10 nF, α =0.5, D = 9×10^{-6} cm^2/s.

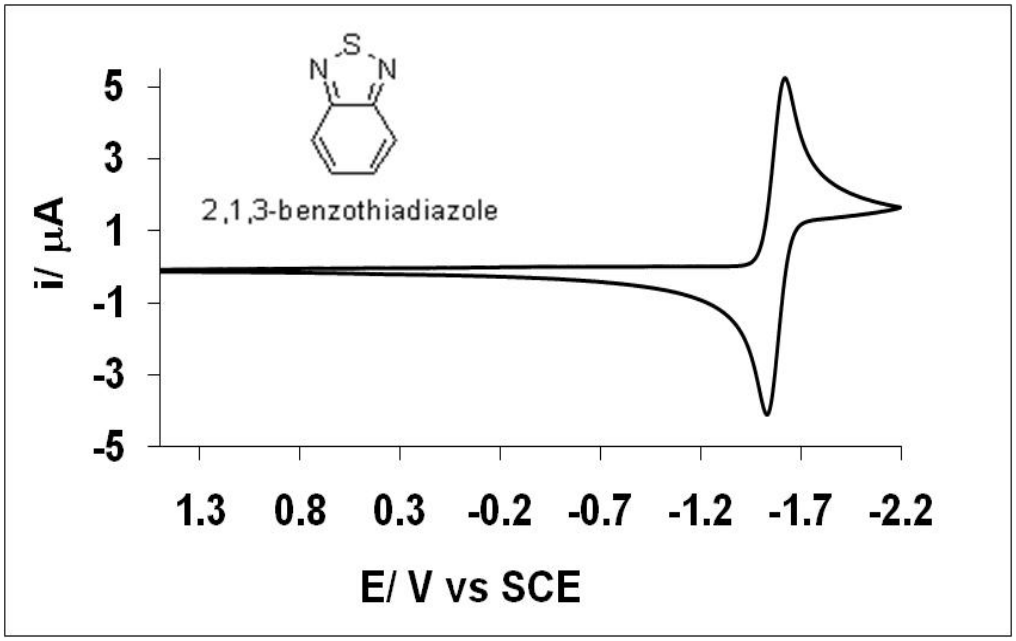

Figure 3.4 Cyclic voltammogram of 2,1,3-benzothiadiazole in MeCN, scan rate: 200mV/s.

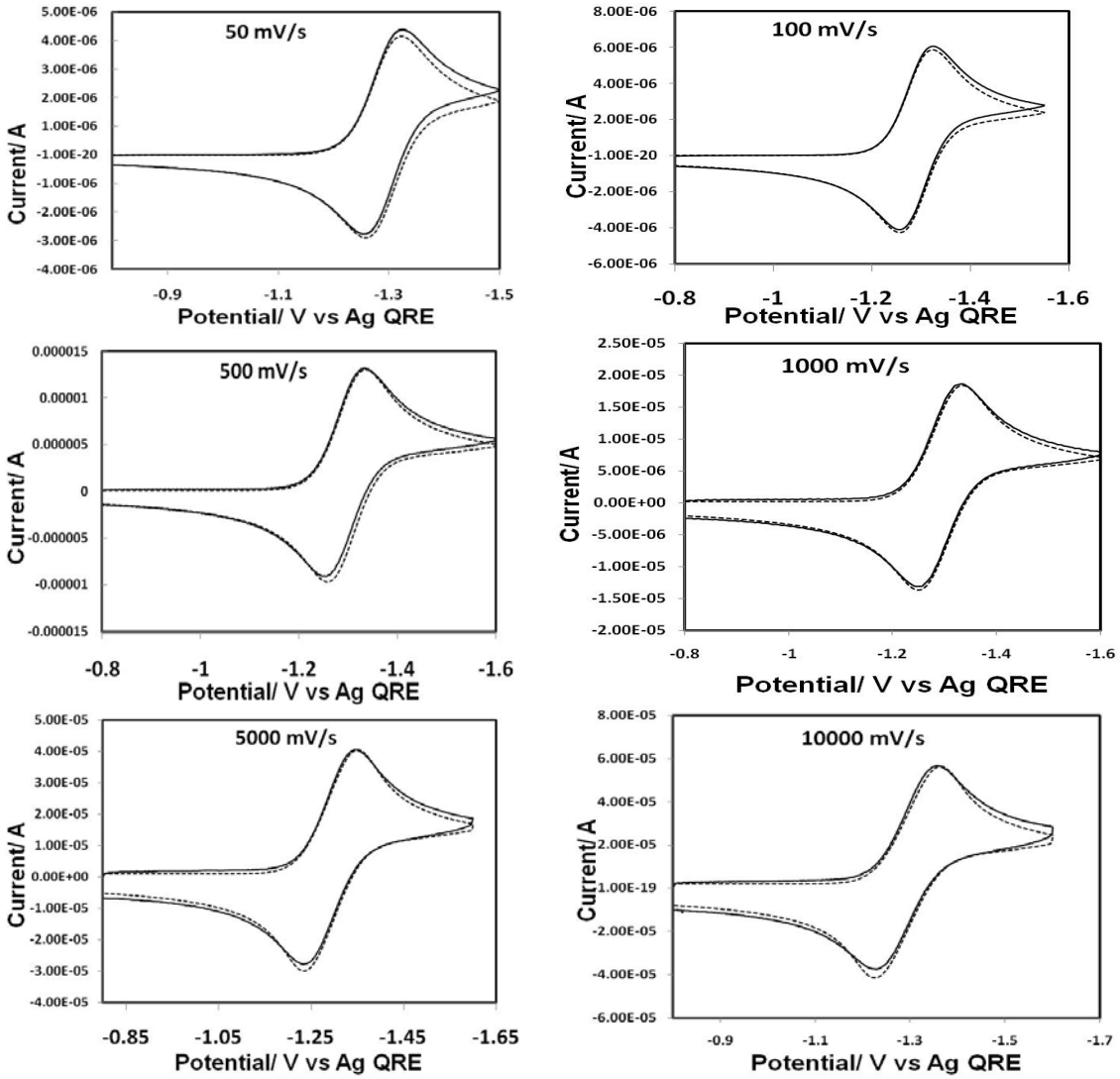

Figure 3.5 Simulation of reduction 1 mM **BH3**, the simulation corrected for resistance and capacitance, experimental (solid line), simulation (dotted line). The reduction is one electron transfer process (k = 1×10^{4} cm/s) Ru = 1.2 kΩ, Cd= 10 nF, α =0.5, D = 9×10^{-6} cm^2/s.

3.4.2 Spectroscopy

Absorption and fluorescence spectra for all the compounds are shown in Figure 3.6. The absorption and emission spectra were obtained in the same solvent mixture used in the electrochemical measurements for the sake of consistency. The optical properties, absorption and emission maxima, extinction coefficient, fluorescence quantum yield, and the optical energy gap are given in Table 3.2. Structureless π-π* absorption bands were observed for fluorene derivatives and **BH0**-**BH3** compounds. Compared with **BH0**, **BH1**- **BH3** are red-shifted by 12 nm (**BH2**), 16 nm (**BH1**) and 18 nm (**BH3**), due to electron donor properties of the terminal groups (OMe > propogyl-O > *tert*butyl). The emission spectra of **BH0-3** show the same trend. Compared to **BH0**, **BH1**-**3**, are red-shifted by 30 nm (**BH2**), 34 nm (**BH1**) and 44 nm (**BH3**). **BH0** emits with a λ_{max} = 512 nm and a Stokes shift of 124 nm, while larger Stokes shifts are observed in **BH1**,**2** and **3**, as summarized in Table 3.2.

The absorption λ_{max} for **AB2** and **C01** are slightly red-shifted because of their greater conjugation. The slightly smaller Stokes shifts for **AB2** and **C01** compared to the **BHs**, which could be due to the smaller solvent polarity used for these compounds, Bz:MeCN, compared to pure MeCN in the case of **BHs**.

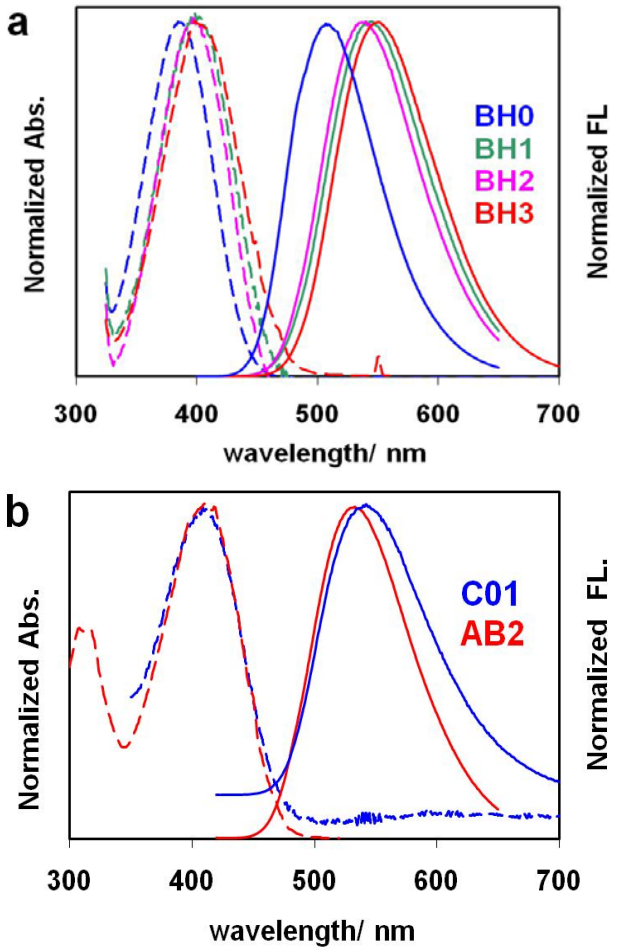

Figure 3.6 Absorption (dotted lines) and emission (solid lines) spectra, (a) **BH0**–**BH3** in MeCN. (b) **C01** and **AB2** in 1:1 Bz:MeCN. Emission spectra were excited at the absorption maxima.

Table 3.2. Spectroscopy results

	λ_{max} - (abs)(nm), [log ε]	λ_{max} (em)(nm)	E_s (eV)[a] 0-0 transition	Φ_{PL}%[b]	Stoke's shifts $\Delta\lambda_{st}$ (nm)
BH0	388,[4.33]	512	2.78	5.0	124
BH1	404,[4.43]	546	2.67	5.5	142
BH2	400,[4.40]	542	2.71	5.2	142
BH3	406,[4.44]	556	2.60	7.0	150
C01	412,[4.61]	544	2.60	90	132
AB2	417,[4.65]	535	2.63	75	118

All spectra recorded in the described solvent at room temperature. [a] Calculated from the wavelength where excitation and emission spectra cross. [b] Quantum yield calculated relative to the fluorescein in solution.

3.4.3 Electrogenerated chemiluminescence (ECL)

All **BHs** and the fluorene derivatives produced strong ECL emission for radical ion annihilation, which can be seen with the naked eye in a dimly lit room; typical results are given in Table 3.3 and Figure 3.7. In all cases the estimated annihilation energy is sufficient to populate the excited singlet state directly, classifying the ECL of these systems as energy sufficient or S-route systems. All ECL spectra were close to the PL spectra; the 5 nm to 15 nm difference between the PL and ECL is probably caused by instrumental differences and the self-absorption (inner filter effect) from the high concentrations of the solutions used for ECL vs. those for PL studies.

BH0 produced only weak ECL by direct annihilation (sweeping or stepping potentials between the first oxidation and reduction peaks). This results from instability of the radical cation, as seen in the oxidative cyclic voltammogram. Because of this instability of the **BH0** radical cation, the ECL intensity decreased with time and a spectrum could not be obtained with the liquid nitrogen cooled CCD camera as a detector during extended pulsing. However in this case, a coreactant approach could be used. Since the radical anion of **BH0** is stable, BPO was used as a coreactant for reductive ECL. BPO, upon reducing electrochemically, produces a strong oxidizing agent (E^{oxd}= 1.5 V vs SCE),[13,1a] which can react with the radical anion of **BH0** populating the excited state. Under these conditions, strong ECL was observed (Figure 3.7a).

Table 3.3. ECL data

Cmpd[a]	λ_{max}^{ECL}/nm	λ_{em}^{FL}/nm	E_s (ev)[b] 0-0 transition	ΔH_{ann}[c] *eV*	Φ_{PL}%	Φ_{ECL} %[d]
BH0	518	512	2.78	3.00	2.0	0.05
BH1	560	546	2.67	2.80	4.5	1.40
BH2	556	542	2.71	2.83	4.2	1.35
BH3	555	556	2.60	2.75	5.0	2.35
C01	548	544	2.60	2.87	75	2.7
AB2	536	535	2.63	2.91	65	7.50

[a]All concentrations ~ 1 mM. [b] $E_s = hc\,(\tilde{\nu}_{abs} + \tilde{\nu}_{PL}) / 2$. [c] $-\Delta H = -(E_{pa} - E_{pc}) - 0.1$ [d]

Quantum efficiency calculated relative to DPA, assuming DPA is 8%.[18]

To estimate the stability of the ECL and the radical ion species involved, potential pulsing ECL transients were collected. For example **BH3** shows two consecutive oxidation waves and one reduction peak (one-electron transfers). When the potential was stepped from the first oxidation wave ($E_{pa,1}$ + 50 mV) to the reduction wave ($E_{pc,1}$ – 50 mV), approximately equal ECL peaks were observed on the cathodic and anodic pulses, consistent with the same quantities of radical anions and cations formed per pulse and stability of the radical ions during the time of the experiment (Figure 3.8a). When the potential was stepped to the second oxidation wave ($E_{pa,2}$ + 50 mV) producing the dication A^{2+}, the anodic current was smaller than the cathodic current and the ECL maximum intensities were about the same as for pulsing to the first oxidation wave (Figure 3.8b). However the decay rate of the anodic ECL transients is higher (Figure 3.8b). Moreover, the ECL intensity of anodic pulse decreased with time, while in cathodic ECL intensity was constant. There have not been many studies of ECL generation between radical anions and dications, and the situation is complicated because of the occurrence of a comproportionation reaction between dication and parent and also by the fact that all of the electrogenerated species are potential quenchers. Although we have tried to simulate the observed behavior by choosing different rate constants for the possible reactions, we were not successful in matching the observed experimental results. Interpreting these kinds of asymmetric ECL generation will probably be easier in a steady state (two-electrode) mode, e.g. by scanning electrochemical microscopy (SECM).

The relative quantum efficiencies were determined for all the ECL emitters, as calculated by the number of photons emitted per injected electron. These were compared to 9,10-diphenylanthracene (DPA) as a standard ECL emitter, even though the emission (λ_{max} = 420 nm) is quite blue-shifted compared to the compounds of interest here. These results are given in Table 4, taking the quantum yield of DPA in acetonitrile as 8%.[13] The ECL emission intensity of **AB2** is about the same as that of DPA, but in the green region of the spectrum.

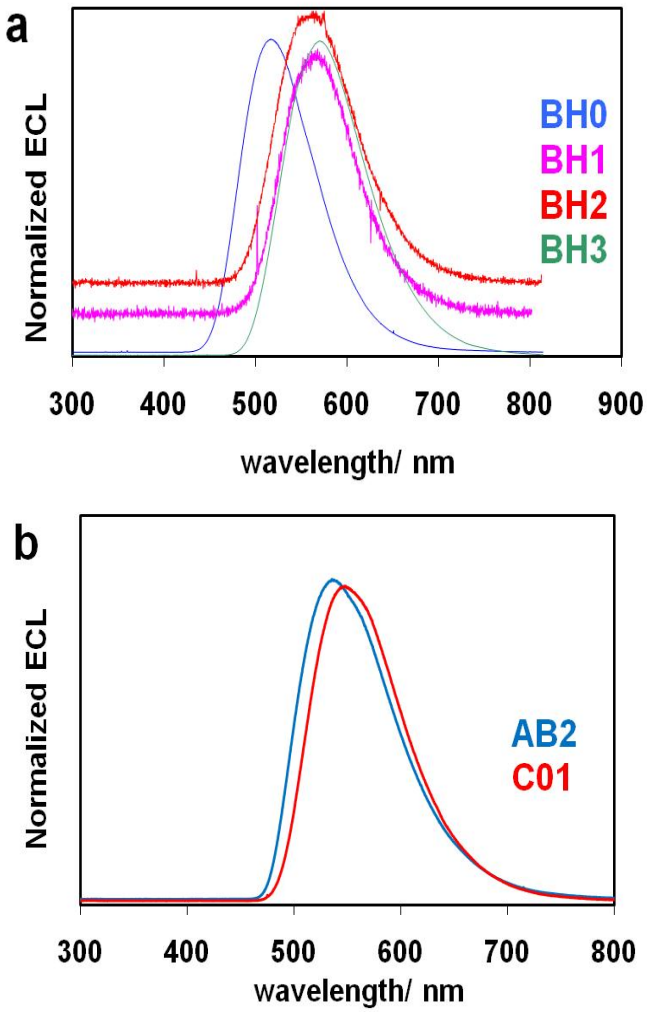

Figure 3.7 (a) ECL spectra of **BHs** in MeCN, **BH1**, **BH2**, **BH3** were taken by annihilation by stepping between (E_p^{red} –50 mV) to the first oxidation potential (E_p^{oxd} +50 mV), integration time: 1 min, slit width: 0.5 mm. **BH0** were recorded using BPO (1 0mM) as a coreactant (b) ECL of fluorene derivatives by annihilation by stepping between (E_p^{red} – 50mV) to the first oxidation potential (E_p^{oxd} + 50 mV).

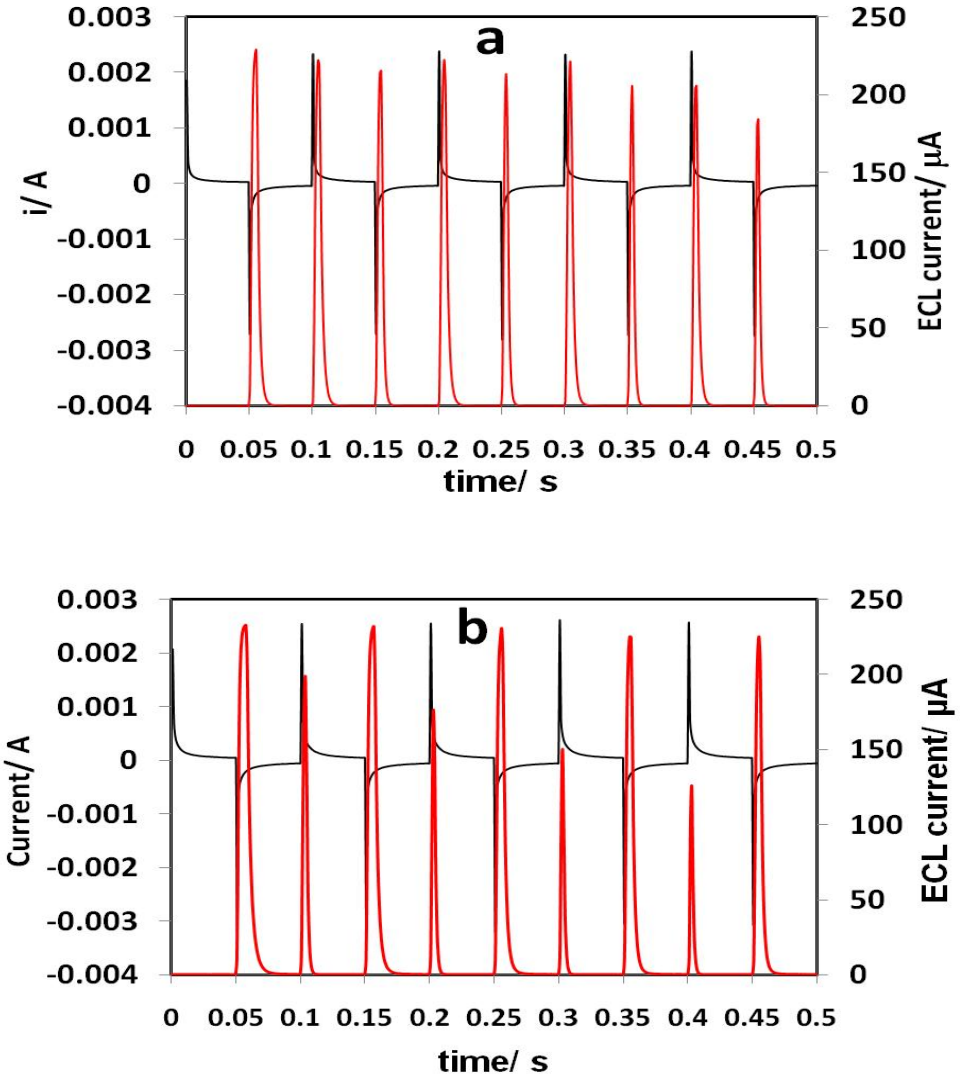

Figure 3.8 Stepping ECL (annihilation) of **BH3** (1 mM), in MeCN, pulse width: 0.1 s, stepping direction is from anodic to cathodic (a) from first oxidation peak (1.35 V) (n~1) to the first reduction peak (–1.50 V) (n=1) (b) from both oxidation peaks (1.50 V) (n=2) to the first reduction pea k(–1.50 V) (n=1), pulse width = 0.0 5s**. (As plotted here the positive electrochemical current is anodic pulse, negative electrochemical current is cathodic pulse)**

3.5 THERMAL PROPERTIES

Differential scanning calorimetry (DSC) and thermogravimetric analysis (TGA) were used to study the thermal properties of the compounds as shown in Table 3.4. **C01** and **AB2** exhibited distinct glass transition temperatures (T_g) at 180 and 190 ^oC, respectively. TGA analysis indicated that the fluorene derivatives (**C01** and **AB2**) were thermally stable, with decomposition temperatures (T_d), relative to 10% weight loss, ranging from 459 to 489 ^oC. TGA analysis for **BHs** show T_d ranging from 243 to 315 ^oC due to their low molecular weights.

Table 3.4. Thermal properties

Compound	T_g	T_d
BH0		307
BH1		243
BH2		268
BH3		315
C01	180	459
AB2	190	489

3.6 CONCLUSIONS

We have synthesized a series of highly fluorescent and strong, green ECL emitters. These compounds were characterized by electrochemistry, spectroscopy and thermal analysis. All the compounds, with the exception of **BH0**, give reversible oxidation and reduction waves in their CV and form stable radical ions. Due to their high PL quantum yield and stable radicals upon oxidizng and reducing, these gave strong and stable green ECL emission. The ECL quantum yield of **AB2** is close to that of the well-known ECL emitter, DPA. Such fluorene derivatives are promising for future applications as nanomaterials and biological luminescent labels.

3.7 REFERENCES

[1] For review on ECL: See (a) *Electrogenerated Chemiluminescence*; Bard, A. J.; Ed.; Marcel Dekker, Inc.; New York, **2004**. (b) Miao, W. *Chem. Rev*. **2008**, *108*, 2506. (c) Richter, M. M. *Chem. Rev*. **2004**, *104*, 3003. (d) Knight, A. W.; Greenway, G. M. *Analyst* **1994**, *119*, 879. (e) Bard, A. J.; Debad, J. D.; Leland, J. K.; Sigal, G. B; Wilbur, J. L.; Wohlstadter, J. N. In *Encyclopedia of Analytical Chemistry: Applications, Theory and Instrumentation*; Meyers, R. A., Ed.; John Wiley & Sons: New York, **2000**; *Vol. 11*, p. 9842.

[2] Yasuda, T.; Imase, T.; Yamamaoto, T. *Macromolecules* **2005**, *38*, 7378.

[3] (a) Wong, K.-T.; Chien, Y.-Y.; Chen, R.-T.; Wang, C.-F.; Lin, Y.-T.; Chiang, H.-H.; Hsieh, P.-Y.; Wu, C.-C.; Chou, C. H.; Su, Y. O.; Lee, G.-H.; Peng, S.-M. *J. Am. Chem. Soc.* **2002**, *124*, 11576. (b) Wu, F-I.; Dodda, R.; Reddy, D. S.; Shu, C-F. *J. Mater. Chem*. **2002**, *12*, 2893. (c) Tsolakis, P. K.; Kallitsis, J. K. *Chem. Eur. J*. **2003**, *9*, 936. (d) Wu, C-C.; Lin, Y-T.; Wong, K-T.; Chen, R-T.; Chien, Y-Y. *Adv. Mater*. **2004**, *16*, 61. (e) Chochos, C. L.; Kallitsis, J. K.; Gregoriou, V. G**.** *J. Phys. Chem. B.* **2005***, 109,* 8755. (f) Chochos, C. L.; Kallitsis, J. K.; Keivanidis, P. E.; Baluschev, S.; Gregoriou, V. G. *J. Phys. Chem. B* **2006,** *110,* 4657. (g) Chen, A. C.-A.; Wallace, J. U.; Klubek, K. P.; Madaras, M. B.; Tang, C. W.; Chen, S. H. *Chem. Mater*. **2007**, *19*, 4043.

[4] (a) Lee, S. H.; Tsutsui, T. *Thin Solid Films* **2000**, *363*, 76. (b) Geng, Y.; Katsis, D.; Culligan, S. W.; Ou, J. J.; Chen, S. H.; Rothberg, L. *J. Chem. Mater.* **2002**, *14*, 463. (c) Li, Y.; Ding, J.; Day, M.; Tao, Y.; Lu, J.; D'iorio, M. *Chem. Mater.* **2003,** *15,* 4936. (d) Culligan, S. W.; Geng, Y.; Chen, S. H.; Klubek, K.; Vaeth, K. M.; Tang, C. W. *Adv. Mater*. **2003**, *15*, 1176. (g). Kanibolotsky, A. L.; Berridge, R.; Skabara, P. J.; Perepichka, I. F.; Bradley, D. D. C.; Koeberg, M. *J. Am. Chem. S*oc. **2004**, *126*, 13695.

(h) Liu, Q-D.; Lu, J.; Ding, J.; Day, M.; Tao, Ye.; Barrios, Pedro.; Stupak, J.; Chan, K.; Li, J.; Chi Y. *Adv. Funct. Mater.* **2007***, 17,* 1028. (i) Kong, Q.; Zhu, D.; Quan, Y.; Chen, Q.; Ding, J.; Lu, J.; Tao, Y. *Chem. Mater.* **2007**, *19,* 3309.

[5] (a) Chang, S.-C.; Li, Y.; Yang, Y. *J. Phys. Chem. B* **2000**, *104*, 11650. (b) Lupton, J. M.; Craig, M. R.; Meijer, E. W. *Appl. Phys. Lett.* **2002**, *80*, 4489. (c) Wong, K.-T.; Chien, Y.-Y.; Chen, R.-T.; Wang, C.-F.; Lin, Y.-T.; Chiang, H.-H.; Hsieh, P.-Y.; Wu, C.-C.; Chou, C. H.; Su, Y. O.; Lee, G.-H.; Peng, S.-M. *J. Am. Chem. Soc.* **2002**, *124*, 11576. (d) Ego, C.; Grimsdale, A. C.; Uckert, F.; Yu, G.; Srdanov, G.; Mullen, K. *Adv. Mater*. **2002**, *14,* 809. (e) Culligan, S. W.; Geng, Y.; Chen, S. H.; Klubek, K.; Vaeth, K. M.; Tang, C. W. *Adv. Mater.* **2003**, *15*, 1176. (f) Wu, W.; Inbasekaran, M.; Hudack, M., Welsh, D.; Yu, W.; Cheng, Y.; Wang, C.; Kram, S.; Tacey, M.; Bernius, M.; Fletcher, R.; Kiszka, K.; Munger, S.; O'Brien, J. *Microelectron. J.* **2004**, *35*, 343. (g) Huang, F.; Wu, H.; Wang, D.; Yang, W.; Cao, Y. *Chem. Mater.* **2004,** *16,* 708. (h) Wong, K.-T.; Liao, Y.-L.; Lin, Y.-T.; Su, H.-C.; Wu, C.-C. *Org. Lett.* **2005**, *7*, 5131. (i) Chen, A. C.-A.; Wallace, J. U.; Wei, S. K.-H.; Zeng, L.; Chen, S. H. *Chem. Mater.* **2006,** *18,* 204. (j) Fan, S.; Sun, M.; Wang, J.; Yang, W.; Cao, Y. *Appl. Phys. Lett*. **2007**, *91*, 213502.

[6] (a) Joshi, H. S.; Jamshidi, R.; Tor, Y. *Angew. Chem. Int. Ed*. **1999**, *38*, 2721. (b) Yoshida, Y.; Tanigaki, N.; Yase, K.; Hotta, S. *Adv. Mater*. **2000**, *12*, 1587. (c) Tsuzuki, T.; Shirasawa, N.; Suzuki, T.; Tokito, S. *Adv. Mater*. **2003**, *15*, 1455. (d) Montes, V. A.; Li, G.; Pohl, R.; Shinar, J.; Anzenbacher, P. *Adv. Mater*. **2004**, *16,* 2001. (e) Gana, J-A.; Song, Q. L.; Hou, X- Y.; Chen, K.; Tian, H. *J. Photochem. Photobiol. A* **2004,** *162*, 399.

[7] (a) Millard, I. S. *Synth. Met.* **2000**, *111–112*, 119. (b) Muller, C. D.; Falcou, A.; Reckefuss, N.; Rojahn, M..; Wiederhirn, V.; Rudati, P.; Frohne, H.; Nuyken, O.; Becker, H.; Meerholz, K. *Nature*, **2003**, *421*, 829. (c) Justin Thomas, K. R.; Lin, J. T.; Velusamy, M.; Tao, Y-T., Chuen, C.-H. *Adv. Funct. Mater*. **2004**, *14*, 83. (d) Lin, J.; Dong, J.; Zhou, Q.; Geng, Y.; Ma, D.; Wang, L.; Jing, X.; Wang; F. *J. Mater. Chem.* **2007**, *17*, 2832.

[8] Choi, J. P.; Wong, K. T.; Chen, Y. M.; Yu, J. K.; Chou, P. T.; Bard, A. J. *J. Phys. Chem. B* **2003**, *107*, 14407.

[9] Fungo, F.; Wong, K.-T.; Ku, S.-Y.; Hung, Y.-Y.; Bard, A. J. *J. Phys. Chem. B* **2005**, *109*, 3984.

[10] Omer, K. M.; Kanibolotsky, A. L.; Skabara, P. J.; Perepichka, I. F.; Bard, A. J. *J. Phys. Chem. B* **2007**, *111*, 6612.

[11] Rashidnadimi, S.; Hung, T.-H.; Wong, K.-T.; Bard, A. J. *J. Am. Chem. Soc.* **2008**, *130*, 634.

[12] (a) Sartin, M. M.; Zhang, H.; Zhang, J.; Zhang, P.; Tian, W.; Wang. Y.; Bard, A. J. *J.Phys. Chem. C*, **2007**, *111*, 16350. (b) Lai, R. Y.; Fleming, J. J.; Merner, B. L.; Vermeij, R. J.; Bodwell, G. J.; Bard, A. J. *J. Phys. Chem A*, **2004**, *108*, 376.

[13] (a) Chandross, E.; Sonntag, F. *J. Am. Chem. Soc*. **1966**, *88*, 1089. (b) Santa Cruz, T. D.; Akins, D. L.; Brike, R. L. *J. Am. Chem. Soc*. **1976**, *98*, 1677.

[14] Ku, S.-Y.; Wong, K.-T.; Bard, A. J. *J. Am. Chem. Soc.* **2008**, *130*, 2392.

[15] Ku, S.-Y.; Chi, L.-C.; Hung, W.-Y.; Yang, S.-W.;Tsai, T.-C.; Wong, K.-T.; Chen, Y.-H.; Wu, C.-I. *J. Mater. Chem.* **2009**, *19*, 773.

[16] Yasuda, T.; Imase, T.; Yamamaoto, T. *Macromol*. **2005**, *38*, 7378.

[17] Gritzner, G.; Kuta, J.; *Pure Appl. Chem.* **1984**, *56*, 462.

[18] Beideman, F. E.; Hercules, M. *J. Am.Chem. Soc*. **1979**, 83, 2203.

Chapter 4: Electrochemistry and Bright and Stable Electrogenerated Chemiluminescence of Fluorene-Substituted Aromatic Hydrocarbons

4.1 INTRODUCTION

Polyaromatic hydrocarbons (PAHs) in aprotic media were the earliest subjects of electrogenerated chemiluminescence (ECL) studies,[1] and substituted PAHs have been widely investigated.[2] Indeed the PAHs 9,10-diphenylanthracene (DPA) and rubrene (R) have been ECL standards in aprotic media.[1a] These are intense ECL emitters because of their high fluorescence quantum yields and stable cation and anion radicals. However, even with DPA and R the ECL decays because of reactions of the ion radicals. This might be attributed to the irreversibility of the second oxidation waves because of the instability of the dication DPA^{2+}. Although ECL pulsing typically only involves potentials of the first oxidation wave, the disproportionation of the monocation radical occurs to a small extent and then the dication instability leads to slow decomposition. If the second oxidation wave is made more chemically reversible, the stability of ECL should be improved. An argument like this has been made in considering the stability of electrochromic devices based on similar generation of radical ions.[3]

In aprotic media ECL is the emission of light due to the electron transfer process in the vicinity of the electrode with the intensity largely governed by the stability of the electrogenerated ion radicals over the time scale of the potential sweeps or steps and the quantum efficiency of the generated excited state.[1a] The model is shown in Scheme 4.1**:**

Scheme 4.1

$$A - e \rightarrow A^{\bullet +} \quad (4.1)$$

$$A + e \rightarrow A^{\bullet -} \quad (4.2)$$

$$A^{\bullet -} + A^{\bullet +} \rightarrow {}^1A^* + A \quad (4.3)$$

$${}^1A^* \rightarrow A + h\nu \quad (4.4)$$

The ECL spectrum of a compound usually is the same as the fluorescence spectrum, because both methods form the same excited state. In ECL the excited state is formed due to electron transfer, while in photoluminescence (PL), the excited state is formed by light absorption. However, the ECL and fluorescence spectra of some PAHs like pyrene show another extra broad and structureless peak at longer wavelengths, which is attributed to the formation of excimer.[4,2d] Equations 5 -7 in Scheme 4.2 show the excimer formation mechanism.

Scheme 4.2

$$A^{\bullet -} + A^{\bullet +} \rightarrow {}^1A_2^* \text{ (excimer formation)} \quad (4.5)$$

$$A^* + A \rightarrow {}^1A_2^* \text{ (excimer formation)} \quad (4.6)$$

$${}^1A_2^* \rightarrow 2A + \boldsymbol{h\nu_2} \text{ (excimer emission)} \quad (4.7)$$

Long wavelength emission can also be caused by formation of a byproduct during the electrolysis, e.g. by decay of the radical cation, as seen with anthracene.[1e]

Fluorene based molecules, like oligofluorenes[2a] and terfluorenes[5] are of interest in ECL and organic light emitting devices (OLED) due to their good electrochemical, thermal stabilities and high quantum yields. The present work shows that insertion of a

DPA derivative (**FDF**), a pyrene (**FPF**), and an anthracene between two fluorene derivatives (**FAF**) (Figure 4.1) produces very interesting ECL behavior and enhanced ECL efficiency and stability compared to the parent PAHs.

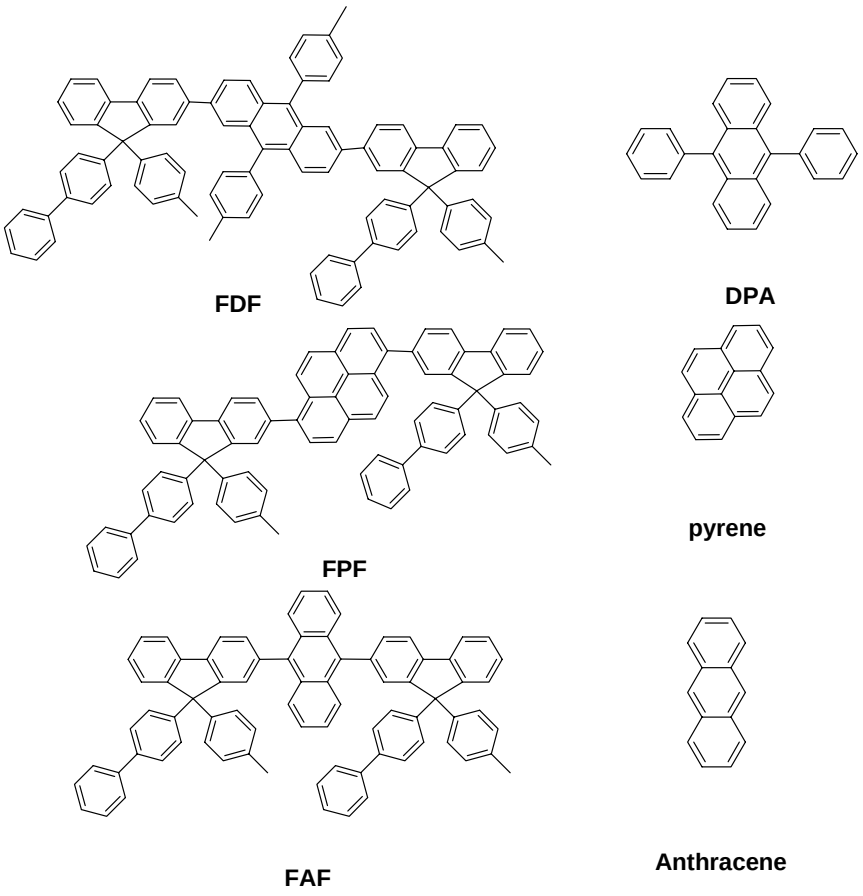

Figure 4.1 Chemical structures of the new series compounds and model compounds

4.2 Synthesis

Scheme 4.3 depicts the synthetic route of compound **1**, which was synthesized by aryl Grignard addition onto the corresponding 2, 6-dibromoanthraquinone,[6] followed by oxidation reaction with potassium iodide (2 steps, 50% yield).

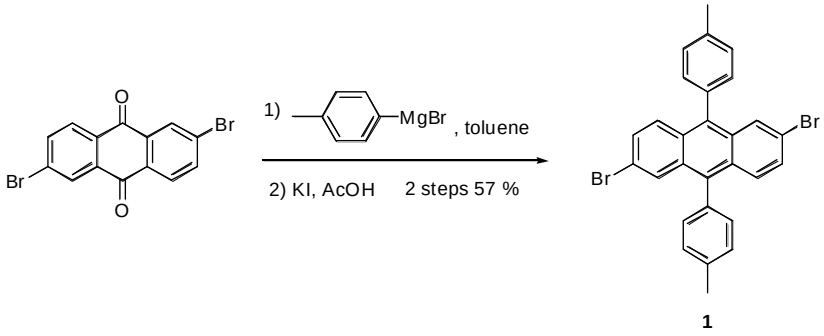

Scheme 4.3. The synthetic route of compound **1**.

Scheme 4.4 shows the synthetic route syntheses of **FDF**, **FPF**, and **FAF**.

Pd-catalyzed Suzuki coupling reactions of boronic esters **2** and dibromo-aromatic rings (1,6-dibromo pyrene, 9,10-dibromoanthracene and compound **1**) were accomplished by adding a catalytic amount of bulky tri-*tert*-butylposphine as a promoter to afford the target **FDF**, **FPF**, and **FAF** in modest yields (60-75%).

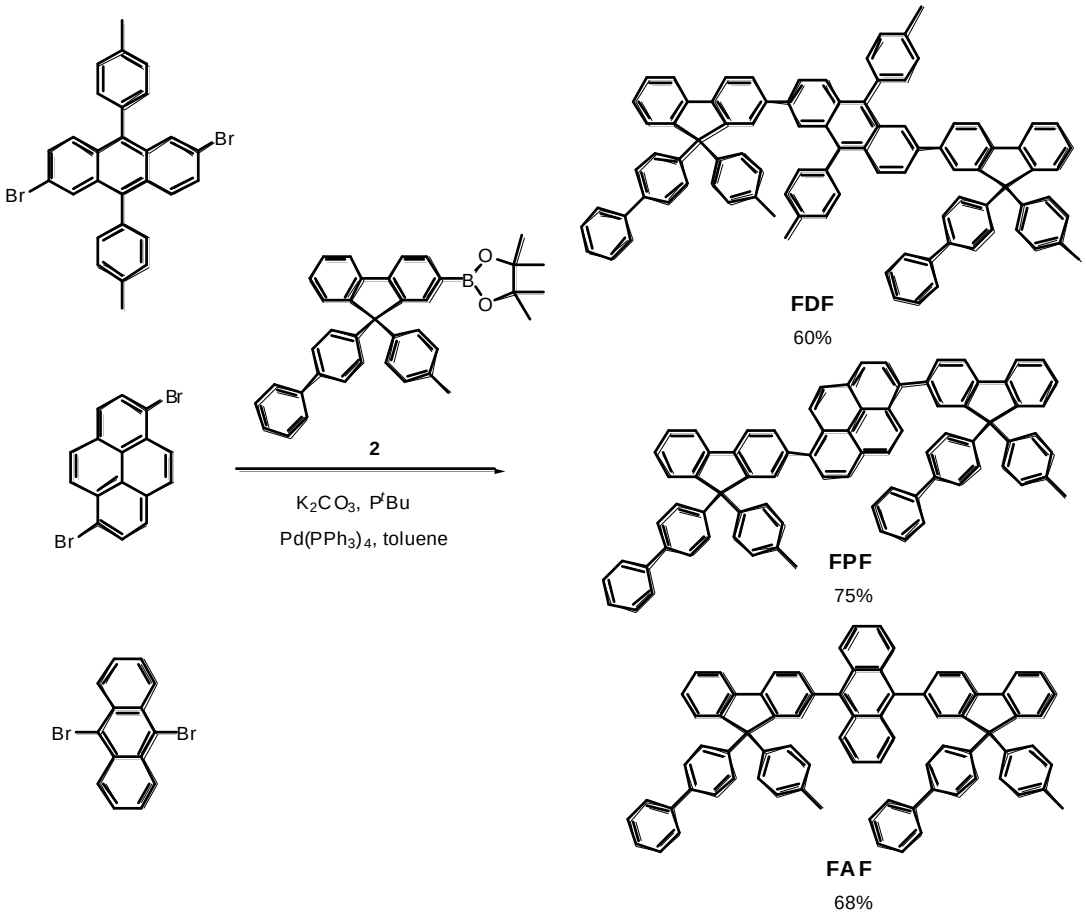

Scheme 4.4. Suzuki coupling reaction for synthesis **FDF**, **FPF**, and **FAF**

(***Synthesis of compound* 1**): Arylmagnesium bromide was first prepared in advance from 4-bromotoluene (3.93 mL, 32 mmol), and magnesium (768 mg, 32 mmol) in dry ether. Then arylmagnesium bromide was added into the flask containing 2,6-dibromo-anthraquinone (1.9 g, 8 mmol) in toluene (80 mL) under reflux. The mixture was refluxed for 8 h, and then quenched with water. It was extracted with EtOAc and dried with $MgSO_4$. Then, the organic solution was concentrated by rotary evaporation. The crude mixture was dissolved in acetic acid (100 mL), and added KI (3.98 g, 24 mmol). After heating for 1 h, it was extracted with dichloromethane two times. Column chromatography of the crude mixture on silica gel ($CHCl_3$/ Hex = 1/ 4) gave **1** (2.34 g, 57% yield) as a yellow solid. IR (KBr) ν 2919, 1606, 1507, 1434, 1361, 1063, 950 cm^{-1}; ^1H NMR ($CDCl_3$, 400 MHz) δ 7.84 (d, *J* = 2.4 Hz, 2H), 7.56 (d, *J* = 10 Hz, 2H), 7.41 (d, *J* = 7.2 Hz, 4H), 7.37~7.34 (dd, *J* = 8.8, 1.6 Hz, 2H), 7.30 (d, *J* = 8.0 Hz, 4H), 2.54 (s, 6H); ^{13}C NMR ($CDCl_3$, 100 MHz) δ 137.5, 136.6, 134.4, 130.8, 129.2, 128.8, 128.7, 128.6, 119.9, 21.5; MS (m/z, FAB^+) 307 (90), 154(100); Anal. Calcd for $C_{28}H_{20}Br_2$ C, 65.14, H, 3.90, found C, 64.96, H, 64.73.

(***Synthesis of* FDF**): The mixture of compound **1** (519 mg, 1.0 mmol), 2-(9-biphenyl-9-tolyl-fluorene) pinacol boronate (1175 mg, 2.0 mmol), K_2CO_3 (1.4 mL, 2.1 mmol), tri-*tert*-butylphosphine (2.0 mL, 0.1 mmol), and $Pd(PPh_3)_4$ (115 mg, 0.1 mmol) was dissolved in toluene (10 mL). The mixture was refluxed for three days. The crude product was extracted with CH_2Cl_2 and the organic layer was washed with water, dried over $MgSO_4$ and the solvent evaporated. Column chromatography of the crude mixture

on silica gel ($CHCl_3$/ toluene/ Hex = 1/ 3/ 4) gave **FDF** (702 mg, 60% yield) as a green solid. IR (KBr) ν 3032, 1619, 1520, 1487, 1440, 1374, 996 cm^{-1}; ^1H NMR ($CDCl_3$, 400 MHz) δ 7.95 (s, 2H), 7.80~7.77 (m, 6H), 7.68 (s, 2H), 7.59 (d, *J* = 8.4 Hz, 4H), 7.55 (d, *J* = 7.2 Hz, 2H), 7.48~7.37 (m, 22H), 7.34~7.26 (m, 8H), 7.16 (d, *J* = 8.0 Hz, 4H), 7.05 (d, *J* = 7.6 Hz, 4H), 2.50 (s, 6H), 2.33 (s, 6H); ^{13}C NMR ($CDCl_3$, 100 MHz) δ151.6, 151.2, 144.9, 142.5, 141.8, 140.5, 139.6, 139.2, 139.1, 137.1, 136.8, 136.0, 135.4, 131.0, 130.0, 129.4, 128.9, 128.8, 128.5, 128.3, 127.8, 127.5, 127.3, 126.9, 126.8, 126.7, 126.0, 124.9, 124.4, 120.3, 120.1, 64.9, 21.5, 21.1; MS (m/z, FAB^+) 1171.6 (15), 307.1 (100); HRMS Cacld for $C_{92}H_{66}$ 1170.5165, found 1170.5128.

(***Synthesis of* FPF**): The mixture of 3,8-dibromo-pyrene (362 mg, 1.0 mmol), 2-(9-biphenyl-9-tolyl-fluorene) pinacol boronate (1175 mg, 2.0 mmol), K_2CO_3 (1.4 mL, 2.1 mmol), tri-*tert*-butylphosphine (2.0 mL, 0.1 mmol), and $Pd(PPh_3)_4$ (115 mg, 0.1 mmol) was dissolved in toluene (10 mL). The mixture was refluxed for three days. The crude product was extracted with CH_2Cl_2 and the organic layer was washed with water, dried over $MgSO_4$ and the solvent evaporated. Column chromatography of the crude mixture on silica gel ($CHCl_3$/ toluene/ Hex = 1/ 4/ 10) gave **FPF** (762 mg, 75% yield) as a white solid. IR (KBr) ν 3025, 1905, 1606, 1493, 1454, 1182, 1016, 837, 738 cm^{-1}; ^1H NMR ($CDCl_3$, 400 MHz) δ 8.18~8.13 (m, 4H), 8.00~7.93 (m, 6H), 7.88 (d, *J* = 7.6 Hz, 2H), 7.76 (s, 2H), 7.69 (dd, *J* = 7.6, 1.2 Hz, 2H), 7.55 (d, *J* = 7.2 Hz, 4H), 7.52~7.45 (m, 8H), 7.44~7.31 (m, 16H), 7.23 (s, 2H), 7.09 (d, *J* = 8.0 Hz, 4H), 2.32 (s, 6H); ^{13}C NMR

($CDCl_3$, 100 MHz) δ 151.4, 151.3, 144.9, 142.6, 140.5, 140.4, 139.7, 139.3, 139.1, 137.6, 136.2, 130.2, 129.9, 128.9, 128.6, 128.5, 128.4, 128.0, 127.7, 127.4, 127.0, 126.8, 126.1, 125.1, 124.3, 120.2, 120.0, 65.1, 21.1; MS (m/z, FAB^+) 1015.5 (100), 1014.5 (90); HRMS Cacld for $C_{80}H_{56}$ 1014.4832, found 1014.4224; Anal. Calcd for $C_{80}H_{56}$ C, 94.45, H 5.55, found C, 94.67, H, 4.60.

(***Synthesis of* FAF**): The mixture of 9,10-dibromoanthracene (336 mg, 1.0 mmol), 2-(9-biphenyl-9-tolyl-fluorene) pinacol boronate (1175 mg, 2.0 mmol), K_2CO_3 (1.4 mL, 2.1 mmol), tri-*tert*-butylphosphine (2.0 mL, 0.1 mmol), and $Pd(PPh_3)_4$ (115 mg, 0.1 mmol) was dissolved in toluene (10 mL). The mixture was refluxed for three days. The crude product was extracted with CH_2Cl_2 and the organic layer was washed with water, dried over $MgSO_4$ and the solvent evaporated. Column chromatography of the crude mixture on silica gel （$CHCl_3$/ toluene/ Hex = 1/ 4/ 8 ） gave **FAF** (673 mg, 68% yield) as a white solid. IR (KBr) ν3071, 3025, 2926, 1911, 1805, 1606, 1547, 1374, 1016, 910 cm^{-1}; ^1H NMR ($CDCl_3$, 400 MHz) δ 8.01~7.98 (dd, *J* = 8.0, 4.4 Hz, 2H), 7.89 (d, *J* = 7.6 Hz, 2H), 7.76~7.72 (m, 4H), 7.60 (d, *J* = 0.8 Hz, 1H), 7.54~ 7.46 (m, 8H), 7.44~7.26 (m, 22H), 7.24~7.17 (m, 5H), 7.05~7.00 (m, 4H), 2.29~2.27 (m, 6H); ^{13}C NMR ($CDCl_3$, 100 MHz) δ151.9, 151.7, 151.6, 145.1, 142.7, 140.9, 140.1, 139.7, 139.5, 138.3, 137.4, 136.4, 131.0, 130.9, 130.0, 129.9, 129.8, 129.1, 128.8, 128.7, 128.2, 128.0, 127.8, 127.2, 127.1, 127.0, 126.5, 125.2, 120.5, 120.2, 65.1, 65.0, 21.0; MS (m/z, FAB^+) 990.6 (100); HRMS

Cacld for $C_{78}H_{54}$ 990.4226, found 990.4213; Anal. Calcd for $C_{78}H_{54}$ C, 94.51, H, 5.49, found C, 94.17, H, 5.21.

4.3 RESULTS AND DISCUSSION

4.3.1 Electrochemistry

Cyclic voltammograms for the three new compounds and their parents are shown in Figure 4.2 and electrochemistry data are tabulated in Table 4.1. **FDF** (which is composed of DPA derivative between two fluorene moieties) oxidizes electrochemically and gives its first reversible oxidation wave $E^{o}_{1,ox}$ = 1.05 V vs SCE (for DPA, $E^{o}_{1,ox}$ = 1.15 V)[7] and the second reversible oxidation peak $E^{o}_{2,ox}$ = 1.48 V (compared to DPA with an irreversible wave $E^{o}_{2,ox}$ = 1.58 V). The formal potential of the first oxidation peak of **FDF** is less positive by 100 mV than DPA, and the second oxidation peak is also less positive by 100 mV, indicating cation radical and dication are more stable in **FDF** than DPA, and this is the effect of the fluorene moiety with an increase of conjugation. The second oxidation wave of DPA is irreversible even at higher scan rates. However, in **FDF** the second oxidation wave, which is associated with the DPA moiety, is almost reversible even at 100 mV/s as shown in Figure 4.2a. This is due to the enhanced conjugation and delocalization of the charge through the fluorene moieties which stabilizes the cation radical and steric hindrance that blocks DPA positions subject to nucleophilic attack. Thus the fluorene moiety leads to tuning of the electrochemical reversibility of the electron transfer reaction. The observed peak separation for the reversible waves was ~80 mV, larger than that expected peak splitting for ideal nernstian

behavior where a one-electron wave is expected to have a peak separation of ~ 59 mV. However, the internal standard material, ferrocene, which is known to show nernstian behavior showed a similar peak separation under these same electrolyte conditions; thus, the observed peak separation can be attributed to ohmic drop (~1200 ohm) that is often observed within aprotic solvents. Scan rate studies showed that the anodic and cathodic peak currents (i_{pa}, i_{pc}) of the first oxidation wave were proportional to the square root of scan rate ($\nu^{1/2}$) while the corresponding peak potentials (E_{pa}, E_{pc}) were independent of ν. Additionally, the peak current ratio (i_{pa}/i_{pc}) was approximately unity down to a scan rate of 100 mV/s, indicating the absence of a following chemical reaction.

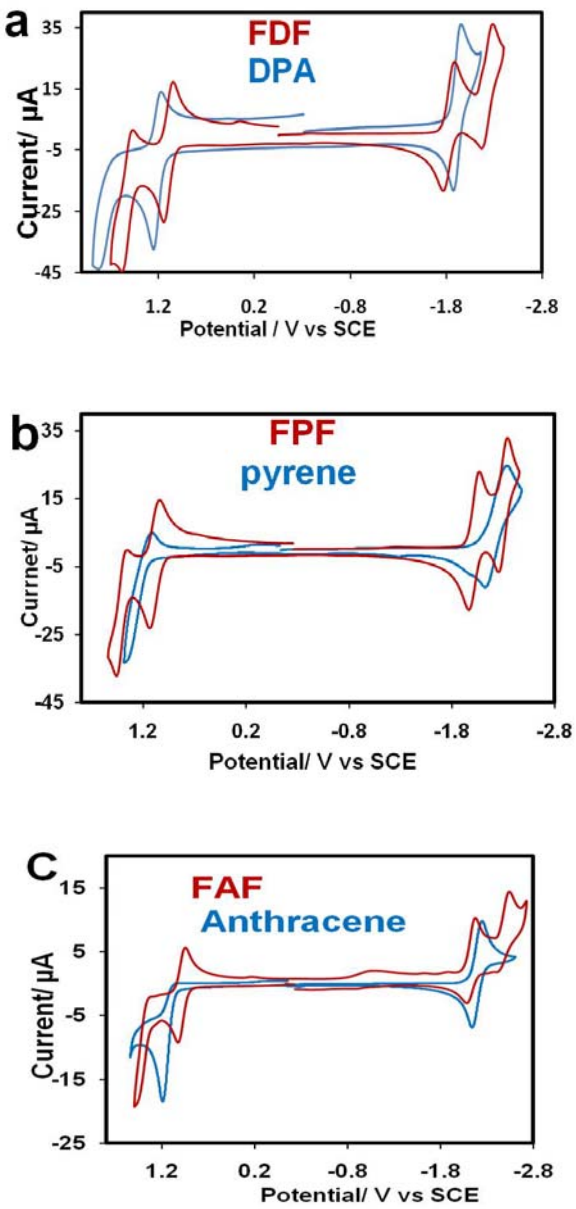

Figure 4.2 Cyclic voltammograms of (a) **FDF** and DPA, (b) **FPF** and pyrene and (c) **FAF** and anthracene. Conditions were 1 mM of compounds, 0.1 M Bu_4NPF_6 as a supporting electrolyte in 1:1 (Bz: MeCN) solvent, scan rate 100 mV/s, working electrode: Pt disk (~1 mm diameter), counter electrode: Pt wire, reference electrode: Ag wire (calibrated verse Fc/Fc^+).

The reduction of **FDF** shows two reversible peaks each reduction peak height was the same as those for the oxidation, indicating a one electron transfer process in each peak. The position of the reduction waves were at $E^{o}_{1,red}$= –1.78 V vs SCE, $E^{o}_{2,red}$ = –2.27 V vs SCE, while (for DPA, $E^{o}_{1,red}$ = –2.06 V vs SCE); the second reduction wave for DPA could not be observed within the window of the solvent used in this experiment. The larger effect of the fluorene moiety on reduction compared to the oxidation indicates that the fluorene moiety behaves more as an electron withdrawing group and decreases the electron density on the DPA moiety. As with the oxidation, the reduction peak separation potential for each wave was ~80 mV, as for ferrocene, assigning each reduction peak is one electron transfer process.

FPF (pyrene between fluorene moieties) also shows two oxidation waves $E^{o}_{1,ox}$ = 1.10, $E^{o}_{2,ox}$ = 1.43 V vs SCE. The first one is reversible at all scan rates from 50 mV to 10 V/s, while the second oxidation peak starts to show reversibility after 250 mV/s (Figure 4.2b). Again **FPF** electrochemically oxidizes more easily than the parent compound (pyrene) by a difference of 60 mV (for pyrene $E^{o}_{1,ox}$= 1.16 V vs SCE).

The reduction of **FPF** shows two sequential reduction peaks ($E^{o}_{1,red}$ = –2.00 V, $E^{o}_{2,red}$ = –2.30 V vs SCE) with both peaks reversible even at low scan rates (Figure 4.2b). Again, the fluorene moiety stabilizes the cation radicals and anion radicals through main backbone conjugation. The **FPF** also reduced more easily by 60 mV. The effect of the

two bulky fluorene moiety on the redox potentials of pyrene is less compared to DPA, perhaps because the two fluorene moieties show better conjugation with DPA than with pyrene, which means in the case of **FDF**, the electronic interaction between fluorene and DPA is stronger than in the case of **FPF** of pyrene with two fluorene moieties (this co-planarity is also seen in the spectroscopy as discussed in the next section).

FAF (9, 10-difluorene-anthrance) shows two oxidation peaks (Figure 4.2c). The first is reversible $E^{o}_{1,ox}$ =1.13 V, but the second is irreversible $E^{o}_{2,ox}$= 1.57 V vs SCE (up to 2000 mV/s). For the first oxidation peak, **FAF** is easier to oxidize than the parent anthracene by 130 mV (anthracene, E_P= 1.24 V vs SCE).[8] The oxidation peak of anthracene is totally irreversible. Aikens et al. suggested that the irreversibility of anthracene can be attributed to the reaction of meso positions by nucleophilic attack by solvent and decomposition of the cation radicals.[9] While for **FAF**, due to the electronic interaction through the backbone and protection of the meso position by the fluorene moieties, the cation radical is stabilized even at low scan rates. The second wave shows a lower reversibility. Additionally, of the structure of **FAF** can be compared to DPA, in that both are substituted in the 9 and 10 positions and explains the similarities of the cyclic voltammetry of **FAF** and DPA (with similar potentials of the oxidation peaks and irreversibility of the second oxidation wave).

The reduction of **FAF** shows two sequential peaks ($E^{o}_{1,red}$ = –1.92 V, $E^{o}_{2,red}$ = –2.29 V vs SCE) comparing with anthracene ($E^{o}_{1,red}$ = –2.09 V vs SCE; no second reduction seen). However if the comparison is made with DPA, the second reduction wave of DPA couldn't be observed within the window of the solvent while second

reduction wave of **FAF** is observed. Again, this results from the fluorene substitution which decreases electron density on the anthracene. The observed peak separation for the reversible waves was again ~80 mV. Scan rate studies showed that the anodic and cathodic peak currents of the first oxidation waves for all the compounds and second oxidation waves for **FDF** and **FPF**, and first reduction waves for all the compounds and second reduction waves for **FDF** and **FPF** were proportional to $\nu^{1/2}$ and, the peak current ratio was approximately unity down to a scan rate of 50 mV/s, indicating the absence of a following chemical reaction. This suggests that the first and second oxidation to the stable radical cation and dication is nearly nernstian. This is not the case in the second oxidation of **FAF,** which is chemically irreversible up to about 10 V/s, probably because the dication reacts with traces of water or acetonitrile. The same is true for its second reduction peak, which is basic enough to take proton from water.[10]

In summary, the electrochemical reversibility is enhanced dramatically by insertion of the polyaromatic hydrocarbons (PAHs) between two fluorene moieties (oligofluorenes). This also influences the ECL properties by increasing the stability of the radical anion and cation and consequently, increasing the lifetime of the oppositely charged radicals which annihilate to form the excited states.

Table 4.1 Electrochemical results. All potentials are versus SCE.

	Oxidation Potential		Reduction Potential			HOMO*	LUMO	Eg
	$E^{o}_{1,ox}$	$E^{o}_{1,ox}$	$E^{o}_{1,red}$	$E^{o}_{2,red}$	**D**(cm^2/s)	eV	eV	eV
FDF	1.05	1.48	–1.87	–2.27	9×10^{-6}	–5.50	–2.58	2.92
DPA	1.15	1.58(E_p)	–2.06	-				
FPF	1.10	1.43	–2.00	–2.30	9×10^{-6}	–5.56	–2.46	3.10
Pyrene	1.16	-	–2.19	-				
FAF	1.13	1.57	–1.92	–2.29	9.5×10^{-6}	–5.59	–2.54	3.05
Anthracene	1.24(*Ep*)	-	–2.09	-				

* HOMO= $-E^{ox}_{vs\ Fc/Fc+} - 4.8$ eV. LUMO = $-E^{red}_{vs\ Fc/Fc+} - 4.8$ eV, Eg = $E^{ox} + E^{red}$

4.3.2 Spectroscopy

Absorption and emission spectra are shown in Figure 4.3 and photophysical data are tabulated in Table 4.2. All of the compounds show a shift to lower energy comparing to their parent compounds because of the increased number of chromophores and increased conjugation by the fluorene moieties. **FDF** shows absorption and emission spectra with a 50 nm red shift compared to DPA, consistent with the effect of the substituted fluorenes. **FPF** exhibits structureless absorption and emission peaks. The emission peak at 431 nm is red shifted by 31 nm compared to pyrene, again due to the conjugation. For **FPF**, unlike pyrene, there is not any evidence for excimer formation, which agrees well with the ECL results discussed in the next section. This is because steric hindrance of the bulky structure of **FPF** prevents formation of an excited state dimer. **FAF** shows a structured absorption spectrum, while the emission is devoid of structure, probably because of rearrangement of the excited state of the molecule before emission.

The entire new oligofluorene compounds generally show small Stoke's shifts, that can be attributed to a rigid structure resulting in a small reorganization energy in the excited state as well as a low polarity of producing as small interaction with solvent.[11] The compounds have high quantum yields over a range of 0.62 for **FAF** to 0.90 for **FDF.**

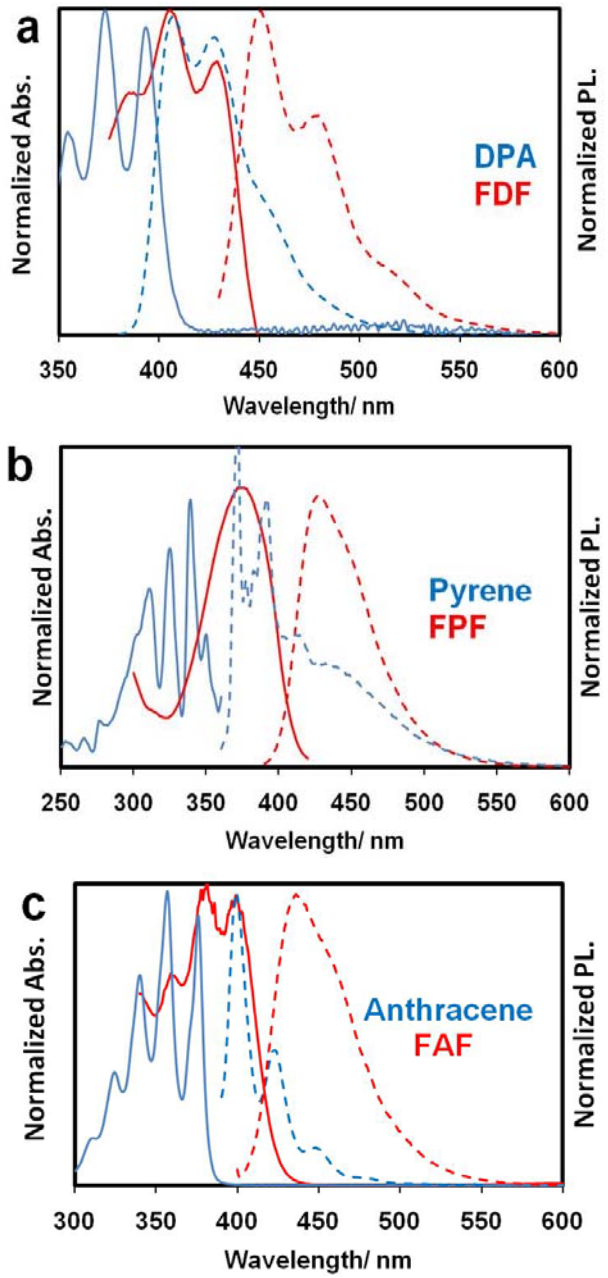

Figure 4.3 Normalized absorption (solid line) and emission spectra (dotted line, excited at absorption maxima) of (a) **FDF** and DPA, (b) **FPF** and pyrene, (c) **FAF** and anthracene, , and in 1:1 MeCN:Bz.

Table 4.2. Photophysical properties of the compounds comparing with their parents.

	$\lambda_{max, Abs}$ (nm)	$\lambda_{max, PL}$(nm)	Φ_{PL}	Stokes shift
FDF	385, 407, 430	452, 485, 516(*sh*)	0.90	22
DPA	355 ,373,393	408, 429, 450(*sh*)		15
FPF	373	430	0.81	57
Pyrene	311, 324, 340	392, 413, 440, 470(*ex*)		52
FAF	341, 360, 380, 400	437	0.62	37
Anthracene	310, 327,340, 357, 376	400, 423, 450, 482		24

Solvent is (1:1) MeCN:Bz for all the compounds.
sh: shoulder, *ex*: excimer

4.3.3 Electrogenerated Chemiluminescence

All the oligofluorene compounds produce bright ECL by direct annihilation in nonaqueous solvents. ECL spectra of the three new highly efficient ECL emitters compared with their parent compounds are shown in Figure 4.4 and the results are tabulated in table 4.3. Red shifts in the spectra of 10 to 15 nm were observed for ECL compared to PL. This shift is attributed to the inner filter effect due to difference in concentrations used for PL and ECL.

ECL spectra of **FDF** compared to DPA are shown in Figure 4.4a. **FDF** gives a maximum ECL emission peak at λ^{ECL} = 485 nm, which is red shifted from DPA by almost 50 nm due to the high conjugation through the DPA and fluorene backbones. Transient ECL of **FDF** (Figure 4.4) shows that with each pulse (pulsing from $\boldsymbol{E_{p1,ox}}$ **+ 80 mV** to $\boldsymbol{E_{p1,red}}$ **− 80 mV**); a constant and equal ECL intensity peak is produced, demonstrating stability of the anion and cation radicals in the multi-potential step experiment.[12] The emission spectra of either PL or ECL for FDF is structured in a similar manner as DPA and they have similar fluorescence quantum yields (Φ^{PL}_{FDF} = 0.90, Φ^{PL}_{DPA}= 0.91, $\Phi^{ECL}_{FDF} \sim \Phi^{ECL}_{DPA}$).

The ECL light observed for **FDF**, was almost as intense as that of DPA under the same conditions. The question of long term stability upon cycling has always been of interest in ECL because of possible device applications.[13] With many ECL couples, although the ion radicals are apparently stable on the CV time scale, the ECL tends to decrease with extended pulsing. However, ECL emission with **FDF** should be more

stable than DPA, because the second oxidation wave of DPA is not stable even at 1 V/s while the second oxidation peak of **FDF** is stable even at 100 mV/s. If one measures the ECL by pulsing the potential between the first oxidation and reduction waves in a three electrode cell, the ECL was stable for at least 20,000 pulses (0.1 s/pulse), (Figure 4.4d).

FPF also shows bright blue ECL (λ^{ECL} = 445 nm). The ECL of pyrene shows only excimer emission in the spectrum from ion radical annihilation, consistent with the dimer-like nature of the intermediate. With **FPF** there is no indication of excimer formation (Figure 4.4b), although the large shift in its emission compared to pyrene monomer places the ECL **FPF** emission just slightly blue-shifted from the eximeric emission of pyrene. As with photoluminescence, the steric hindrance in **FPF** prevents orbital pi-stacking for excimer formation even during the electron transfer reaction. Thus while pyrene and **FPF** spectra occur near one another (Figure 4.4b), the ECL of pyrene is from excimer emission while ECL of **FPF** is from monomer emission. Because, **FPF** fluoresces at 430 nm and gives ECL near 445 nm, pyrene; gives PL excimer at 470 nm[14] and ECL of pyrene gives a maximum at the same position, assigned to excimer formation.[4]

Anthracene shows poor ECL via the direct annihilation reaction in aprotic solvents characterized by long wavelength emission from side products, because of the irreversibility of the anthracene oxidation wave and instability of the cation radical (Figure 4.2c).[15] The cation has a very short life-time even with a pulse width of 0.05 s, and its anodic production requires rigorous purification of DMF for the ECL of

anthracene to be observed. **FAF**, which is blocked in the 9 and 10 anthracene positions, as in DPA, however, gives very strong and stable ECL, with good electrochemical reversibility of the oxidation wave. Bright blue and relatively stable ECL (450 nm) was observed.

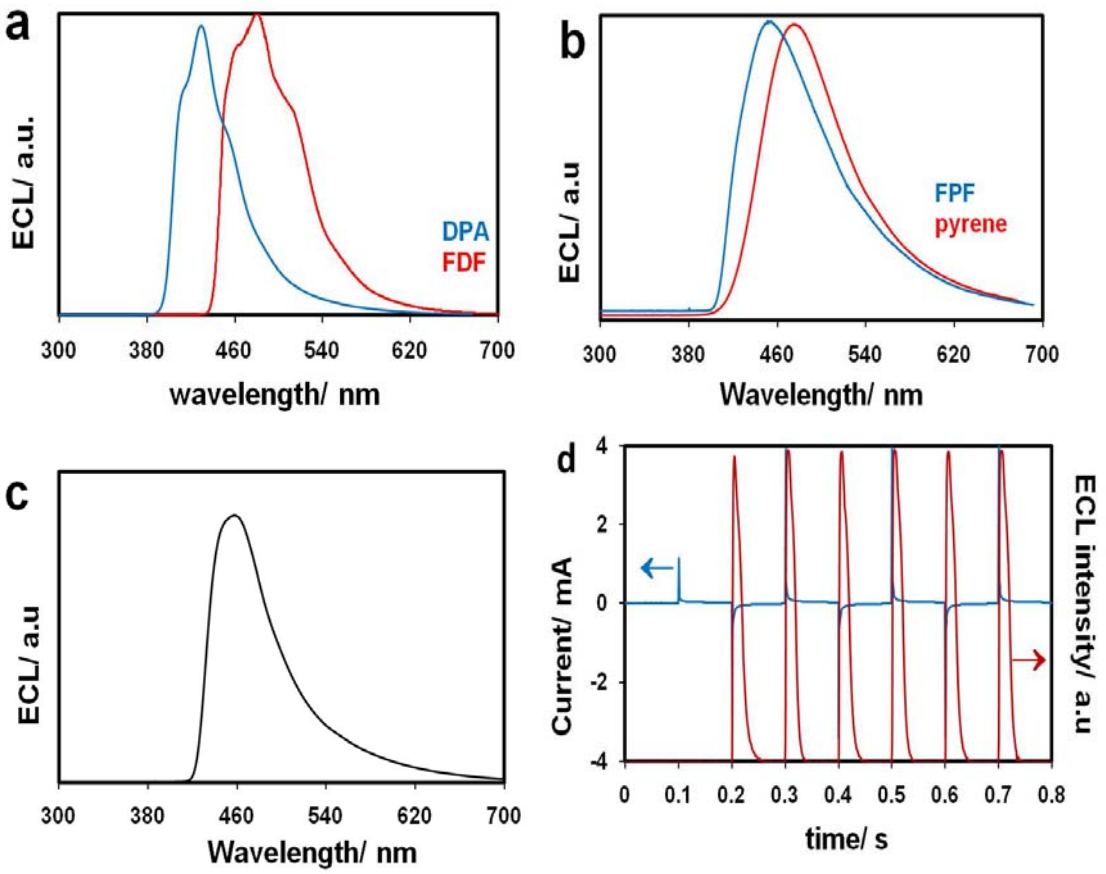

Figure 4.4. Normalized ECL spectra of (a) DPA and **FDF** (b) pyrene and **FPF,** (c) **FAF** taken in the same solution used for electrochemistry experiments shown in Figure 4.1. Pulsing is from $E_p{}^1{}_{ox}$ +80 mV to $E_p{}^1{}_{red}$ −80 mV with integration time of 10s for each sample and a slit width of 0.5 mm. (d) Transient ECL experiment, electrochemical current (blue line), ECL intensity (dark red line) for **FDF**. Pulse width: 0.1 s, sampling time: 1 ms, pulsing pattern: zero volts to negative ($E_p{}^1{}_{red}$−80 mV) to anodic ($E_p{}^1{}_{ox}$ +80 mV).

Table 4.3. photophysical and ECL paremeters

	$\lambda_{max,\ PL}$(nm)	$\lambda_{max,\ ECL}$(nm)	E_s [a]	$\Delta H^o{}_{an}$ [b]	Φ_{PL}	$\Phi_{r,\ ECL}$ [c]
FDF	451, 482, 516(*sh*)	460, 485, 513(sh)	2.81	2.82	0.90	0.90
FPF	430	445	3.05	3.00	0.81	0.85
FAF	437	450	2.92	2.95	0.62	0.65

[a] E_s calculated based on ½($E_{abs} + E_{emission}$). [b] $\Delta H^o_{an} = E^o_{1,ox} - E^o_{1,red} - 0.1V$. [c] $\Phi_{r,ECL}$ is the relative ECL compared to DPA, assuming Φ_{ECL}DPA = 1.

By comparing of enthalpy of annihilation reaction ($\Delta H_{an} = E^{o}_{ox} - E^{o}_{red} - 0.1$) eV to the energy required for excited state formation E_s as shown in Table 4.3, ECL for all three compounds follows the S-route, i.e. availability of enough energy in the electron transfer reaction to populate to the singlet excited state directly.[1]

4.4 CONCLUSIONS

Three novel highly fluorescent and ECL emitters were synthesized and characterized. Electrochemistry data demonstrated that these novel compounds form stable anion and cation radicals which are the basic requirements for ECL. ECL experiments show that they are potential candidates for ECL applications. **FDF** shows very bright and stable ECL that may consider as one of "Super ECL" emitters. Due to stable electrochemistry and high PL quantum yields these new blue emitters could be good materials for organic light emitting devices (OLEDs).

4.5 REFERENCES

[1] a) Bard, A. J Ed., Electrogenerated Chemiluminescence; Marcel Dekker: New York, **2004**; b) Hercules, D.M. Science **1964,** *145* **,**808-809; c) Visco,R. E. Chandross, E. A. *J. Am. Chem. Soc*. **1964,** *86,* 5350-5351; d) Santhanam, K. S. V.; Bard, A. J. *J. Am.Chem. Soc*. **1965**, *87*, 139-140; e) Faulkner, L. R.; Bard, A. J. *J. Am. Chem. Soc*. **1968,** *90***,** 6284-6290**.**

[2] a) Sartin, M. M.; Shu, C.; Bard, A. J. *J. Am. Chem. Soc*. **2008**, *130*, 5354-5360; b) Sartin, M. M.; Zhang, H.; Zhang, J.; Zhang,P.; Tian, W.; Wang,Y.; Bard, A. J. *J. Phys. Chem. C* **2007**, *111*, 16345-16350; c) Omer, K. M.; Kanibolotosky, A. L.; Skabara, P. J.; Perepichka, I . F.; Bard, A. J. *J. Phys. Chem B* **2007**, *111*, 6612-6619; d) Lai, R. Y.; Fleming, J. J.; Merner, M. L.; Vermeij, R. J.; Bodwell, G. J.; Bard, A. J. *J. Phys. Chem A* **2004**, *108*, 376-383; e) Becker, W. G.; Seung, H. S.; Bard, A. J. *J. Electroanal. Chem.***1984**, *167,* 127-140; f) Beideman, F. E.; Hercules, D. M. *J. Phys. Chem*. **1979**, *83*, 2203-2209; g) SantaCruz, T. D.; Akins, D. L.; Birke, R. L. *J. Am. Chem Soc*. **1976**, *98*, 1677-1682; h) Faulkner, L. R.; Tachikawa, H.; Bard, A. J. *J. Am. Chem. Soc*. **1972**, *94*, 691-699; h) Fleet,B.; Kirkbright, G. F.; Pickford, D.J. *J. Electroanal. Chem*. **1971**, *30*, 115-121.

[3] Byker, H. J. United States Patent 4,902,108 (February 20, 1990).

[4] a) Chandross, E. A.; Longworth, J. W.; Visco, R. E. *J. Am. Chem. Soc*. **1965**, *87*, 3259-3260; b) Hercules, D. M.; Chang, J.; Werner, T. C. *J. Am. Chem. Soc*. **1970**, *92*, 5560-5565; c) Maloy, J. T.; Bard, A. J. *J. Am. Chem. Soc*. **1971,** *93*, 5968-5981. d) Kira, T.; Sukigara, M. ; Honda, K. *J. Electroanal. Chem*. **1973**, *47*, 161-166; e) Keszthelyi,C. P. ; Bard, A. J. *Chem. Phys. Letter*. **1974**, *24*, 300-304; f) Tachikawa, H.; Bard, A. J. *Chem. Phys. Lett*. **1974**, *26*, 568-573; g) Suminaga,T. ; Hayakawa, S. S. *Bull. Chem. Soc. Jpn.* **1980**, *53*, 315-318.

[5] **For OLED** a) Wong, K-T.; Chen, R-T.; Fang, F-C.; Wu,C-C.; Lin, Y-T. *Organic Lett*. **2005**, *7,* 1979-1982; b) Geng, Y.; Katsis, D.; Culligan, S. W.; Ou, J. J.; Chen, S. H. ; Rothberg, L. *J. Chem. Mater*. **2002**, *14*, 463-470; c) Wong, K-T.; Chien, Y-Y.; Chen, R-

T.; Wang, C-F. ; . Lin, Y-T.; Chiang, H-H. ; Hsieh, P-Y. ; Wu, C-C.; Chou, C. H.; Su,Y. O.; Lee, G-H.; Peng, S-M. *J. Am. Chem. Soc.* **2002**, *124*, 11576-11577.

for ECL d) Choi, J-P. ; Wong, K-T.; Chen, Y-M.; Yu, J-K.; Chou, P-T.; Bard, A. J. *J. Phys. Chem B.* **2003**, *107*, 14407-14413.

[6] Lee, S. K.; Yang, W. J.; Choi, J. J.; Kim, C. H.; Jeon, D-J.; Cho, B. R. *Org. Lett.* **2005**, *7*, 323-326.

[7] Sartin, M. M.; Shu, C.; Bard, A. J. *J. Am. Chem. Soc*. **2008**, *130*, 5354-5360.

[8] Mann, C. K.; Barnes, K. K. Electrochemical Reaction in Nonaqueous Systems, Marcel Dekker, New York, **1970**.

[9] (a) Coleman, A. E.; Richtol, H. H.; Aikens, D. A. *J. Electroanal.Chem*. **1968**, *18*, 165-174. (b) Werner, T. C.; Chang, J.; Hercules, D. M. J. *Am. Chem. Soc*. **1970**, *92*, 763-768.

[10] Andruzzi, R. ; Trazza, A.; Greci,L.; Marchetti, L. L. *J. Electroanal Chem*. **1980**, *108*, 49-58.

[11] Reichardt,C. *Solvents and Solvent Effects in Organic Chemistry*. John Wiley and Sons: **2003.**

[12] Cruser, S. A.; Bard, A. J. *J. Am. Chem. Soc.* **1969**, *91*, 267-275.

[13] Laser, D.; Bard, A. J. *J. Electrochem. Soc*. **1975**, *122*, 632-640.

[14] Birks, J. B. Christopherou, L. G. *Spectrochim. Acta* **1963**, *19*, 401-410.

[15] a) Faulkner, L. R.; Bard, A. J. *J. Am. Chem. Soc.* **1968,** 90, 6284-6290; b) Faulkner, L. R.; Bard, A. J. *J. Am. Chem. Soc*. **1969**, *91*, 209-210.

Chapter 5: Electrochemistry, Spectroscopy and Electrogenerated Chemiluminescence of some Star-shaped Truxene–Oligofluorene Compounds

5.1 INTRODUCTION

Electrogenerated chemiluminescence (ECL) is a unique type of electron transfer that generates excited states by the reaction of radical ions (or other highly oxidized or reduced species). It has been extensively investigated and has found several applications.[1] Fluorene-based materials are often highly fluorescent species and are promising candidates for various optoelectronic applications. Over the last decade, polyfluorenes have emerged as leading electroluminescent materials in polymeric light-emitting devices (PLED) for display technologies demonstrating bright blue emission coupled with high charge mobility, excellent thermal and electrochemical stability and tunable properties through chemical modifications and copolymerizations.[2], Other electronic and photonic applications of fluorene-based homopolymers and copolymers include, e.g. photovoltaics,[3,4] field-effect transistors (FET),[5] and solid-state lasers.[6] Homologous series of oligofluorenes, as monodisperse, well-defined π-conjugated systems[7] have been fruitful in providing a correlation between electronic, optical, morphological properties and chemical structure and molecular conformation, serving as models for polyfluorenes and providing deep insights into the photophysics of this promising class of conjugated polymers.[8,9] They were also successfully used as efficient emitters in organic light-

emitting devices (OLED).[9,10] Generally, the environmental stability of monodisperse oligofluorenes (towards photooxidation or as materials in devices) is higher than those of polyfluorenes.[11] With the polymer analogs, faster degradation and the appearance of undesirable green emission during the PLED operation occurs due to the formation of fluorenone defects on the polymer chains; this chemical instability serves to decrease the device performance by quenching emission.[12]

The basic reactions in these OLEDs/PLEDs are the same as that in ECL in solution where light emission is produced by an energetic electron transfer reaction (equivalent to electron-hole recombination) between electrochemically generated species at an electrode. Typically in ECL, radical ions of an organic compound (A) are generated sequentially at the surface of an electrode by cycling the potential within a short time interval, and react (annihilate) during their interdiffusion. The annihilation by ECL between cation and anion radicals produces an excited state (A^*) if the energy provided by the electron transfer reaction is sufficient to produce A^*. When A^* is the singlet state, equations (1–4), this is called the S-route or an "energy sufficient system".

$$A - e^- \rightarrow A^{+\bullet} \quad (5.1)$$

$$A + e^- \rightarrow A^{-\bullet} \quad (5.2)$$

$$A^{+\bullet} + A^{-\bullet} \rightarrow {}^1A^* + A \quad (5.3)$$

$${}^1A^* \rightarrow A + h\nu \quad (5.4)$$

If the energy provided by the ion radicals is not sufficient to populate the singlet state, the triplet state can be populated (eq. 5), followed by triplet-triplet annihilation to generate the singlet state (eq. 6). This is called the T-route or an "energy deficient system".

$$A^{+\bullet} + A^{-\bullet} \rightarrow {}^3A^* + A \quad (5.5)$$

$$^3A^* + {}^3A^* \rightarrow {}^1A^* + A \quad (5.6)$$

Another possibility, referred to as the E-route, results from the production of an excimer in the annihilation reaction (eq. 7).

$$A^{+\bullet} + A^{-\bullet} \rightarrow A_2^* \quad (5.7)$$

$$A_2^* \rightarrow 2A + h\nu \quad (5.8)$$

ECL can also be produced by oxidation alone by using a coreactant, a compound that can produce a strong reducing agent from a reaction that follows the electrochemical ET reaction. These reductants must be energetic enough to react with the cation radicals of the emitters to produce their excited states. Typical coreactants for oxidations are tri-*n*-propylamine (TPrA), which produces a strong reducing agent ($TPrA^{\cdot}$),[13,14] and oxalate ($C_2O_4^{2-}$), which produces a strong reductant, $CO_2^{-\bullet}$.[15-17] Alternatively a coreactant can be used in a reducing step by an analogous route. For example, peroxydisulfate ($S_2O_8^{2-}$)[18] and benzoyl peroxide (BPO)[19,20] produce strong oxidizing agents on reduction.

Star-shaped conjugated oligomers as intrinsically two-dimensional conjugates (compared to more widely study linear 1D conjugated system) have been of great interest in recent years. The 2D character of such architectures allows further deep insight into the electronic processes in these compounds, including aspects of electronic interactions between the arms, and opens the door for new materials for optoelectronics.[21] Various star-shaped conjugated oligomers with different cores and arms (oligofluorenes,[22,23] oligothiophenes,[24] oligo(phenylenevinylenes),[25] oligo(phenyleneethynylenes),[26] etc.)

have been synthesized and their applications in OLEDs,[22b-e] photovoltaics,[24f,g] FETs,[24b,e,f] and non-linear optics[25c,27] have been demonstrated.

In this chapter we describe the electrochemistry, spectroscopy and ECL of a series of star-shaped oligofluorene compounds (Scheme 5.1). We describe both the electrochemistry and the spectroscopy of oligomers **T1–T4** containing an hexahexyl-truxene core with three oligofluorene arms of different lengths, from one fluorene unit (**T1**) to four fluorene units (**T4**) in the arms.

Scheme 5.1 Truxene-oligofluorenes (T1-T4)

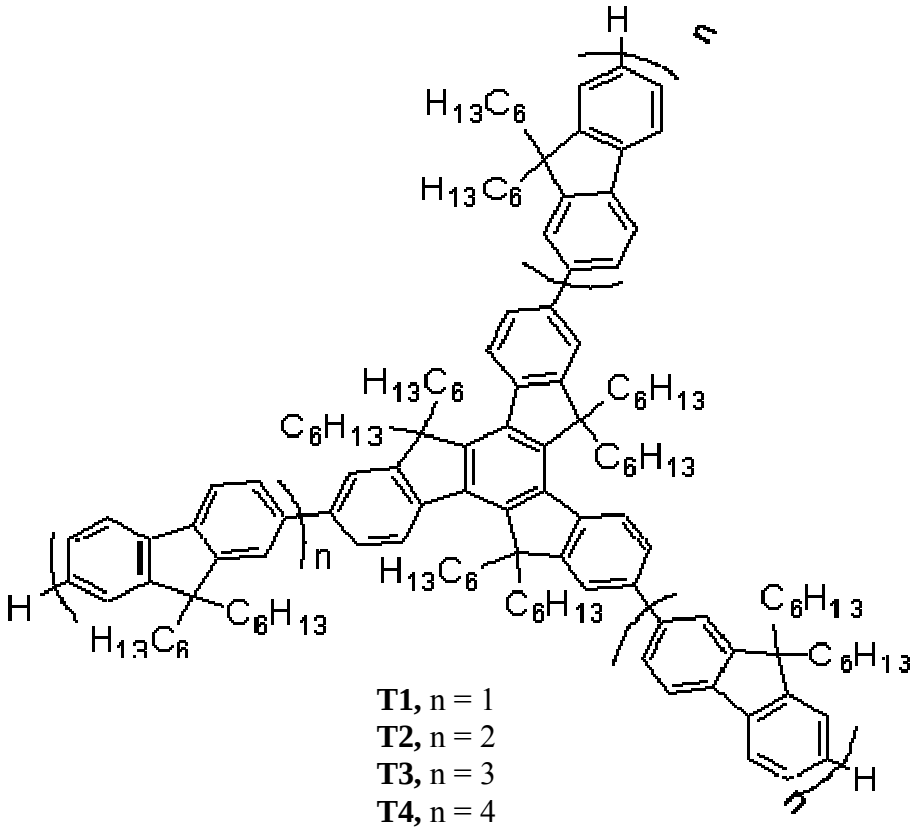

T1, n = 1
T2, n = 2
T3, n = 3
T4, n = 4

5.2 EXPERIMENTLA SECTION.

5.2.1 Chemicals.

The synthesis of **T1** to **T4** has been described previously.[23] Tetra-*n*-butylammonium oxalate (TBAOX) was prepared by mixing oxalic acid (EM Science) and tetra-*n*-butylammonium hydroxide in methanol (Fluka) in a mole ratio of 1:2 followed by evaporation and drying in a rotary evaporator. All solutions were prepared in the dry box in an airtight cell for measurements completed outside the dry box.

5.3 RESULTS AND DISCUSSION

5.3.1 Electrochemistry

All electrochemical measurements were carried out in 1:1 v/v of MeCN:Bz (except for **T4** where, because of poor solubility, 1:2 v/v MeCN:Bz was used instead) with 0.1 M $TBAPF_6$ as supporting electrolyte. Although cyclic voltammetry studies of **T1**–**T4** had been performed previously, oxidation in CH_2Cl_2 and reduction in THF,[23] these solvents are not appropriate for ECL because they have rather narrow potential windows. CVs of **T1** and **T2** in MeCN:Bz at a scan rate v = 0.5 V/s showed two anodic reversible waves and a single reversible cathodic wave before background oxidation of the solvent/supporting electrolyte (Figure 5.1), while **T3** showed two reversible anodic waves and two reversible cathodic waves. Oxidation of **T4** showed two reversible anodic waves followed by a split quasi-reversible second wave then an irreversible peak that partially overlapped with background, and two reversible cathodic waves followed by a smaller, less well-defined second wave. The observed peak splitting (ΔE_p) for the reversible waves were ~100 mV, larger than the expected nernstian one–electron wave ΔE_p of ~59 mV. However, the internal standard, ferrocene, which is known to show nernstian behavior, showed a similar ΔE_p under these same electrolyte conditions suggesting that uncompensated resistance (~2 kΩ), frequently observed with aprotic solvents, is the cause of the slightly larger ΔE_p-values. All peak potentials of oxidations (E_{pa}^{ox}) and reductions (E_{pc}^{red}) are summarized in Table 5.1. Scan rate studies showed that the anodic and reverse cathodic peak currents of the first oxidation waves (i_{pa}^{ox}, i_{pc}^{ox})

were proportional to $v^{1/2}$. Additionally the peak current ratio for the first oxidation waves of **T1** to **T4** (i_{pa}^{ox}/i_{pc}^{ox}) was approximately unity down to a scan rate 50 mV/s, indicating the absence of significant contributions from following chemical reactions.

Diffusion coefficients, *D*, were found by plotting the peak current vs. $v^{1/2}$ and are listed in Table 1, assuming each wave was a single electron transfer step. To confirm the $n = 1$ assumption, chronoamperometric measurements for **T1** were also carried out at an ultramicroelectrode (UME) (Figure 5.2).[28] With this technique, *D* can be determined without knowledge of *n* or concentration (*C*), and *n* can be determined from the steady state limiting current, if *C* is known. The *D*-value found from the current transient agreed with that from CV, which confirmed the $n = 1$ nature of the reduction wave (this was also confirmed by comparison with CV i_p-values for the oxidation process). For the oligomers **T1** to **T4** there is a positive shift in E_{pc}^{red} (from –2.52 to –2.23 V vs. SCE) and a negative shift in E_{pa}^{ox} for **T1** to **T4** (from +1.28 to +1.23 V vs. SCE) with an increase of the size of molecules. This can be attributed to easier reduction and oxidation with increased delocalization. In summary, the results are consistent with formation of stable radical anions and radical cations for the first electron transfer reactions, consistent with good ECL behavior.

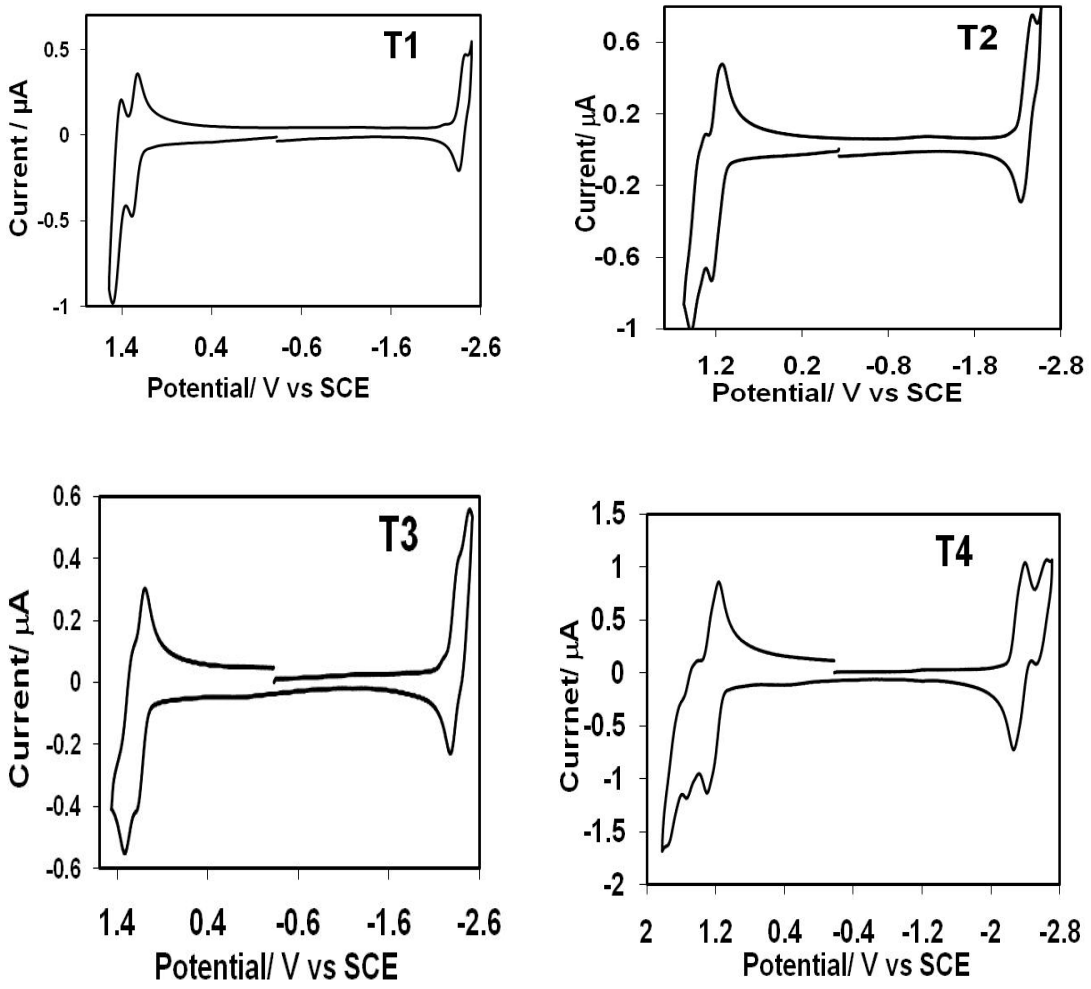

Figure 5.1 Cyclic voltammograms of **T1**–**T3** MeCN:Bz (1:1 v/v) and **T4** in MeCN:Bz (1:2 v/v), 0.1 M $TBAPF_6$, scan rate 0.5 V/s, 0.5 mm Pt disk electrode.

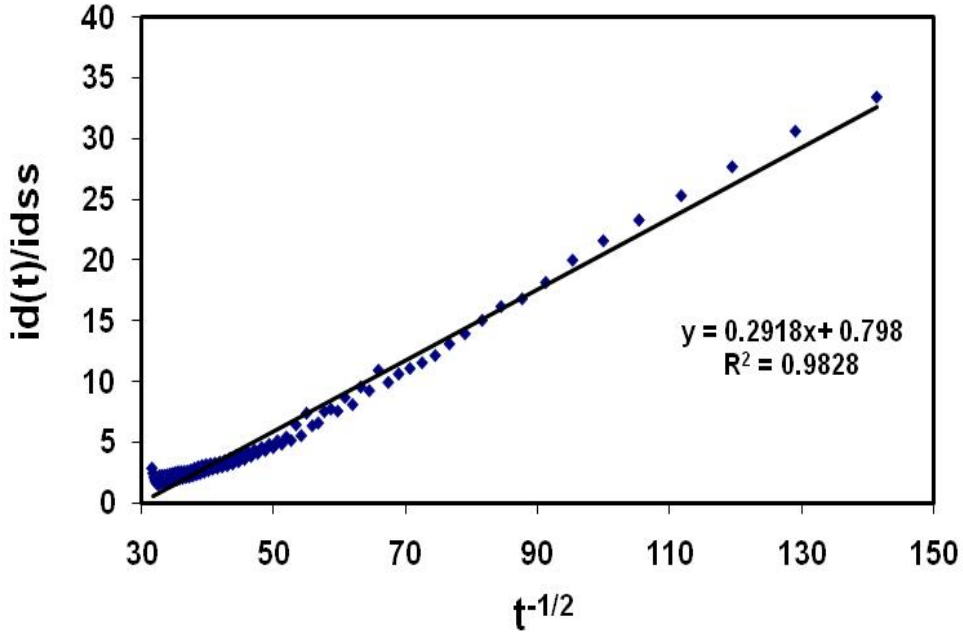

Figure 5.2 Plot of experimental ratio id(t)/idss against the inverse square root of time for the oxidation of 0.4 mM **T1** in MeCN:Bz (1:1 v/v), 0.1 M Bu_4NPF_6, 10 μm diameter Pt microdisk, the sampling rate is 10 μs per point. The results of the linear regression are also shown.

Digital simulations of the CVs at different scan rates were carried out and compared to the experimental results to obtain better insight into the mechanisms and rates of both the anodic and cathodic reactions; the results are summarized in Table 5.1 (see also Figure 5.3). The uncompensated resistance and capacitance were determined by performing a potential step in the relevant solvent system in a region where faradaic reactions did not appear. The geometric electrode surface area used in simulations was determined by a potential step experiment performed in a solution of ferrocene in acetonitrile ($D = 1.2 \times 10^{-5}$ cm^2/s).

Although both the first anodic and first cathodic wave always involved a single electron transfer, the nature of the waves depended on the chain length. The cathodic CV of **T1** was characterized by one reversible electron transfer, with a heterogeneous rate constant, k^o, of about 0.01 cm/s, (assuming complete resistance compensation) (Figures 5.3b). The cathodic reaction for **T2** also showed one reversible electron transfer, with i_{pc}^{red} essentially the same as i_{pa}^{red} for the re-oxidation (3×10^{-7} A) (Figure 5.3d). In contrast, the cathodic scan of **T3** showed two reversible electron transfers with nearly the same peak current values for both reduction waves, indicating $n = 1$ for both reduction processes ($k^o_1 = 0.08$ cm/s, $k^o_2 = 0.05$ cm/s), which corresponds to the formation of radical anion and dianion species (Figure 5.3f). The first and second reduction waves were essentially nernstian with i_{pa}^{red} and i_{pc}^{red} proportional to $\nu^{1/2}$, indicating diffusion control. **T4** showed two reduction waves with the first composed of two reversible peaks

that partially overlap at –2.23 V vs. SCE for the first one and –2.31 V vs. SCE for the second. The i_{pc}^{red} ~ 9.25×10^{-7} A for both overlapped peaks, which is approximately two times larger than the i_{pc}^{red} for **T1** and **T2**, suggesting the reduction peak is an overall two electron transfer reaction, followed by another quasi-reversible peak at –2.57 V vs. SCE (Figure 5.3h).

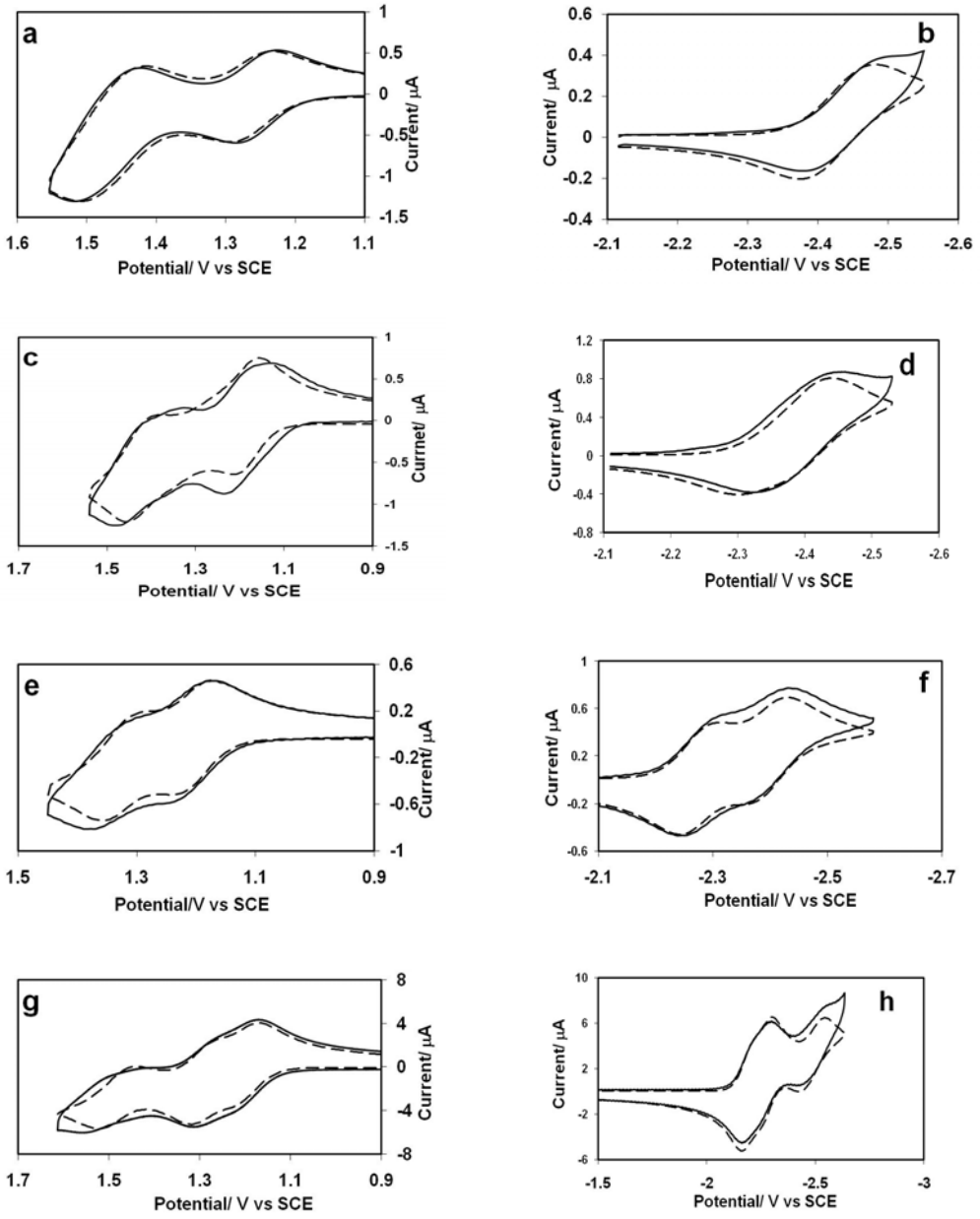

Figure 3. Comparison between simulated and experimental oxidation and reduction waves for **T1**–**T4** at 1 V/s. The model for these simulations: **oxidation** – a) **T1** (E,EE; k^o_1 = 0.01 cm/s, k^o_2 = 0.1 cm/s, k^o_3 = 0.5 cm/s), c) **T2** (E,EE; k^o_1 = 0.1 cm/s, k^o_2 = 0.01 cm/s, k^o_3 = 0.5 cm/s), e) **T3** (E,E; k^o_1 = 0.06 cm/s, k^o_2 = 0.02 cm/s), g) **T4** (E,E,E; k^o_1 = 1 cm/s, k^o_2 = 3 cm/s, k^o_3 = 0.1 cm/s); **reduction** – b) **T1** (E; k^o = 0.01 cm/s; at 0.5 V/s), d) **T2** (E, k^o = 0.01 cm/s), f) **T3** (E,E; k^o_1 = 0.08 cm/s, k^o_2 = 0.05 cm/s), h) **T4** (E,E,E; k^o_1 = 0.5 cm/s, k^o_2 = 0.5 cm/s, k^o_3 = 0.01 cm/s). ------ simulated, —— experimental.

The anodic CV of **T1** was characterized by two reversible waves. The first anodic peak was a one electron transfer ($i_{pa}^{ox1} \sim 3\times10^{-7}$ A), while the second peak was about twice as high ($i_{pa}^{ox2} \sim 5\times10^{-7}$ A) suggesting $n = 2$ (Figure 5.3a). This mechanism was supported by simulation results, using a heterogeneous electron transfer for the first peak of $k^o = 0.01$ cm/s. The same trend was observed for the **T2** oxidation, with the first anodic wave of $n = 1$ and the second wave of $n = 2$, as two partially overlapped peaks, as demonstrated by simulation (Figure 5.3c). However, the longer oligomer, **T3**, showed two consecutive reversible oxidations with nearly the same peak current values ($\sim 3\times10^{-7}$ A), indicating the same number of electrons ($n = 1$) were involved in both oxidation processes (Figure 5.3e). This was confirmed by simulations of the difference in behavior with the shorter oligomer, **T1**, where the second oxidation wave was twice as large as the first, suggesting some difference in electronic interactions between the oligofluorene arms and the truxene core, or a difference in ion pairing of the two species. The longest oligomer, **T4,** showed a broadened wave of two partially overlapping peaks at +1.23 V and +1.35 V vs. SCE followed by a reversible peak at +1.54 and an irreversible peak at +1.79 V vs. SCE. Simulation indicated that the first wave consisted of two overlapping peaks (Figure 5.3g).

These results can be interpreted as interplay of the charge delocalization over the arms and electronic interactions between the arms in **T1**–**T4**. For shorter oligomers, **T1** and **T2**, the truxene core is substantially involved in an initial one-electron transfer during the oxidation process. As a result, the next anodic electron transfer occurs at substantially higher potentials ($\Delta E_{pa}^{(ox1-ox2)} = 0.23$ V and 0.24 V, for **T1** and **T2**, respectively; Table

1). It involves the arms, and as there is not good charge delocalization with the truxene cation radical, the next two electron transfers occur at about the same potential (ΔE = 0.05 V, from simulation; Table 5.1), i.e. essentially no interaction between the arms. The longer oligomer **T3** demonstrates better delocalization of the charge on the arm, thus the first oxidation has a smaller effect on the further electron transfer potential resulting in decreased $\Delta E_{pa}^{(ox1-ox2)}$ = 0.16 V; the arms interact in a stepwise one-electron process. In the longest oligomer **T4**, the radical cation is almost completely delocalized over the terfluorene arms increasing the interactions between the arms, so further splitting of the two first electron transfers is observed ($\Delta E_{pa}^{(ox1-ox2)}$ = 0.12 V). Next (third) one-electron oxidation in **T4** is significantly shifted (by 0.19 V; *cf.* 0.05 V for **T1** and **T2** from simulation) indicating increased interaction between the arms (Table 5.1).

Table 5.1. Summary of Electrochemical Data[a]

		Oxidation peaks (V vs. SCE)			Reduction peaks (V vs. SCE)			D cm^2/s
		1st oxidation peak	2nd oxidation peak	3rd oxidation peak	1st reduction peak	2nd reduction peak	3rd reduction peak	
T1	E_{pa}^{ox} or E_{pc}^{red} (experimental)	+1.28	+1.51		–2.52			
	E^o (from simulation)	+1.26	+1.47, +1.52		–2.45			7×10^{-6}
	n	1	2		1			
T2	E_{pa}^{ox} or E_{pc}^{red} (experimental)	+1.24	+1.48		–2.45			
	E^o (from simulation)	+1.20	+1.44, +1.49		–2.41			5×10^{-6}
	n	1	2		1			
T3	E_{pa}^{ox} or E_{pc}^{red} (experimental)	+1.24	+1.4		–2.30	–2.46		
	E^o (from simulation)	+1.20	+1.34		–2.27	–2.41		3×10^{-6}
	n	1	1		1	1		
T4	E_{pa}^{ox} or E_{pc}^{red} (experimental)	+1.23	+1.35	+1.54[b]	–2.23	–2.31	–2.57	
	E^o (from simulation)	+1.20	+1.29	+1.52	–2.20	–2.27	–2.52	1×10^{-6}
	n	1	1	1	1	1	1	

[a] All electrochemical measurements were performed at a ~0.5 mm Pt disc electrode in MeCN:Bz (1:1 v/v) for **T1-T3** and MeCN:Bz (1:2 v/v) for **T4**); E^o was obtained by simulation, E_{pa}^{ox} is anodic peak potential for oxidation process, E_{pc}^{red} is cathodic peak potential for reduction process, *n* is number of electrons involved in the electron transfer.

[b] There is another irreversible peak at +1.79 which is partially overlapped with the solvent.

5.3.2 Spectroscopy.

The truxene-fluorene oligomers are highly fluorescent species both in solution and in the solid state, with the photoluminescence quantum efficiencies (ϕ_{PL}) for higher oligomers close to those for linear polyfluorene. Absorption and fluorescence spectra were taken in the same solvent systems as used for electrochemistry (1:1 v/v MeCN:Bz for **T1–T3** and 1:2 v/v MeCN:Bz for **T4**) (Figure 5.4). The results are summarized in Table 5.2. The fluorescence spectra of **T1** to **T4** taken with an excitation at the absorption maxima display a fine vibronic progression typical for rigid-rod oligofluorene/polyfluorene structures. The position of the absorption and fluorescence peaks shifted toward the red from **T1** to **T4**, again consistent with increasing delocalization. The intensity of fluorescence was increased from **T1** to **T4** and no luminescence above 500 nm was observed.

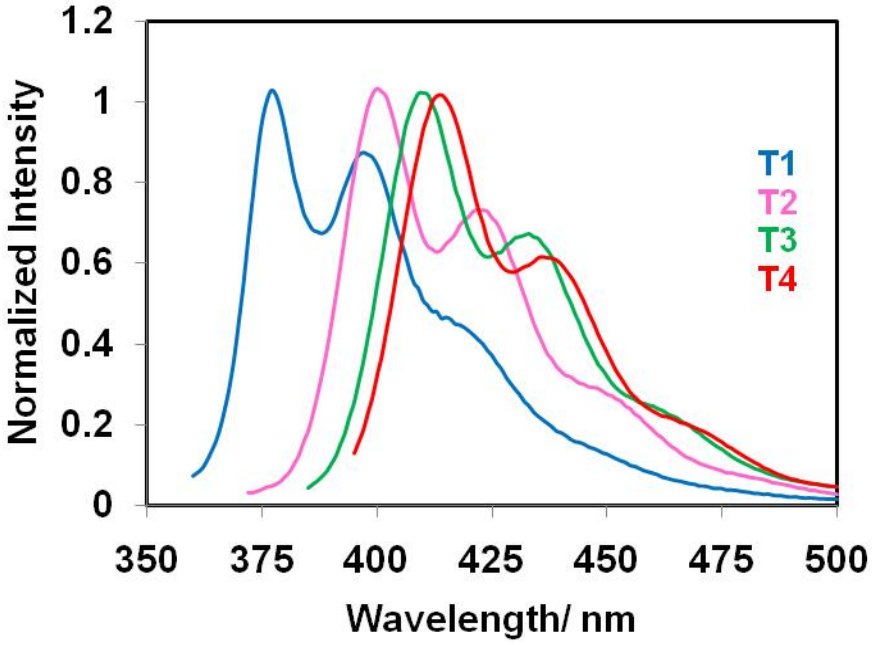

Figure 5.4 Normalized fluorescence spectra of **T1**–**T3** in a mixture MeCN:Bz (1:1 v/v), and **T4** in MeCN:Bz (1:2 v/v), the solutions were excited at their absorption maxima.

Table 5.2. Summary of Spectroscopic Data

Compound	Absorbance, λ_{max} (nm) (Log ε)	Fluorescence, λ_{max} (nm)
T1	343 (5.07)	377, 398, 416sh
T2	362 (5.24)	400, 424, 452sh
T3	372 (5.41)	410, 434, 457sh
T4	377 (5.46)	414, 438, 467sh

5.3.3. Electrogenerated Chemiluminescence (ECL):

5.3.3.1 Ion Annihilation.

When ECL was obtained by continuous pulsing (pulse width 0.1 s) between the first oxidation peak and the first reduction peak in the same solutions as used in the electrochemical studies, with mM levels of **T1** to **T4**, all compounds produced ECL emission, with **T1** easily observed with the naked eye in a semi-darkened room and the longer oligomers **T2-T4** seen even with the lights on. Typical ECL spectra are shown in Figure 5.5. Since the ECL of **T2** to **T4** was very intense and could be seen with the naked eye, even under ambient lighting, a comparison of **T4** with 9,10-diphenylanthracene (DPA), a very bright ECL emitter, was carried out. The ECL from **T4** was about 80% of the ECL emission of DPA under the same conditions. However, the ECL of **T4** decreased to non-detectable levels after ~1000 s of pulsing probably because of the formation of a polymer film on the surface of the electrode (anodic electropolymerization of oligofluorenes is described in the literature[29]). If the cell was returned to the glove box and the electrode polished after this loss of ECL, emission was again restored, consistent with filming of the electrode during pulsing.

The red shift observed in the ECL emission peaks proceeding from **T1** to **T4** is consistent with the fluorescence spectra (Table 5.3). The differences in the resolution due to the wider slit width (0.5–1 mm) used in recording the ECL spectra account for any apparent differences with the fluorescence spectra, except for **T1**. The energy available (enthalpy of annihilation, ΔH_{ann}) between the radical cations and radical anions of the

oligomers for the annihilation reaction, as calculated from the electrochemical, E_p, results (shown in Table 5.4) is much greater than the singlet energy, E_s, from the emission spectra. Species **T2** to **T4** displayed ECL spectra that closely corresponded to the fluorescence emission. However, **T1** showed, in addition to the more intense emission corresponding to the fluorescence at 377 nm, a significant emission at longer wavelength (470 nm) (Figure 5.5, Table 5.3). Such ECL is usually ascribed to emission from excimers or byproducts from side reactions of the radical ions. However, for **T1**, immediately after ECL measurement the fluorescence spectrum of the solution was taken and found to be identical to that measured before ECL experiments, suggesting there were no side reactions to produce bulk byproducts fluorescing at longer wavelengths (consistent with the good stability of the radical ions).

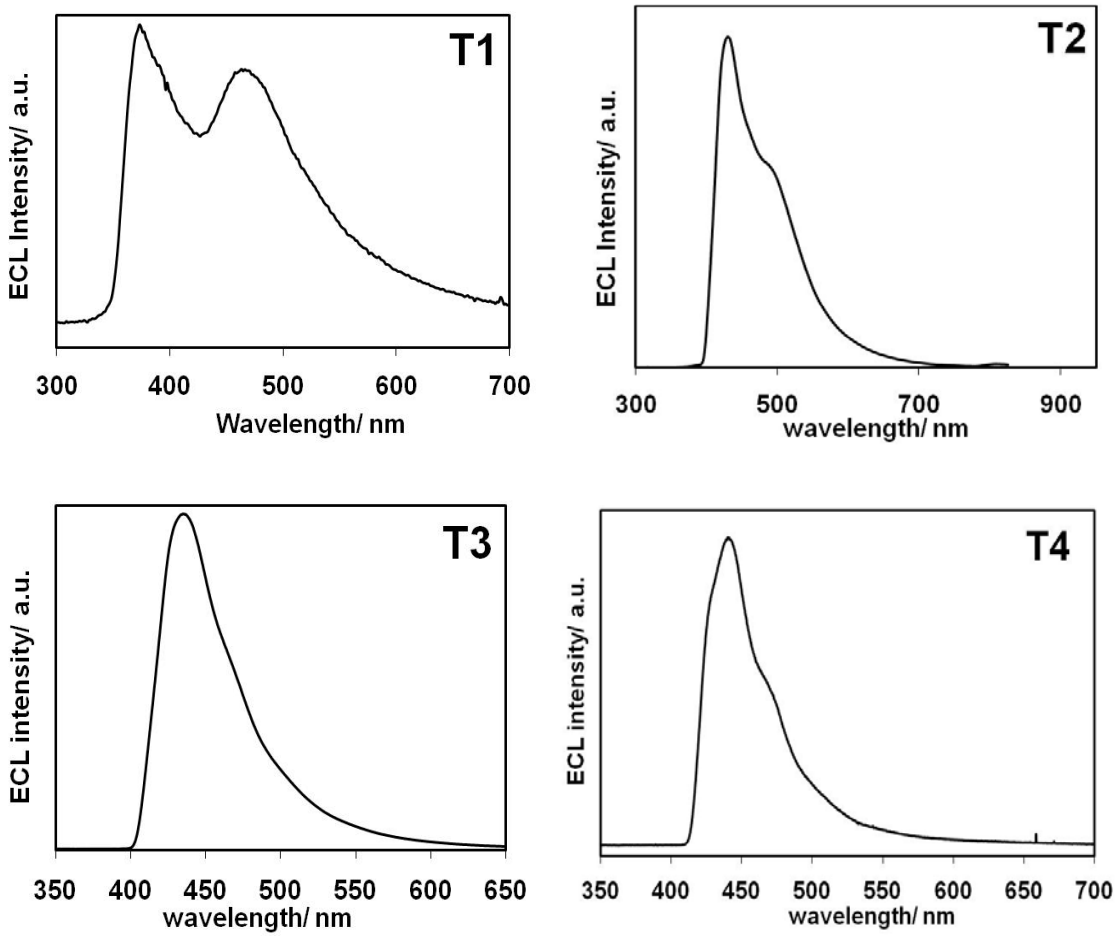

Figure 5.5 ECL spectra of 0.4 mM **T1**–**T3** in MeCN:Bz (1:1 v/v), 0.4 mM **T4** in MeCN:Bz (1:2, v/v); 0.1 s pulses by alternating potential between +1.65 and –2.21 V vs. Ag wire (QRE) for **T1**, +1.6 and –2.22 V for **T2**, +1.58 and –1.95 V for **T3**, and +1.5 and –2.3 V vs. Ag wire for **T4;** integration time was 3 min.

Table 5.3. ECL Peaks of Ion Annihilation Reactions and Fluorescence Emission

Compound	ECL, λ_{max} (nm)	Fluorescence, λ_{max} (nm)
T1	377, 470	377, 398
T2	425	400, 424
T3	434	410, 434
T4	443	414, 438

Table 5.4. Physical Data of Ion Annihilation Reaction for ECL

Compound	E_{pa}^{ox} (V vs. SCE)[a]	E_{pc}^{red} (V vs. SCE)[b]	$-\Delta G_{ann}$ (eV)[c]	$-\Delta H_{ann}$ (eV)[d]	E_s (eV)[e]
T1	+1.28	–2.52	3.80	3.70	3.29
T2	+1.24	–2.45	3.69	3.59	3.10
T3	+1.24	–2.30	3.54	3.44	3.02
T4	+1.23	–2.23	3.46	3.36	2.99

[a] Oxidation, anodic peak potentials of **T1**–**T3** in MeCN:Bz (1:1 v/v) and **T4** in MeCN:Bz (1:2 v/v); 0.1 M $TBAPF_6$;

[b] Reduction, cathodic peak potentials of **T1**–**T4** V vs. SCE; [c] $-\Delta G_{ann} = E_{pa}^{ox} - E_{pc}^{red}$; [d] $-\Delta H_{ann} = -\Delta G_{ann} - 0.1$;[30] [e] $E_s = 1239.85/\lambda_{max}^{PL}$ (nm).

5.3.3.2 Coreactant ECL

The second possibility for the longer wavelength emission was the formation of an excimer that produces a structureless broad emission band. Such excimers (and the equivalent exciplexes) are sometimes found in ECL, even when they are not seen in photoluminescence, as a result of the direct formation by the ion annihilation reaction (eq. 5.7).[31] Thus, we recently observed formation of excimers from poly(9,9-dioctylfluorene)[32] and ter(9,9-diaryl)fluorenes[20] in ECL experiments. If this is the case, the probability of a generated excimer would be much less if a coreactant was used as one of the reactants to generate ECL. To test this possibility TBA oxalate was used as a coreactant. Oxalate ion generates a strong reductant, $CO_2^{-\bullet}$, following oxidation of oxalate[17] as in equations 5.9 to 5.11 below:

$$C_2O_4^{2-} - e \rightarrow C_2O_4^{-\bullet} \quad (5.9)$$

$$C_2O_4^{-\bullet} \rightarrow CO_2 + CO_2^{-\bullet} \quad (5.10)$$

$$A^{+\bullet} + CO_2^{-\bullet} \rightarrow CO_2 + {}^1A^* \quad (5.11)$$

However, some excimers can also form from the route:

$$A + CO_2^{-\bullet} \rightarrow CO_2 + A^{-\bullet} \quad (5.12)$$

followed by annihilation of the radical ions.

The emission from the ECL of the oxalate coreactant with **T1** was weak and could not be obtained with the CCD camera. However, we could study the ECL emission with the photomultiplier (PMT) using filters to estimate the emission wavelengths. To test the excimer, a LP-425 nm long pass filter was used to cut off all wavelengths below 425 nm.

As demonstrated in (Figures 5.6 and 5.7), the ECL emission with the filter was close to the emission without it, so excimer formation was not demonstrated.

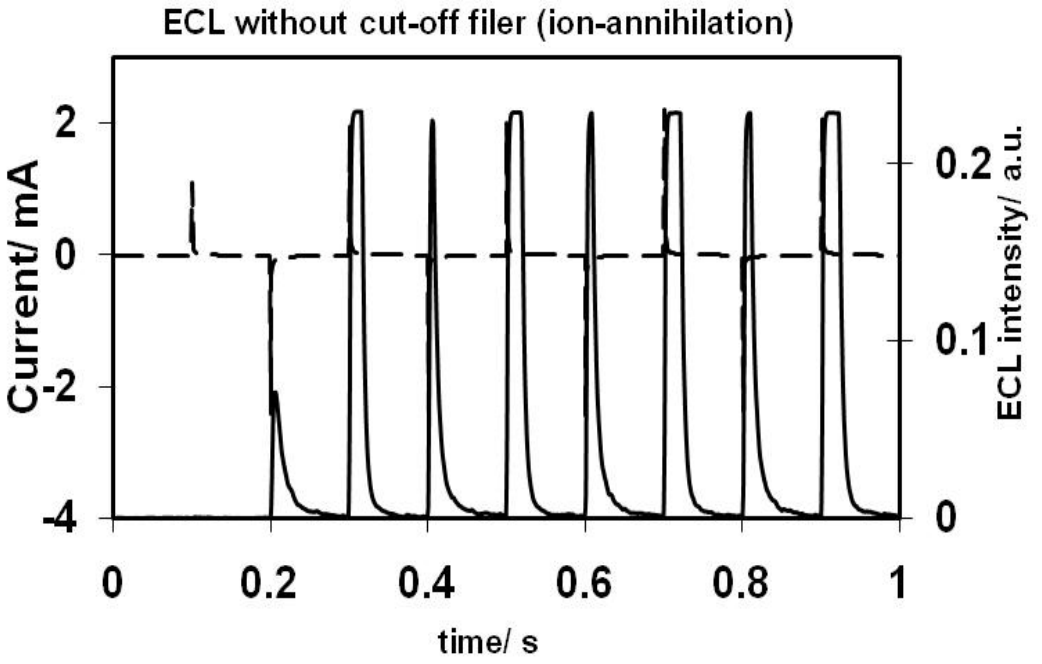

Figure 5.6. Intensity –time curve for annihilation ECL for compound **T1**, 0.1 s pulsing by alternating potential between +1.65 and –2.21 V vs. Ag wire QRE. ------ current, —— light.

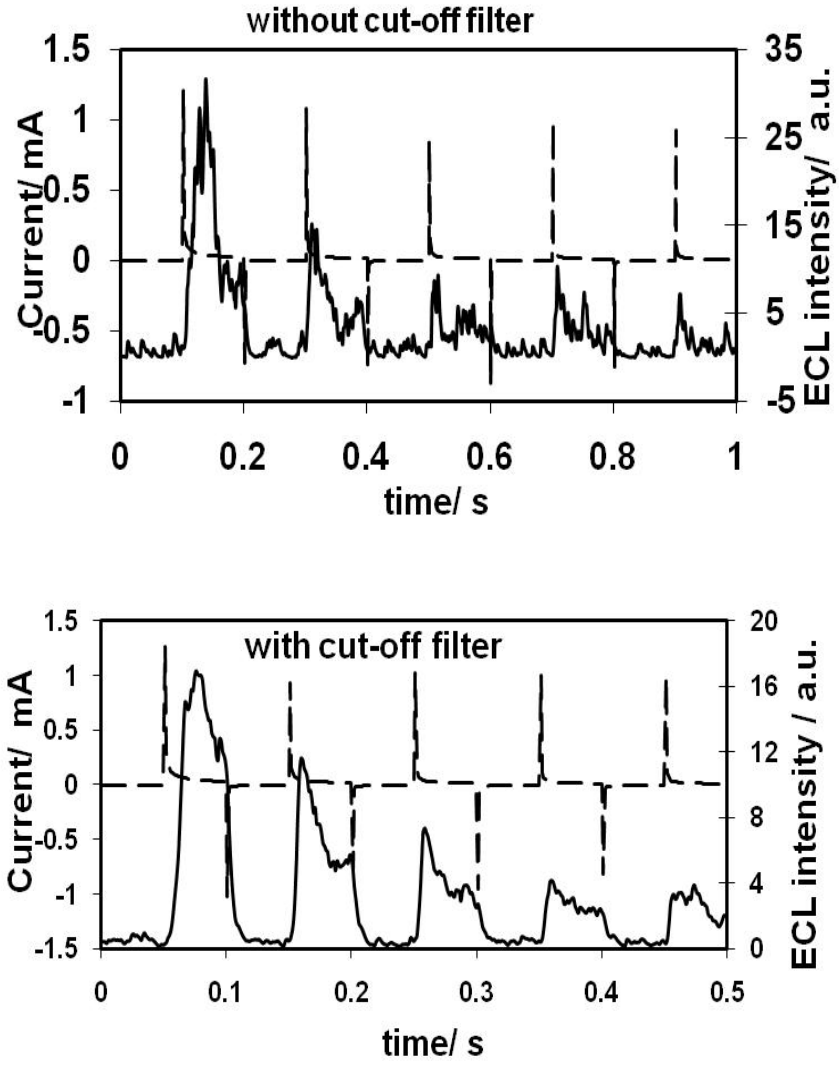

Figure 5.7 Intensity–time curve for coreactant ECL for compound **T1**, pulsing by alternating potential between +1.65 and 0 V vs. Ag wire QRE. Without cut-off filter (0.1 s pulse width) and with cut-off LP 425 nm (0.05 s pulse width). ------ current, —— light.

5.4 CONCLUSION

Truxene-oligofluorene star-shaped oligomers show clean electrochemistry in MeCN:Bz solution with good stability of both the anion and cation radicals. They show intense blue ECL emission that is clearly visible to the naked eye when generated by ion annihilation when the potential is pulsed between the first reduction and first oxidation potentials. The ECL emission for the larger oligomers, **T2** to **T4,** produce ECL spectra at the wavelengths very close to fluorescence emission, while **T1**, the smallest oligomer, also shows some longer wavelength emission of unknown origin.

5.5 REFERENCES

[1] Bard, A. J., Ed., *Electrogenerated Chemiluminescence,* Marcel Dekker: N.Y. 2004**.**

[2] (a) Perepichka, D. F.; Perepichka, I. F.; Meng, H.; Wudl, F. In: *Organic Light-Emitting Materials and Devices*, Li, Z. R.; Meng, H., Eds.; CRC Press: Boca Raton, FL, 2006, Chapter 2, pp. 45–293. (b) Scherf, U.; List, E. J. W. *Adv. Mater.* **2002**, *7*, 477. (c) Neher, D. *Macrom. Rap. Commun.* **2001**, *22*, 1366. (d) Leclerc, M. *J. Polym. Sci. Part A: Polym. Chem.* **2001**, *39*, 2867. (e) Bernius, M. T.; Inbasekaran, M.; O'Brien, J.; Wu, W. *Adv. Mater.* **2000**, *12*, 1737.

[3] (a) Snaith, H. J.; Greenham, N. C.; Friend, R. H. *Adv. Mater.* **2004**, *16*, 1640. (b) Russell, D. M.; Arias, A. C.; Friend, R. H.; Silva, C.; Ego, C.; Grimsdale, A. C.; Müllen, K. *Appl. Phys. Lett.* **2002**, *80*, 2204.

[4] (a) Kim, Y.; Cook, S.; Choulis, S. A.; Nelson, J.; Durrant, J. R.; Bradley, D. D. C. *Chem. Mater.* **2004,** *16,* 4812. (b) Snaith, H. J.; Friend, R. H. *Thin Solid Films* **2004**, *451–452,* 567. (c) Zhang, F.; Perzon, E.; Wang, X.; Mammo,; W. Andersson, M. R.; Inganäs, O. *Adv. Funct. Mater.* **2005**, *15*, 745. (d) Kim, Y. M.; Lim, E.; Kang, I.-N.; Jung, B.-J.; Lee, J.; Koo, B. W.; Do, L.-M.; Shim, H.-K. *Macromolecules* **2006**, *39,* 4081.

[5] (a) Zaumseil, J.; Donley, C. L.; Kim, J.-S.; Friend, R. H.; Sirringhaus, H. *Adv. Mater.* **2006**, *18*, 2708. (b) Yan, H.; Yoon, M.-H.; Facchetti, A.; Marks, T. J. *Appl. Phys. Lett.* **2005**, *87*, 183501.

[6] (a) Rabe, T.; Hoping, M.; Schneider, D.; Becker, E.; Johannes, H.-H.; Kowalsky, W.; Weimann, T.; Wang, J.; Hinze, P.; Nehls, B. S.; Scherf, U.; Farrell, T.; Riedl, T. *Adv. Funct. Mater.*, **2005**, *15*, 1188. (b) Heliotis, G.; Xia, R.; Bradley, D. D. C.; Turnbull, G. A.; Samuel, I. D. W.; Andrew, P.; Barnes, W. L. *Appl. Phys. Lett.* **2003**, *83*, 2118. (c) Heliotis, G.; Bradley, D. D. C.; Turnbull, G. A.; Samuel, I. D. W. *Appl. Phys. Lett.* **2002**, *81*, 415.

[7] *Electronic Materials: The Oligomer Approach*, Müllen, K.; Wegner, G., Eds.; Wiley-VCH: Weinheim, New York, 1998.

[8] (a) Anémian, R.; Mulatier, J.-C.; Andraud, C.; Stéphan, O.; Vial, J.-C. *Chem. Commun.* **2002**, 1608. (b) Geng, Y.; Katsis, D.; Culligan, S. W.; Ou, J. J.; Chen, S. H.; Rothberg, L. J. *Chem. Mater.* **2002**, *14*, 463. (c) Katsis, D.; Geng, Y. H.; Ou, J. J.; Culligan, S. W.; Trajkovska, A.; Chen, S. H.; Rothberg, L. J. *Chem. Mater.* **2002**, *14*, 1332. (d) Geng, Y.; Trajkovska, A.; Katsis, D.; Ou, J. J.; Culligan, S. W.; Chen, S. H. *J. Am. Chem. Soc.* **2002**, *124*, 8337. (e) Geng, Y.; Culligan, S. W.; Trajkovska, A.; Wallace, J. U.; Chen, S. H. *Chem. Mater.* **2003**, *15*, 542. (f) Jo, J.; Chi, C.; Höger, S.; Wegner, G.; Yoon, D. Y. *Chem. Eur. J.* **2004**, *10*, 2681. (g) Chi, C.; Im, C.; Enkelmann, V.; Ziegler, A.; Lieser, G.; Wegner, G. *Chem. Eur. J.* **2005**, *11*, 6833. (h) Li, J.; Li, M.; Bo, Z. *Chem. Eur. J.* **2005**, *11*, 6930. (i) Chi, C.; Wegner, G. *Macromol. Rapid Commun.* **2005**, *26*, 1532. (j) Li, Z. H.; Wong, M. S. *Org. Lett.* **2006**, *8*, 1499.

[9] (a) Geng, Y.; Trajkovska, A.; Culligan, S. W.; Ou, J. J.; Chen, H. M. P.; Katsis, D.; Chen, S. H. *J. Am. Chem. Soc.* **2003**, *125*, 14032. (b) Geng, Y.; Chen, A. C. A.; Ou, J. J.; Chen, S. H. *Chem. Mater.* **2003**, *15*, 4352. (c) Li, Z. H.; Wong, M. S.; Tao, Y.; Lu, J. *Chem. Eur. J.* **2005**, *11*, 3285.

[10] (a) Wong, K.-T.; Chien, Y.-Y.; Chen, R.-T.; Wang, C.-F.; Lin, Y.-T.; Chiang, H.-H.; Hsieh, P.-Y.; Wu, C.-C.; Chou, C. H.; Su, Y. O.; Lee, G.-H.; Peng, S.-M. *J. Am. Chem. Soc.* **2002**, *124*, 11576. (b) Culligan, S. W.; Geng, Y.; Chen, S. H.; Klubek, K.; Vaeth, K. M.; Tang, C. W. *Adv. Mater.* **2003**, *15*, 1176. (c) Wong, K.-T.; Liao, Y.-L.; Lin, Y.-T.; Su, H.-C.; Wu, C.-C. *Org. Lett.* **2005**, *7*, 5131. (d) Chen, A. C.-A.; Wallace, J. U.; Wei, S. K.-H.; Zeng, L.; Chen, S. H. *Chem. Mater.* **2006,** *18,* 204.

[11] Lupton, J. M.; Craig, M. R.; Meijer, E. W. *Appl. Phys. Lett*. **2002**, *80*, 4489.

[12] (a) List, E. J. W.; Guentner, R.; Scanducci de Freitas, P.; Scherf, U. *Adv. Mater*. **2002**, *14*, 374. (b) Gaal, M.; List, E. J. W.; Scherf, U. *Macromolecules* **2003**, *36*, 4236. (c) Gong, X.; Iyer, P. K.; Moses, D.; Bazan, G. C.; Heeger, A. J.; Xiao, S. S. *Adv. Funct.*

Mater. **2003**, *13*, 325. (d) Romaner, L.; Pogantsch, A.; Scandiucci de Freitas, P.; Scherf, U.; Gaal, M.; Zojer, E.; List, E. J. W. *Adv. Funct. Mater.* **2003**, *13*, 597. (e) Gamerith, S.; Gadermaier, C.; Scherf, U.; List, E. J. W. *Phys. Stat. Sol. (a)* **2004**, *201*, 1132. (f) Sims, M.; Bradley, D. D. C.; Ariu, M.; Koeberg, M.; Asimakis, A.; Grell, M.; Lidzey, D. G. *Adv. Funct. Mater.* **2004**, *14*, 765.

[13] Faulkner, L. R.; *J. Electrochem. Soc.* **1997**, *124*, 1724.

[14] Noffsinger, J. B.; Danielson, N. D. *Anal. Chem.* **1987**, *59*, 865.

[15] Zu, Y.; Bard, A. J. *Anal. Chem*. **2000**, *72*, 3223.

[16] Miao, W.; Choi, J.-P.; Bard, A. J. *J. Am. Chem. Soc*. **2002**, *124*, 14478.

[17] Chang, M.-M.; Saji, T.; Bard, A. J. *J. Am. Chem. Soc*. **1977**, *99*, 5399.

[18] Rubinstein, I.; Bard, A. J. *J. Am. Chem. Soc*. **1981**, *103*, 512.

[19] White, H. S.; Bard, A. J. *J. Am. Chem. Soc*. **1982**, *104*, 6891.

[20] Choi, J.-P.; Wong, K.-T.; Chen,Y.-M.;Yu, J.-K.; Chou, P.-T.; Bard, A. J. *J. Phys. Chem. B* **2003**, *107*, 14407.

[21] Wu, C.; Malinin, S. V.; Tretiak, S.; Chernyak, V. Y. *Nature Physics* **2006**, *2*, 631.

[22] (a) Zhou, X.-H.; Yan, J.-C.; Pei, J. *Org. Lett.*, **2003**, *5*, 3543. (b) Li, B.; Li, J.; Fu, Y.; Bo, Z. *J. Am. Chem. Soc.* **2004**, *126*, 3430. (c) Li, B.; Xu, X.; Sun, M.; Fu, Y.; Yu, G.; Liu, Y.; Bo, Z. *Macromolecules* **2006**, *39,* 456. (d) Montes, V. A.; Pérez-Bolívar, C.; Agarwal, N.; Shinar, J.; Anzenbacher, Jr., P. *J. Am. Chem. Soc.* **2006**, *128*, 12436. (e) Lai, W.-Y.; Zhu, R.; Fan, Q.-L.; Hou, L.-T.; Cao, Y.; Huang, W. *Macromolecules* **2006**, *39,* 3707.

[23] Kanibolotsky, A. L.; Berridge, R.; Skabara, P. J.; Perepichka, I. F.; Bradley, D. D. C.; Koeberg, M. *J. Am. Chem. Soc*. **2004**, *126*, 13696.

[24] (a) Geng, Y.; Fechtenkötter, A.; Müllen, K. *J. Mater. Chem.*, **2001**, *11*, 1634. (b) Ponomarenko, S. A.; Kirchmeyer, S.; Elschner, A.; Huisman, B.-H.; Karbach, A.; Drechsler D. *Adv. Funct. Mater.* **2003**, *13*, 591. (c) Pei, J.; Wang, J.-L.; Cao, X.-Y.; Zhou, X.-H.; Zhang, W.-B. *J. Am. Chem. Soc.* **2003**, *125*, 9944. (d) Nicolas, Y.; Blanchard, P.; Levillain, E.; Allain, M.; Mercier, N.; Roncali, J. *Org. Lett.*, **2004**, *6*,

273. (e) Sun, Y.; Xiao, K.; Liu, Y.; Wang, J.; Pei, J.; Zhu, D. *Adv. Funct. Mater.* **2005**, *15*, 818. (f) Cravino, A.; Roquet, S.; Alévêque, O.; Leriche, P.; Frère, P.; Roncali, J. *Chem. Mater.* **2006,** *18,* 2584. (g) Cremer, J.; Bäuerle, P. *J. Mater. Chem.* **2006**, *16*, 874.

[25] (a) Holst, H. C.; Oehlhof, A. *Eur. J. Org. Chem.* **2003**, 4173. (b) Fratiloiu, S.; Senthilkumar, K.; Grozema, F. C.; Christian-Pandya, H.; Niazimbetova, Z. I.; Bhandari, Y. J.; Galvin, M. E.; Siebbeles, L. D. A. *Chem. Mater.* **2006,** *18,* 2118. (c) Brunel, J.; Mongin, O.; Jutand, A.; Ledoux, I.; Zyss, J.; Blanchard-Desce, M. *Chem. Mater.* **2003**, *15,* 4139.

[26] (a) Rodríguez, J. G.; Esquivias, J.; Lafuente, A.; Díaz, C. *J. Org. Chem.* **2003**, *68*, 8120. (b) Yamaguchi, Y.; Ochi, T.; Miyamura, S.; Tanaka, T.; Kobayashi, S.; Wakamiya, T.; Matsubara, Y.; Yoshida, Z.-I. *J. Am. Chem. Soc.* **2006**, *128*, 4504.

[27] (a) Wang, Y.; He, G. S.; Prasad, P. N.; Goodson III, T. *J. Am. Chem. Soc.* **2005**, *127*, 10128. (b) Yan, Y.-X.; Tao, X.-T.; Sun, Y.-H.; Wang, C.-K.; Xu, G.-B.; Yang, J.-X.; Ren, Y.; Zhao, X.; Wu, Y.-Z.; Yua, X.-Q.; Jiang, M.-H. *J . Mater. Chem.* **2004**, *14* , 2995.

[28] Denuault, G.; Mirkin, M. V.; Bard, A. J. *J. Electroanal. Chem.* **1991**, *308*, 27.

[29] Hapiot, P.; Lagrost, C.; Le Floch, F.; Raoult, E.; Rault-Berthelot, J. *Chem. Mater.* **2005,** *17,* 2003.

[30] Santa Cruz, T. D.; Akins, D. L.; Birke, R. L. *J. Am. Chem. Soc*. **1976**, *98*, 1677.

[31] Lai, R. Y.; Fleming, J. J.; Merner, B. L.; Vermeij, R. J.; Bodwell, G. J.; Bard, A. J. *J. Phys. Chem. A* **2004,** *108,* 376.

[32] Prieto, I.; Teetsov, J.; Fox, M. A.; Vanden Bout, D. A.; Bard, A. J. *J. Phys. Chem. A* **2001,** *105,* 520.

Chapter 6: Electrogenerated Chemiluminescence of Aromatic Hydrocarbon Nanoparticles in Aqueous Solution

6.1 INTRODUCTION

We report in this chapter electrogenerated chemiluminescence (ECL) from dispersed (colloidal solutions) of nanoparticles (NP) of aromatic hydrocarbon compounds in an aqueous medium. Aromatic hydrocarbons in nonaqueous solvents like acetonitrile, under conditions of very small water and oxygen concentrations, were some of the earliest species studied by ECL.[1] However the low solubility of aromatic hydrocarbons in water and high reactivity of their radical ions with water have prevented their investigations in aqueous media. It was of interest to see if NPs, which have sizes (in the nm regime) between those of molecules and bulk crystals and often exhibit characteristics different from those observed in the corresponding bulk materials,[2] would produce ECL. In general, organic NPs might have practical applications, because their fluorescence spans a wide wavelength region and NPs of these can be prepared with a range of sizes and shapes.[3] Compared to inorganic NPs, fewer studies have been conducted on the properties of organic NPs, e.g. on the size effect of organic NPs on their spectroscopic and other properties.[2] ECL has been extensively studied for organic molecules,[1] but only relatively few studies have been done on semiconductor NPs.[4] To our knowledge there has been no report on ECL of organic compound NPs, probably because their nucleation

and growth mechanisms are less understood and the basic properties, e.g. effect of NP size on spectroscopy, are less well-established. The search for methods of controlling size, shape, and optical properties of organic NPs is still under development.[5]

In this chapter, we describe ECL from rubrene and DPA NPs in aqueous solutions prepared by a simple reprecipitation method, in which a small amount of organic compound in a good solvent (such as THF, DMF or MeCN) is injected rapidly and stirred vigorously into a poor solvent (such as water), in which the organic compound has a very low solubility. Characterization of the NPs using different techniques, e.g. scanning electron microscopy (SEM), transmission electron microscopy (TEM), dynamic light scattering (DLS), UV-vis absorption and luminescence spectroscopies are discussed.

6.2 EXPERIMENTAL SECTION

6.2.1 Synthesis of nanoparticles.

The reprecipitation method was used for this synthesis.[2] The rubreneNPs were synthesized by dissolving the rubrene at a 5 mM concentration in THF and quickly injecting 100 μL of this solution into 10 mL of deionized water under an argon atmosphere with vigorous stirring at room temperature. The resulting NP solution, after filtering through a 0.22 μm pore-size filter (Millex GP, PES membrane), had a clear pale red color. The same procedure was followed for the preparation of DPA NPs by using MeCN, DMF or THF as the solvent.

6.2.2. Instrumentation.

UV-vis spectra were recorded on a Milton Roy Spectronic 3000 array spectrophotometer. Fluorescence spectra were recorded on a Fluorolog-3spectrofluorimeter (ISA-JobinYvon Horiba, Edison, NJ) using a 1 cm path length quartz cuvette. Scanning electron microscopy (SEM) was performed with a LEO 1450VP microscope at an accelerating voltage of 20 kV and linked with an Oxford Instruments X-ray analysis system. The organic nanoparticles sample were coated with a metal layer of silver to increase the conductivity of the organic nanoparticle layer and decreasing the charging problem in taking SEM image.

Transmission electron microscopy (TEM) analysis and selected area electron diffraction (SAED) were conducted using a JEOL 2100F microscope at an accelerating

voltage of 200 kV. Fluorescence imaging was carried out with an inverted optical microscope (Model TE 300, Nikon) and images of the emission were taken with a Model 7404-0001, Roper Scientific Inc. camera. Current and ECL transients were simultaneously recorded using an Autolab electrochemical workstation (Eco Chemie, The Netherlands) coupled with a photomultiplier tube (PMT, Hammamatsu R4220p) held at –750V with a high-voltage power supply (Kepco, Flushing, NY). The photocurrent produced at the PMT was converted to a voltage signal by an electrometer/ high resistance system (Keithley, Cleveland, OH) and fed into the external input channel of an analog-to-digital converter (ADC) of the Autolab. The electrochemical/ECL cell was composed of J-type inlaid platinum disk as a working electrode which was polished with alumina of different sizes between each experiment. The other electrodes were a platinum coiled wire counter electrode and Ag/AgCl reference electrode.

6.3. RESULTS AND DISCUSSION

6.3.1 Microscopic and spectroscopic characterization.

Figure 6.1 shows that rubrene NPs are fairly monodisperse with a hydrodynamic radius of about 50 nm based on dynamic light scattering (DLS) measurements. From DLS measurements, the relative standard deviation for particle size was 0.6 % (for n=5) for the DPA NPs and 0.5% (for n=5) for the rubrene NPs. The sizes of rubrene NPs determined from TEM images were in good agreement with DLS measurements (see Figure 6.1). The kinetics of formation of aggregates is determined by the interaction potential between particles, the particle size, and the flow conditions during synthesis.[6] Ionic additives, low molecular weight molecules such as surfactant, and neutral or charged polymers can also dramatically affect the formation process and stability of the NPs. For example, particles formed in the presence of Triton X-100 were smaller (~ 40 nm in diameter, according to DLS measurement) and the size distribution was narrower than in its absence. However, the presence of surfactant had a negative effect on generation of ECL probably because the encapsulation of a particle within a layer of surfactant decreased the electron transfer rate between the particle and the electrode. NPs of rubrene in water were unstable in ambient atmosphere under room light exposure for 10 h, while they were stable for a month in the dark (although the slow formation of aggregates was seen as shown Figure 6.1).

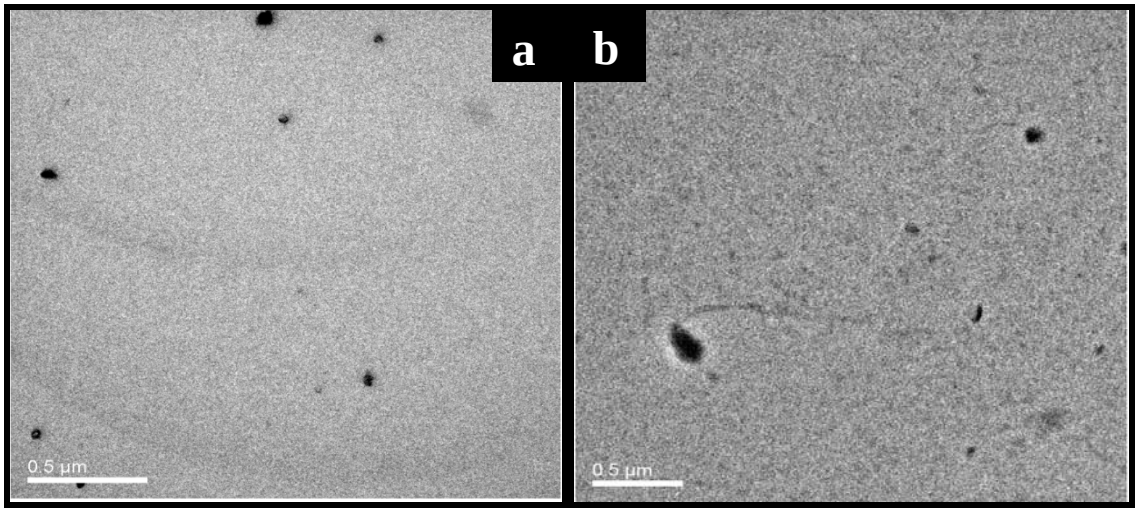

Figure 6.1 TEM images of freshly-prepared rubreneNCs (a) and NCs after one-week aging in solution (b).

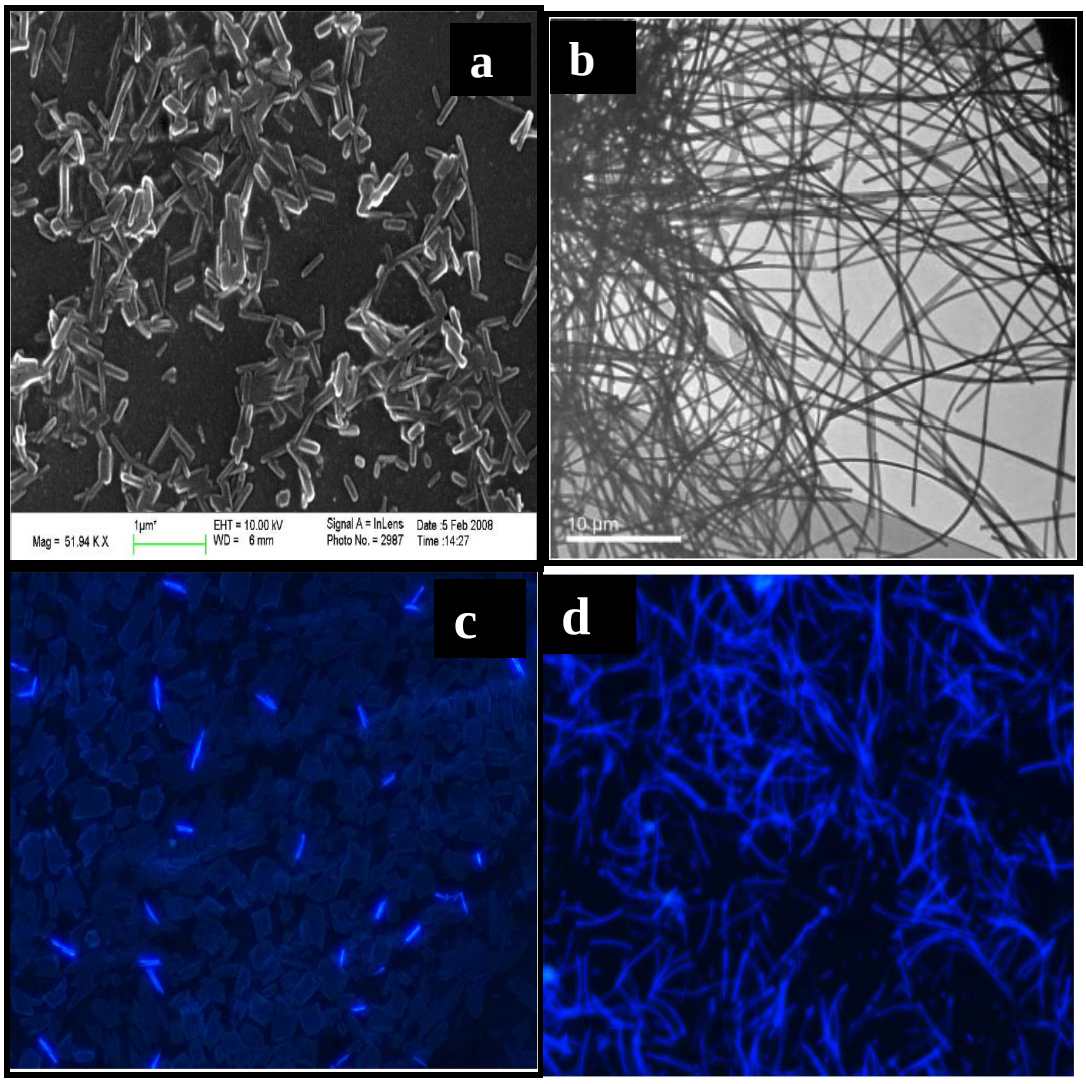

Figure 6.2 (a) SEM image of DPA nanoparticles; (b) TEM image of nanowires of DPA; (c) fluorescence image of freshly prepared DPA nanorods; (d) fluorescence image of DPA nanowires (after one-week aging in solution).

ONPs of 9,10-diphenylanthracene (DPA), a well-known blue ECL emitter, prepared by using THF as a solvent did not show appreciable ECL. However DPA NPs prepared with MeCN as the solvent were larger, ~250 nm, as shown in Figure 6.2a and b and produced appreciable ECL with oxalate as a coreactant, as discussed below. We attribute the difference in ECL behavior for THF and MeCN-based preparations to the size and shape of the crystals formed during nanocrystallization process, which have been attributed to the difference in the solubility of the organic compound in water (a poor solvent) and the polarity of the good solvent. A more detailed characterization of the shape of the DPA NPs was revealed by SEM and TEM. As shown in Figure 6.2, DPA nanorods (50 nm in diameter and 500 nm in length) were initially formed; these changed with time and after about one week were converted into larger nanowires, about 1 μm in diameter and 10 μm in length. This shape change might be attributed to crystal-to-crystal photodimerization which has been proposed to explain the observed shape changes in organic NPs.[7]

DPA nanorods deposited on a glass substrate were used to examine the fluorescence image of individual rods with fluorescence microscopy (see Figure 6.2c and d). Under UV excitation, the rods produced blue fluorescence characteristic of DPA emission. The dimensions of individual nanorods shown in the fluorescence image were in good agreement with the TEM image, indicating that in a freshly prepared aqueous NP solution, rods are the predominant forms that grow into longer wires with time. However, Zhang at el[8], reported that nanorods of DPA are formed when a large volume of

DPA/THF (~1mL) is injected to 5mL of water containing cetyltrimethyl ammonium bromide (CTAB). Although they reported that surfactant is necessary to get stable nanorods, in our work surfactant gave a negative effect on ECL, so it was avoided.

Absorption spectra of both rubrene and DPA exhibited evenly-spaced vibronic peaks that generally mirrored the emission spectra, Figure 6.3. The absorption and emission spectra of rubrene NPs in water is red shifted by 5 nm, while the DPA NPs red shifted by 10 nm compared to the molecular solution in an organic solvent. This shift has been attributed to the polarizable environment of the surrounding NPs in water, which lowers the energy of the transition.[9]

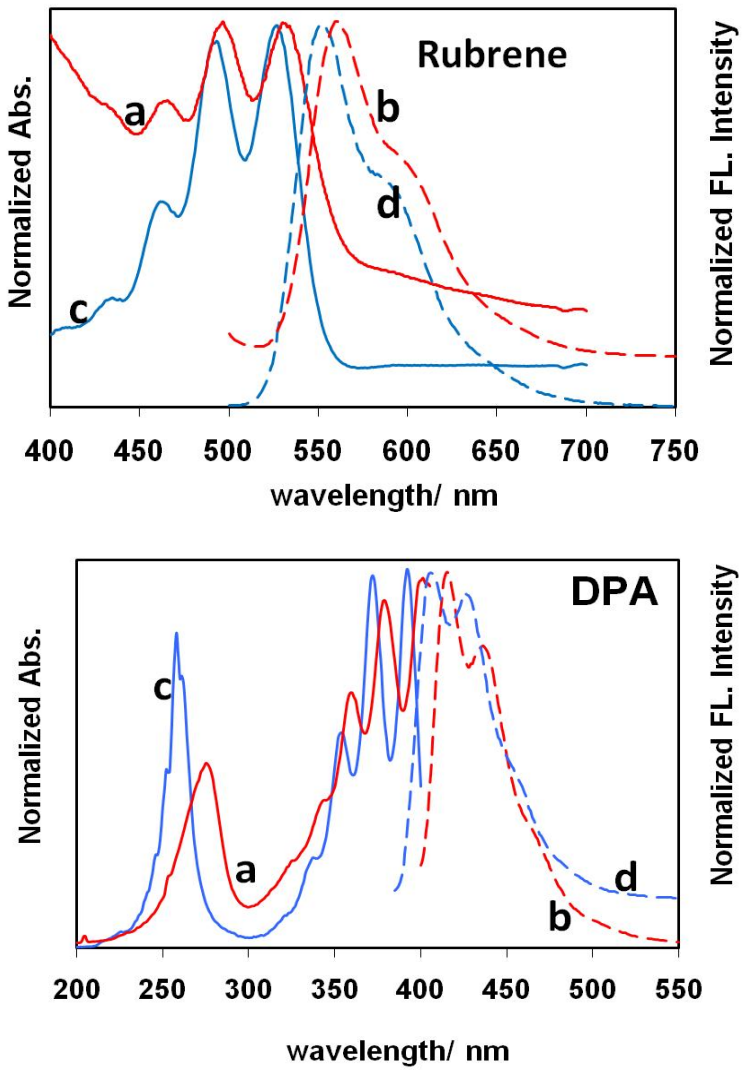

Figure 6.3 (a) Absorbance of NPs in aqueous solution (red solid line); (b) fluorescence of NPs in aqueous solution (red dashed line); (c) absorbance of rubrene dissolved THF or DPA dissolved in MeCN (blue solid line); (d) fluorescence of rubrene in THF or DPA in MeCN (blue dashed line).

6.3.2 Electrochemistry and electrogenerated chemiluminescence.

Because of the limited potential window for electrochemical studies in aqueous solutions, the reduction of water generally prevents observation of the reduction of aromatic hydrocarbons, even those that are more easily reduced, like rubrene NPs. Cyclic voltammograms (CV) of the dispersed organic NPs in aqueous 0.1 M $NaClO_4$ however displayed no distinctive features which could be clearly assigned to either the oxidation or reduction of the NPs. The lack of a measureable electrochemical signal can be attributed to the low concentration of the NPs (C), as well as their small diffusion coefficients (D) (because of their large radii) in the solution. The electrochemical current is governed by the flux of the NPs to the electrode surface, which is a function of both C and D.

However one can obtain information about the redox behavior by observing ECL with a coreactant. For example the oxidation of rubrene NPs in the presence of coreactant, such as tri-n-propylamine (TPrA) or oxalate ion, which form strong reducing agents ($E_{red} \leq -1.7$ V vs SCE) on oxidation, has been shown to produce emission.[1,10] NPs could be oxidized by a potential sweep or step to a sufficiently positive potential, where the coreactant is also oxidized. ECL emission was observed when the electrogenerated oxidized NPs ($R^{+\bullet}$) reacted with the strong reducing agent ($TPrA^{\cdot}$ or $CO_2^{\cdot -}$) produced by oxidation of the coreactant to produce the excited states of NPs. The coreactant mechanism has been described previously.[10,11] All of the observed electrochemical current observed in these experiments can be attributed to the coreactant oxidation.

Transient ECL generated from the reaction of oxidized NPs and the energetic intermediate of the coreactant was obtained by stepping the electrode potential from 0.0 V to +1.1 V vs Ag/AgCl. For rubrene NPs, as shown in Figure 6.4a, the ECL emission was produced when the electrode potential was stepped to +1.1 V to oxidize both NPs and TPrA; no ECL was produced when the electrode potential was stepped back to 0.0 V. The ECL signal was sharp but weak, probably because of instabilities of the intermediates by reaction with water molecules and oxygen, and also because of the low concentrations and diffusion coefficients of the NPs. The ECL intensity decreased with time, as shown in Figure 4d, probably because of the instability of the radical cations at the surface of the NPs.

The ECL vs. potential curve (at a scan rate of 500 mV/s) is shown in Figure 6.4b, in which ECL emission was produced in the potential region where rubrene was oxidized (estimated from results in MeCN). The ECL intensity generated from rubrene NPs was strong enough to be detected with the PMT, but could not be observed with the naked eye.

Poor electrochemistry was observed for NPs alone, in which the CVs were featureless. Similar behavior was found for semiconductor NPs.[12,4] Unlike those prepared in THF, rubreneNPs prepared in DMF, produced a much smaller ECL signal that was difficult to detect at the same preparation concentration conditions (i.e. injecting 100 μL of 1 mM rubrene in DMF into 10 mL deionized water). However by increasing the concentration (e.g. injecting 500 μL of 1 mM rubrene in DMF into 10 mL water), an ECL signal could be detected as shown in Figure 6.4c. This might be attributed to the smaller

solubility of rubrene in DMF vs. THF and the different miscibility of these two solvents with water during the reprecipitation process.[13]

ECL of DPA by an annihilation reaction (i.e. reaction between cation and anion radical of DPA) in MeCN solution produces strong blue light. As mentioned earlier, due to the limited potential window of an aqueous solution at a Pt working electrode, we are limited to study only the oxidation of DPA in the presence of a coreactant such as TPrA or oxalate. As reported previously in nonaqueous media,[10] $TPrA^{\bullet}$ is not energetic enough to generate the excited state of DPA but oxalate is, because oxalate oxidation produces the more reducing $CO_2^{\bullet -}$ (Figure 6.4e). The ECL intensity was small, however, probably because of the very low diffusion coefficients of the rather large particles of DPA. The ECL intensity is governed by the flux of the NPs to the electrode, which decreases as the diffusion coefficient decreases. Scheme 6.1 shows the proposed mechanism of organic ECL emission.

In summary, ECL, particularly coreactant type was produced for dispersed NPs of DPA and rubrene in aqueous media. Methods of preparation of the NPs, which in turn have effects on the nanocrystallization processes, affect the intensity of the ECL signal. Increases in intensity require formation of smaller NPs, which should produce higher concentrations and significantly larger diffusion coefficients.

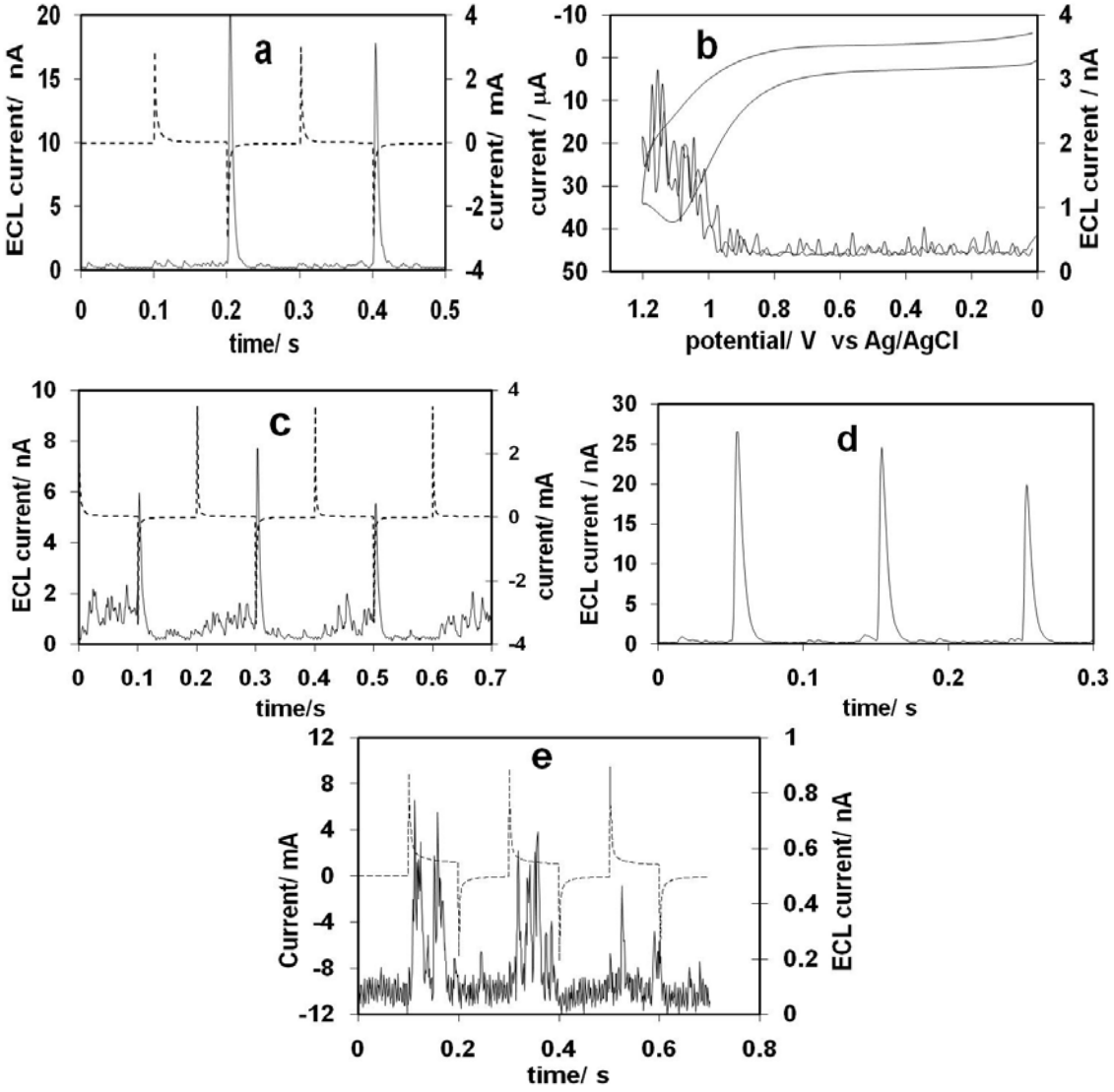

Figure 6.4. (a) Chronoamperometry (dotted line) and ECL transient (solid line) for rubreneNCs (prepared from THF) in aqueous 0.1 M TPrA and 0.1 M $NaClO_4$, pulse width = 0.1 s. (b) Cyclic voltammogram of rubreneNCs at scan rate of 500 mV/s, blank experiment: 0.1 M TPrA in 0.1 M $NaClO_4$. (c) Chronoamperometry (dotted line) and ECL transient (solid line) of rubreneNCs (prepared from DMF) in aq. 0.1 M TPrA and 0.1 M $NaClO_4$, pulse width = 0.1 s. (d) ECL transient (solid line) of rubreneNCs (prepared from THF) in 0.1 M TPrA and 0.1 M $NaClO_4$, pulse width = 0.05 s. (e) ECL (solid line) and current (dotted line) of DPA NCs in 0.1 M $Na_2C_2O_4$aqueous solution.

Scheme 6.1 Proposed mechanism of ECL of organic nanoparticles in water solution in the presence of Tripropoylamine as acoreactant.

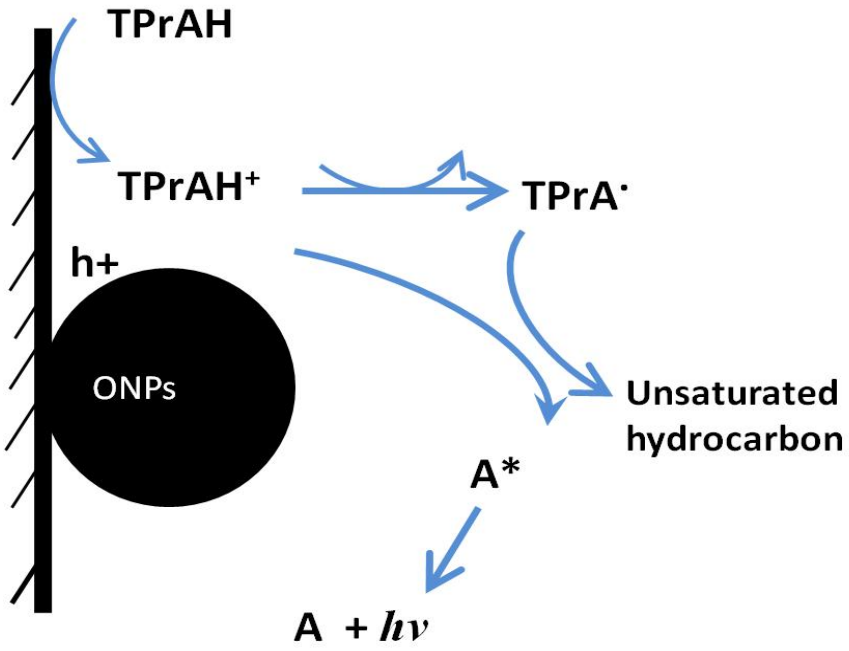

6.4 CONCLUSION

NPs (average radius ~ 50 nm) of two ECL emitters, rubrene and DPA were synthesized and characterized. ECL of these dispersed NPs was observed in aqueous 0.1 M $NaClO_4$solutions containing suitable coreactants. Rubrene formed spherical NPs which were stable for at least one week in the dark with no significant aggregation, while DPA NPs first formed nanorods, which grew into nanowires within a week due to the instability of the initially-formed NPs. The ECL intensity from the rubrene NPs was sufficient to suggest their use as labels for ECL analytical methods. However, we are attempting the preparation of smaller particles. The addition of surfactant generates smaller NPs, however surfactant decreases the ECL intensity, probably because it interferes with electron transfer reactions at the NP surface. Alternative approaches are being investigated.

6.5 REFERENCES

[1] Reviews of ECL, see (a) *Electrogenerated chemiluminescence*; Bard, A. J.; Ed; Marcel Dekker, INC.; New York, 2004. (b) Miao, W.; *Chem. Rev.* **2008,** *108,* 2506 (c) Richter, M. M. *Chem. Rev*. **2004**, 104, 3003. (d) Knight, A. W.; Greenway, G. M. *Analyst* **1994**, *119*, 879 (e) Bard, A. J.; Debad, J. D.; Leland, J. K.; Sigal, G. B; Wilbur,J . L.; Wohlstadter, J. N. In Encyclopedia of Analytical Chemistry: Applications, Theory and Instrumentation; Meyers, R.A., Ed.; John Wiley & Sons: New York, 2000; vol 11, p.9842.

[2] (a) Mori , J.; Miyashita, Y.; Oliveira,D.; Kasai, H.; Oikawa, H.; Nakanishi, H. *Journal of Crystal Growth* ,**2009**, *311*, 553 (b) Wu, C.; Peng, H.; Jiang,Y.; McNeill**,** J**.** *J. Phys. Chem. B* **2006,** *110,* 14148 (c) Kaneko, K.; Shimada, S.; Onodera, T.; Kimura, T.; Matsuda, H.; Okada S.; Kasa, H.; Oikawa, H.; Kakudate, Y.; Nakanishi, H, *Jpn. J. Appl. Phys*, **2007**, *46*, 6893, (d) Kasai, H.; Nalwa, H. S.; Oikawa, H.; Okada, S.; Matsuda, H.; Minami, N.; Kakuta, A.; Ono, K.; Mukoh,A.; Nakanishi, H.; *Jpn. J. Appl. Phys*, **1992**, *31*, 1132 (e) Kasai, H.; Oikawa, H.; Okada, S.; and Nakanishi, H.; *Bull.chem. Soc. Jpn*, **1998**, *71*, 2597.

[3] An, B.-K.; Kown, S.-K.; Jung, S.-D.; Park, S.-Y. *J. Am. Chem. Soc.* **2002**, *124*, 14410.

[4] (a) Ding, Z.; Quinn, B. M.; Haram, S. K.; Pell, L. E.; Korgel, B. A.; Bard, A. J. *Science*, **2002**, *296*, 1293. (b) Bard, A. J.; Ding, Z; Myung, N.; *Structure and Bonding*, **2005**, *118*, 1. (c) Myung, N.; Lu, X.; Johnston, K. P.; Bard, A. J. *Nano Letters*, **2004**, *4*, 183. (d) Myung, N.; Lu, X.; Ding, Z.; Bard, A. J. *Nano Letters*, **2004**, *2*,1315. (e) Ren, T.; Xu, J.-Z.; Tu, Y.-F.; Xu, S.; Zhu, J.-J. *Electrochemistry communications*, **2005**, *7*, 5.

[5] Fu, H.; Loo, H.; Xiao, D.; Xie, R.; Ji, X.; Yao, J.; Zhang, B.; Zhang, L. *Angew. Chem. Int. Ed*. **2002**, *41*, 962

[6] Horn, D.; Rieger, J.; *Angew Chem. Int. Ed*. **2001**, *40*, 4330

[7] Al-Kaysi, R. O.; Muller, A. M.; Bardeen, C. J. *J. Am. Chem. Soc*. **2006**, *128*, 15938.

[8] Zhang, X.; Yuan, G.; Li, Q.; Wang, B.; Zhanh, X.; Zhang, R.; Chang, J.C.; Lee, C-S.; Lee, S-T. *Chem. Mater*. **2008**, *20*, 6945

[9] Kim, H. Y.; Bjoklund, S. - H. Lim.; Bardeen, C. J. *Langmuir*, **2003**, *19*, 3941

[10] Lai, R.Y.; Bard, A. J. *J. Phys. Chem* A. **2003**, *107*, 3335

[11] (a) Miao, W.; Choi, J-P.; Bard, A.J. *J. Am. Chem. Soc* . **2002**, *124*, 14478. (b) Zu, Y.; Bard, A. J. *Anal. Chem*. **2000**, *72*, 3223. (c) Leland, J. K.; Powell, M. J. *J. Electrochem.Soc*. **1990**, *137*, 3127. (d) Kanoufi, F.; Zu, Y.; Bard, A. J. *J. Phys. Chem B* **2001,** *105*, 210.

[12] Myung, N.; Bae, Y.; Bard, A.J. *Nano Lett*. **2003**, *3*, 1053.

[13] Chung, H.-R.; Kown, E.; Oikawa, H.; Kasai, H.; Nakanishi, H. *Journal of Crystal Growth*, **2006**, *294*, 459.

Chapter 7: Concluding Remarks

The ECL of series of highly fluorescent new green emitters was examined. Green emission in ECL (which were seldom seen in ECL) was obtained after insertion of a good acceptor (or energy gap lower) of 2,1,3 benzothiadiazole in a central part between different donor groups. Except the molecule with a very weak donor group (**BH0**) which gives weak ECL, the others, produce intense green ECL, due to stability of the radical cation and anion in the solution. ECL spectrum of **BH0** (the one which shows quasi reversible oxidation peak) was hard to record it, however, using BPO as a coreactant and taking advantage of just reduction side, intense ECL peak could be recorded same as PL spectrum. As expected, the ECL pulses were of equal intensity when pulsing between the first oxidation peak and the first reduction peak, but that symmetry was lost when pulsing between the second oxidation peak and the first reduction peak.

Tuning of electrochemical reversibility has been observed when the well-known studied molecules as DPA (9,10 diphenylanthracene), pyrene, anthracene inserted between fluorene derivative moieties. The introduction of fluorene groups imparts steric hindrance that prevents interchromophore interactions, giving these molecules high PL quantum yields. The fluorene substitutions also block the active positions of the PAH cores subject to electrochemical decomposition permitting the formation of stable radical ions and enhancing π-conjugation facilitating the charge delocalization. More

importantly, the C2 and C6 substitutions on the DPA core provide extra stabilization for the highly charged species (dication and dianion), allowing **FDF** to have highly efficient (Φ_{ECL} FDF =0.90) and stable (up to 20 000 pulses) blue ECL. The calculated enthalpies of these annihilation reactions indicate that the electron transfer reactions for ECL follow an S-route.

Star-shaped molecules were interesting molecules to study due to they have rigid structure and high PL quantum yield. Truxene core –oligofluorene arms star-shaped oligomers were studied. Electrochemistry in a MeCN/Bz solution showed reversible oxidation and reduction peaks. They show intense blue EL emission that is clearly visible to the naked eye when generated by ion annihilation when the potential is pulsed between the first reduction and first oxidation potentials.

All the above molecules have been tested in nonaqueous media because of their insolubility in aqueous solution. Insolubility in aqueous media, will limit their application and hinder them to be used in a real sample analysis and in physiological pHs. Well-dispersed organic Nanoparticles (ONPs) in aqueous solutions were chosen to be an alternative for such a problem.

Well- dispersed organic nanoparticles of common ECL emitters like rubrene and DPA in aqueous solution gave ECL. The intensity of ECL was small because of the small diffusion coefficient of the particles due to the size of the particles were big (50 nm in case of rubrene, and 250 nm in case of fresh DPA/H_2O). It was observed that rubrene NPs were stable even during a month without any stabilizer, while DPA NPs make

nanowire after one week. Size , shape, and aggregation of the ONPs are strongly depend on the nature of the material, solubility in the "poor and good" solvents, presence of the stabilizer (surfactant), and method of fabrication of the particles. Our ECL experiments were limited to use of ONPs without surfactant due to the blocking of ECL light by the surfactant which it was surrounding the particles and obstacle the electrochemistry.

However, research work toward decreasing the particle size is in process, in a hope to overcome the lower intensity problem. Although science in ONPs (like fabrication of nanoparticles, controlling of shape and size) is not as mature as other nano-sized particles like metallic and semiconductor, but tailoring organic molecules are easier, so ONPs holds a higher potential application in future.

Appendix. List of symbols

Roman Symbols

A	Ground state molecule (or Acceptor molecule)
^{1}A*	Excited singlet state molecules
^{2}A*	Excited triplet state molecules
A_2*	Excimer molecules (excited state dimer)
A•–	Radical anion
A•+	Radical cation
D	diffusion coefficient (cm^2/s)
D	Donor molecules
E	Potential (V)
Eo	Standard formal Potential (V)
*E*p	Peak potential (V)
$E_{1/2}$	Half-wave potential (V)
Δ*E*p	Peak potential separation
*E*p,a	Anodic peak potential (V)
*E*p,c	Cathodic peak potential (V)
*E*s	Lowest excited singlet state (eV)
ΔHann	Enthalpy of annihilation reaction (eV)
h	Planck's constant (Js)
i	Current (A or mA or μA)
k	Homogenous rate constant
k^o	Heterogeneous rate constant

*k*b	Homogenous rate constant for backward reaction
*k*f	Homogenous rate constant for forward reaction
R	Nuetral ground state molecules
R•–	Radical anion molecule in solution
R•+	Radical cation molecule in solution
R*	Excited state molecules
T	Temperature

Greek Symbols

α	Transfer coefficient
λmax, ab	Maximum wavelength of absorption
λmax, PL	Maximum wavelength of fluorescence
λECL	Maximum wavelength of ECL emission
ν	Scan rate
ΦPL	PL quantum yield
ΦECL	ECL quantum yield

Glossary

An	Anthracene
BPO	Benzoyl peroxide
BZ	Benzene
CCD	Charge coupled device
CE	Counter electrode
CV	Cyclic Voltammetry (or cyclic voltammogram)
DPA	9,10 diphenyl anthracene
ECL	Electrogenerated Chemiluminescence
FAF	Fluorene derivatives~Anthracene~Fluorene derivatives
FDF	Fluorene derivatives~DPA~Fluorene derivatives
FPF	Fluorene derivatives~Pyrene~Fluorene derivatives
HOMO	Highest occupied molecular orbital
LUMO	Lowest unoccupied molecular orbital
MeCN	Acetonitile
MS	Mass Spectroscopy
NMR	Nuclear magnetic resonance
NP	Nanoparticles
OLED	Organic light emitting diode
ONP	Organic nanoparticles
PLED	Polymer light emitting diode
PV	Photovoltaic

RE	Reference Electrode
THF	Tetrahydrofuran
TPrA	Tri-n-propylamine
WE	Working Electrode
UME	Ultramicroelectrode

References

Chapter 1

(1) For review on ECL: (a) ElectrogeneratedChemiluminescence; Bard, A. J.; Ed.; MarcelDekker, Inc.: New York, 2004. (b) Miao, W. *Chem. ReV*. **2008**, *108*, 2506. (c) Richter, M. M. *Chem. ReV*. **2004**, *104*, 3003. (d) Knight, A. W.; Greenway, G. M. *Analyst* **1994**, *119*, 879. (e) Bard, A. J.; Debad, J. D.; Leland, J. K.; Sigal, G. B.; Wilbur,J. L.; Wohlstadter, J. N. In Encyclopedia ofAnalytical Chemistry:Applications, Theory and Instrumentation; Meyers, R. A., Ed.; John Wiley & Sons: New York, 2000; Vol. 11, p 9842.

(2) (a) Hercules, D. M. *Science* **1964**, *145*, 808.; (b) Santhanam, K. S. V.; Bard, A. J. *J. Am. Chem. Soc*. **1965**, *87*, 139. (c) Visco, R. E.; Chandross, E. A. *J. Am. Chem. Soc.* **1964**, *86,* 5350.

(3) Bard, A. J.; Debad, J. D.; Leland, J. K.; Sigal, G. B.; Wilbur, J. L.; Wohlstadter, J. N. Encyclopedia of Analytical Chemistry; Meyers, R. A., Ed.; Wiley: Chichester, U.K., **2000**; pp 9842.

(4) (a) Faulkner, L. R.; Tachikawa, H.; Bard, A. J. *J. Am. Chem. Soc*. **1972**, *94*, 691. (b) Beideman, F. E.; Hercules, D. M. *J. Phys. Chem*. **1979**, *83*, 2203.

(5) (a) Faulkner, L. R.; Bard, A. J. *J. Am. Chem. Soc*. **1969**, *91*, 209. (b) Faulkner, L. R.; Tachikawa, H.; Bard, A. J. *J. Am. Chem. Soc*. **1972**,*94*, 691.

(6) Rubinstein, I.; Bard, A. J. *J. Am. Chem. Soc*. **1981**, *103*, 512.

(7) Leland, J.; Powell, M. *J. Electrochem. Soc.* **1990**, *137*, 3127.

(8) White, H.; Bard, A. *J. Am. Chem. Soc.* **1982**, *104*, 6892.

(9) Chandross, E.; Sonntag, F. *J. Am. Chem. Soc.* **1966**, *88*, 1089.

(10) Lai, R. Y.; Bard, A. J. *J. Phys. Chem. A* **2003**, *107*, 3335.

(11) Chandoross E.; Longworth, J.; Visco, R. *J. Am. Chem. Soc.* **1965**, *87*, 3259.

(12) Maloy, J.; Bard, A. *J. Am. Chem. Soc.* **1971**, *93*, 5968.

(13) (a) Brus, L. E. *J. Chem. Phys*. **1984**, *80*, 4403. (b) Alivisatos, A. P. *Science* **1996**, *271*, 933. (c) Empedocles, S. A.; Bawendi, M. G. *Science* **1997**, *278*, 2114.

(14) An, B.-K.; Kown, S.-K.; Jung, S.-D.; Park, S.-Y. *J. Am. Chem.Soc*. **2002**, *124*, 14410.

(15) Burda, C.; Chen, X.; Narayanan, R.; El-Sayed, M. A. *Chem. Rev*. **2005**, *105*, 1025.

(16) (a) Kasai, H.; Oikawa, H.; Okada, S.; Nakanishi, H. *Bull. Chem. Soc. Jpn*.**1998**, *71*, 2597. (b) Horn, D.; Rieger, *J. Angew.Chem., Int. Ed***. 2001**, *40*, 4330.

(17) Ibanez, A.; Maximov, S.; Guiu, A.; Chaillout, C.; Baldeck, P. L . *Adv. Mater*. **1998,** *10*,1540.

(18) Seko, T.; Ogura, K.; Kawakami, Y.; Sugino, H.; Toyotama, H.; Tanaka, *J.Chem. Phys. Lett*. **1998,** *291*, 438.

(19) (a) Tamaki, Y.; Asahi, T.; Masuhara, H. *Applied Surface Science.* **2000**, *168*, 85. (b) Tamaki, Y.; Asahi, T.; Masuhara, H. *Jpn. J. Appl. Phys*. **2003**, *42*, 2725. (c) Kita, S.; Masuo, S.; Machida, S.; Itaya, A. *Jpn. J. Appl. Phys*. **2006**, *45,* 6501.

(20) (a) Omer, K. M.; Bard, A. J. *J. Phys. Chem. C* **2009,** *113*, 11575. (b) Yu, J.; Fan, F-R F. Pan, S.; Lynch, V.M.; Omer, K. M.. Bard, A.J. *J. Am. Chem. Soc***. 2008**, *130*, 7196.

(21) DiCesare, J.; Grossman, B.; Katz, E.; Picozza, E.; Ragusa, R.; Woundenberg, T. *Biotechniques* **1993**, *15*, 152.

(22) (a) Uchikura, K.; Kirisawa, M. *Anal.Sci.* **1991**, *7*, 971. (b) Skotty, D. R.; Lee, W. Y.; Nieman, T. A. *Anal. Chem.* **1996**, *68*, 1530.

(23) (a) Yokoyama, K.; Sasaki, S.; Ikebukuro, K.; Takeuchi, T.; Karube, I.; Tokitsu, Y.; Masuda, Y. *Talanta* **1994**, *31*, 1035. (b) Jameison, F.; Sanchez, R. I.; Dong, L.; Leland J. K.; Yost, D.; Martin, M. T. *Anal. Chem.* **1996**, *68*, 1298.

Chapter 2

(1) (a) Mori , J.; Miyashita, Y.; Oliveira,D.; Kasai, H.; Oikawa, H.; Nakanishi, H. *Journal of Crystal Growth* ,**2009**, *311*, 553 (b) Wu, C.; Peng, H.; Jiang,Y.; McNeill**,** J**.** *J. Phys. Chem. B* **2006,** *110,* 14148 (c) Kaneko, K.; Shimada, S.; Onodera, T.; Kimura,

T.; Matsuda, H.; Okada S.; Kasa, H.; Oikawa, H.; Kakudate, Y.; Nakanishi, H, *Jpn. J. Appl. Phys*, **2007**, *46*, 6893, (d) Kasai, H.; Nalwa, H. S.; Oikawa, H.; Okada, S.; Matsuda, H.; Minami, N.; Kakuta, A.; Ono, K.; Mukoh,A.; Nakanishi, H.; *Jpn. J. Appl. Phys*, **1992**, *31*, 1132 (e) Kasai, H.; Oikawa, H.; Okada, S.; and Nakanishi, H.; *Bull.chem. Soc. Jpn*, **1998**, *71*, 2597.

Chapter 3

(1) For review on ECL: See (a) *Electrogenerated Chemiluminescence*; Bard, A. J.; Ed.; Marcel Dekker, Inc.; New York, **2004**. (b) Miao, W. *Chem. Rev*. **2008**, *108*, 2506. (c) Richter, M. M. *Chem. Rev*. **2004**, *104*, 3003. (d) Knight, A. W.; Greenway, G. M. *Analyst* **1994**, *119*, 879. (e) Bard, A. J.; Debad, J. D.; Leland, J. K.; Sigal, G. B; Wilbur, J. L.; Wohlstadter, J. N. In *Encyclopedia of Analytical Chemistry: Applications, Theory and Instrumentation*; Meyers, R. A., Ed.; John Wiley & Sons: New York, **2000**; *Vol. 11*, p. 9842.

(2) Yasuda, T.; Imase, T.; Yamamaoto, T. *Macromolecules* **2005**, *38*, 7378.

(3) (a) Wong, K.-T.; Chien, Y.-Y.; Chen, R.-T.; Wang, C.-F.; Lin, Y.-T.; Chiang, H.-H.; Hsieh, P.-Y.; Wu, C.-C.; Chou, C. H.; Su, Y. O.; Lee, G.-H.; Peng, S.-M. *J. Am. Chem. Soc.* **2002**, *124*, 11576. (b) Wu, F-I.; Dodda, R.; Reddy, D. S.; Shu, C-F. *J. Mater. Chem*. **2002**, *12*, 2893. (c) Tsolakis, P. K.; Kallitsis, J. K. *Chem. Eur. J*. **2003**, *9*, 936. (d) Wu, C-C.; Lin, Y-T.; Wong, K-T.; Chen, R-T.; Chien, Y-Y. *Adv. Mater*. **2004**, *16*, 61. (e) Chochos, C. L.; Kallitsis, J. K.; Gregoriou, V. G**.** *J. Phys. Chem. B.* **2005***, 109,* 8755. (f) Chochos, C. L.; Kallitsis, J. K.; Keivanidis, P. E.; Baluschev, S.; Gregoriou, V. G. *J. Phys. Chem. B* **2006,** *110,* 4657. (g) Chen, A. C.-A.; Wallace, J. U.; Klubek, K. P.; Madaras, M. B.; Tang, C. W.; Chen, S. H. *Chem. Mater*. **2007**, *19*, 4043.

(4) (a) Lee, S. H.; Tsutsui, T. *Thin Solid Films* **2000**, *363*, 76. (b) Geng, Y.; Katsis, D.; Culligan, S. W.; Ou, J. J.; Chen, S. H.; Rothberg, L. *J. Chem. Mater.* **2002**, *14*, 463. (c) Li, Y.; Ding, J.; Day, M.; Tao, Y.; Lu, J.; D'iorio, M. *Chem. Mater.* **2003,** *15,* 4936. (d) Culligan, S. W.; Geng, Y.; Chen, S. H.; Klubek, K.; Vaeth, K. M.; Tang, C. W. *Adv.*

Mater. **2003**, *15*, 1176. (g). Kanibolotsky, A. L.; Berridge, R.; Skabara, P. J.; Perepichka, I. F.; Bradley, D. D. C.; Koeberg, M. *J. Am. Chem. S*oc. **2004**, *126*, 13695.

(h) Liu, Q-D.; Lu, J.; Ding, J.; Day, M.; Tao, Ye.; Barrios, Pedro.; Stupak, J.; Chan, K.; Li, J.; Chi Y. *Adv. Funct. Mater.* **2007***, 17,* 1028. (i) Kong, Q.; Zhu, D.; Quan, Y.; Chen, Q.; Ding, J.; Lu, J.; Tao, Y. *Chem. Mater.* **2007**, *19,* 3309.

(5) (a) Chang, S.-C.; Li, Y.; Yang, Y. *J. Phys. Chem. B* **2000**, *104*, 11650. (b) Lupton, J. M.; Craig, M. R.; Meijer, E. W. *Appl. Phys. Lett.* **2002**, *80*, 4489. (c) Wong, K.-T.; Chien, Y.-Y.; Chen, R.-T.; Wang, C.-F.; Lin, Y.-T.; Chiang, H.-H.; Hsieh, P.-Y.; Wu, C.-C.; Chou, C. H.; Su, Y. O.; Lee, G.-H.; Peng, S.-M. *J. Am. Chem. Soc.* **2002**, *124*, 11576. (d) Ego, C.; Grimsdale, A. C.; Uckert, F.; Yu, G.; Srdanov, G.; Mullen, K. *Adv. Mater*. **2002**, *14,* 809. (e) Culligan, S. W.; Geng, Y.; Chen, S. H.; Klubek, K.; Vaeth, K. M.; Tang, C. W. *Adv. Mater.* **2003**, *15*, 1176. (f) Wu, W.; Inbasekaran, M.; Hudack, M., Welsh, D.; Yu, W.; Cheng, Y.; Wang, C.; Kram, S.; Tacey, M.; Bernius, M.; Fletcher, R.; Kiszka, K.; Munger, S.; O'Brien, J. *Microelectron. J.* **2004**, *35*, 343. (g) Huang, F.; Wu, H.; Wang, D.; Yang, W.; Cao, Y. *Chem. Mater.* **2004,** *16,* 708. (h) Wong, K.-T.; Liao, Y.-L.; Lin, Y.-T.; Su, H.-C.; Wu, C.-C. *Org. Lett.* **2005**, *7*, 5131. (i) Chen, A. C.-A.; Wallace, J. U.; Wei, S. K.-H.; Zeng, L.; Chen, S. H. *Chem. Mater.* **2006,** *18,* 204. (j) Fan, S.; Sun, M.; Wang, J.; Yang, W.; Cao, Y. *Appl. Phys. Lett*. **2007**, *91*, 213502.

(6) (a) Joshi, H. S.; Jamshidi, R.; Tor, Y. *Angew. Chem. Int. Ed*. **1999**, *38*, 2721. (b) Yoshida, Y.; Tanigaki, N.; Yase, K.; Hotta, S. *Adv. Mater*. **2000**, *12*, 1587. (c) Tsuzuki, T.; Shirasawa, N.; Suzuki, T.; Tokito, S. *Adv. Mater*. **2003**, *15*, 1455. (d) Montes, V. A.; Li, G.; Pohl, R.; Shinar, J.; Anzenbacher, P. *Adv. Mater*. **2004**, *16,* 2001. (e) Gana, J-A.; Song, Q. L.; Hou, X- Y.; Chen, K.; Tian, H. *J. Photochem. Photobiol. A* **2004,** *162*, 399.

(7) (a) Millard, I. S. *Synth. Met.* **2000**, *111–112*, 119. (b) Muller, C. D.; Falcou, A.; Reckefuss, N.; Rojahn, M..; Wiederhirn, V.; Rudati, P.; Frohne, H.; Nuyken, O.; Becker, H.; Meerholz, K. *Nature*, **2003**, *421*, 829. (c) Justin Thomas, K. R.; Lin, J. T.; Velusamy, M.; Tao, Y-T., Chuen, C.-H. *Adv. Funct. Mater*. **2004**, *14*, 83. (d) Lin, J.; Dong, J.; Zhou, Q.; Geng, Y.; Ma, D.; Wang, L.; Jing, X.; Wang; F. *J. Mater. Chem.* **2007**, *17*, 2832.

(8) Choi, J. P.; Wong, K. T.; Chen, Y. M.; Yu, J. K.; Chou, P. T.; Bard, A. J. *J. Phys. Chem. B* **2003**, *107*, 14407.

(9) Fungo, F.; Wong, K.-T.; Ku, S.-Y.; Hung, Y.-Y.; Bard, A. J. *J. Phys. Chem. B* **2005**, *109*, 3984.

(10) Omer, K. M.; Kanibolotsky, A. L.; Skabara, P. J.; Perepichka, I. F.; Bard, A. J. *J. Phys. Chem. B* **2007**, *111*, 6612.

(11) Rashidnadimi, S.; Hung, T.-H.; Wong, K.-T.; Bard, A. J. *J. Am. Chem. Soc.* **2008**, *130*, 634.

(12) (a) Sartin, M. M.; Zhang, H.; Zhang, J.; Zhang, P.; Tian, W.; Wang. Y.; Bard, A. J. *J.Phys. Chem. C*, **2007**, *111*, 16350. (b) Lai, R. Y.; Fleming, J. J.; Merner, B. L.; Vermeij, R. J.; Bodwell, G. J.; Bard, A. J. *J. Phys. Chem A*, **2004**, *108*, 376.

(13) (a) Chandross, E.; Sonntag, F. *J. Am. Chem. Soc*. **1966**, *88*, 1089. (b) Santa Cruz, T. D.; Akins, D. L.; Brike, R. L. *J. Am. Chem. Soc*. **1976**, *98*, 1677.

(14) Ku, S.-Y.; Wong, K.-T.; Bard, A. J. *J. Am. Chem. Soc.* **2008**, *130*, 2392.

(15) Ku, S.-Y.; Chi, L.-C.; Hung, W.-Y.; Yang, S.-W.;Tsai, T.-C.; Wong, K.-T.; Chen, Y.-H.; Wu, C.-I. *J. Mater. Chem.* **2009**, *19*, 773.

(16) Yasuda, T.; Imase, T.; Yamamaoto, T. *Macromol*. **2005**, *38*, 7378.

(17) Gritzner, G.; Kuta, J.; *Pure Appl. Chem.* **1984**, *56*, 462.

(18) Beideman, F. E.; Hercules, M. *J. Am.Chem. Soc*. **1979**, 83, 2203.

Chapter 4

(1) a) Bard, A. J Ed., Electrogenerated Chemiluminescence; Marcel Dekker: New York, **2004**; b) Hercules, D.M. Science **1964,** *145* **,**808-809; c) Visco,R. E. Chandross, E. A. *J. Am. Chem. Soc*. **1964,** *86***,** 5350-5351; d) Santhanam, K. S. V.; Bard, A. J. *J. Am.Chem. Soc*. **1965**, *87*, 139-140; e) Faulkner, L. R.; Bard, A. J. *J. Am. Chem. Soc*. **1968,** *90***,** 6284-6290**.**

(2) a) Sartin, M. M.; Shu, C.; Bard, A. J. *J. Am. Chem. Soc*. **2008**, *130*, 5354-5360; b) Sartin, M. M.; Zhang, H.; Zhang, J.; Zhang,P.; Tian, W.; Wang,Y.; Bard, A. J. *J. Phys. Chem. C* **2007**, *111*, 16345-16350; c) Omer, K. M.; Kanibolotosky, A. L.; Skabara, P. J.; Perepichka, I . F.; Bard, A. J. *J. Phys. Chem B* **2007**, *111*, 6612-6619; d) Lai, R. Y.; Fleming, J. J.; Merner, M. L.; Vermeij, R. J.; Bodwell, G. J.; Bard, A. J. *J. Phys. Chem A* **2004**, *108*, 376-383; e) Becker, W. G.; Seung, H. S.; Bard, A. J. *J. Electroanal. Chem.***1984**, *167,* 127-140; f) Beideman, F. E.; Hercules, D. M. *J. Phys. Chem*. **1979**, *83*, 2203-2209; g) SantaCruz, T. D.; Akins, D. L.; Birke, R. L. *J. Am. Chem Soc*. **1976**, *98*, 1677-1682; h) Faulkner, L. R.; Tachikawa, H.; Bard, A. J. *J. Am. Chem. Soc*. **1972**, *94*, 691-699; h) Fleet,B.; Kirkbright, G. F.; Pickford, D.J. *J. Electroanal. Chem*. **1971**, *30*, 115-121.

(3) Byker, H. J. United States Patent 4,902,108 (February 20, 1990).

(4) a) Chandross, E. A.; Longworth, J. W.; Visco, R. E. *J. Am. Chem. Soc*. **1965**, *87*, 3259-3260; b) Hercules, D. M.; Chang, J.; Werner, T. C. *J. Am. Chem. Soc*. **1970**, *92*, 5560-5565; c) Maloy, J. T.; Bard, A. J. *J. Am. Chem. Soc*. **1971**, *93*, 5968-5981. d) Kira, T.; Sukigara, M. ; Honda, K. *J. Electroanal. Chem*. **1973**, *47*, 161-166; e) Keszthelyi,C. P. ; Bard, A. J. *Chem. Phys. Letter*. **1974**, *24*, 300-304; f) Tachikawa, H.; Bard, A. J. *Chem. Phys. Lett*. **1974**, *26*, 568-573; g) Suminaga,T. ; Hayakawa, S. S. *Bull. Chem. Soc. Jpn.* **1980**, *53*, 315-318.

(5) For OLED a) Wong, K-T.; Chen, R-T.; Fang, F-C.; Wu,C-C.; Lin, Y-T. *Organic Lett*. **2005**, *7,* 1979-1982; b) Geng, Y.; Katsis, D.; Culligan, S. W.; Ou, J. J.; Chen, S. H. ; Rothberg, L. *J. Chem. Mater*. **2002**, *14*, 463-470; c) Wong, K-T.; Chien, Y-Y.; Chen, R-T.; Wang, C-F. ; . Lin, Y-T.; Chiang, H-H. ; Hsieh, P-Y. ; Wu, C-C.; Chou, C. H.; Su,Y. O.; Lee, G-H.; Peng, S-M. *J. Am. Chem. Soc.* **2002**, *124*, 11576-11577.

for ECL d) Choi, J-P. ; Wong, K-T.; Chen, Y-M.; Yu, J-K.; Chou, P-T.; Bard, A. J. *J. Phys. Chem B.* **2003**, *107*, 14407-14413.

(6) Lee, S. K.; Yang, W. J.; Choi, J. J.; Kim, C. H.; Jeon, D-J.; Cho, B. R. *Org. Lett.* **2005**, *7*, 323-326.

(7) Sahami, S.; Weaver, M. *J. Electroanal. Chem*. **1981**, *122*, 155-170.

(8) Hamai, S.; Hirayama, F. *J. Phys. Chem*. **1983**, *87*, 83-89.

(9) Sartin, M. M.; Shu, C.; Bard, A. J. *J. Am. Chem. Soc*. **2008**, *130*, 5354-5360.

(10) Mann, C. K.; Barnes, K. K. Electrochemical Reaction in Nonaqueous Systems, Marcel Dekker, New York, **1970**.

(11) (a) Coleman, A. E.; Richtol, H. H.; Aikens, D. A. *J. Electroanal.Chem*. **1968**, *18*, 165-174. (b) Werner, T. C.; Chang, J.; Hercules, D. M. J. *Am. Chem. Soc*. **1970**, *92*, 763-768.

(12) Andruzzi, R. ; Trazza, A.; Greci,L.; Marchetti, L. L. *J. Electroanal Chem*. **1980**, *108*, 49-58.

(13) Reichardt,C. *Solvents and Solvent Effects in Organic Chemistry*. John Wiley and Sons: **2003.**

(14) Cruser, S. A.; Bard, A. J. *J. Am. Chem. Soc.* **1969**, *91*, 267-275.

(15) Laser, D.; Bard, A. J. *J. Electrochem. Soc*. **1975**, *122*, 632-640.

(16) Birks, J. B. Christopherou, L. G. *Spectrochim. Acta* **1963**, *19*, 401-410.

(17) a) Faulkner, L. R.; Bard, A. J. *J. Am. Chem. Soc.* **1968,** 90, 6284-6290; b) Faulkner, L. R.; Bard, A. J. *J. Am. Chem. Soc*. **1969**, *91*, 209-210.

Chapter 5

(1) Bard, A. J., Ed., *Electrogenerated Chemiluminescence,* Marcel Dekker: N.Y. 2004**.**

(2) (a) Perepichka, D. F.; Perepichka, I. F.; Meng, H.; Wudl, F. In: *Organic Light-Emitting Materials and Devices*, Li, Z. R.; Meng, H., Eds.; CRC Press: Boca Raton, FL, 2006, Chapter 2, pp. 45–293. (b) Scherf, U.; List, E. J. W. *Adv. Mater.* **2002**, *7*, 477. (c) Neher, D. *Macrom. Rap. Commun.* **2001**, *22*, 1366. (d) Leclerc, M. *J. Polym. Sci. Part A: Polym. Chem.* **2001**, *39*, 2867. (e) Bernius, M. T.; Inbasekaran, M.; O'Brien, J.; Wu, W. *Adv. Mater.* **2000**, *12*, 1737.

(3) (a) Snaith, H. J.; Greenham, N. C.; Friend, R. H. *Adv. Mater.* **2004**, *16*, 1640. (b) Russell, D. M.; Arias, A. C.; Friend, R. H.; Silva, C.; Ego, C.; Grimsdale, A. C.; Müllen, K. *Appl. Phys. Lett.* **2002**, *80*, 2204.

(4) (a) Kim, Y.; Cook, S.; Choulis, S. A.; Nelson, J.; Durrant, J. R.; Bradley, D. D. C. *Chem. Mater.* **2004,** *16,* 4812. (b) Snaith, H. J.; Friend, R. H. *Thin Solid Films* **2004**, *451–452,* 567. (c) Zhang, F.; Perzon, E.; Wang, X.; Mammo,; W. Andersson, M. R.; Inganäs, O. *Adv. Funct. Mater.* **2005**, *15*, 745. (d) Kim, Y. M.; Lim, E.; Kang, I.-N.; Jung, B.-J.; Lee, J.; Koo, B. W.; Do, L.-M.; Shim, H.-K. *Macromolecules* **2006**, *39,* 4081.

(5) (a) Zaumseil, J.; Donley, C. L.; Kim, J.-S.; Friend, R. H.; Sirringhaus, H. *Adv. Mater.* **2006**, *18*, 2708. (b) Yan, H.; Yoon, M.-H.; Facchetti, A.; Marks, T. J. *Appl. Phys. Lett.* **2005**, *87*, 183501.

(6) (a) Rabe, T.; Hoping, M.; Schneider, D.; Becker, E.; Johannes, H.-H.; Kowalsky, W.; Weimann, T.; Wang, J.; Hinze, P.; Nehls, B. S.; Scherf, U.; Farrell, T.; Riedl, T. *Adv. Funct. Mater.*, **2005**, *15*, 1188. (b) Heliotis, G.; Xia, R.; Bradley, D. D. C.; Turnbull, G. A.; Samuel, I. D. W.; Andrew, P.; Barnes, W. L. *Appl. Phys. Lett.* **2003**, *83*, 2118. (c) Heliotis, G.; Bradley, D. D. C.; Turnbull, G. A.; Samuel, I. D. W. *Appl. Phys. Lett.* **2002**, *81*, 415.

(7) *Electronic Materials: The Oligomer Approach*, Müllen, K.; Wegner, G., Eds.; Wiley-VCH: Weinheim, New York, 1998.

(8) (a) Anémian, R.; Mulatier, J.-C.; Andraud, C.; Stéphan, O.; Vial, J.-C. *Chem. Commun.* **2002**, 1608. (b) Geng, Y.; Katsis, D.; Culligan, S. W.; Ou, J. J.; Chen, S. H.; Rothberg, L. J. *Chem. Mater.* **2002**, *14*, 463. (c) Katsis, D.; Geng, Y. H.; Ou, J. J.; Culligan, S. W.; Trajkovska, A.; Chen, S. H.; Rothberg, L. J. *Chem. Mater.* **2002**, *14*, 1332. (d) Geng, Y.; Trajkovska, A.; Katsis, D.; Ou, J. J.; Culligan, S. W.; Chen, S. H. *J. Am. Chem. Soc.* **2002**, *124*, 8337. (e) Geng, Y.; Culligan, S. W.; Trajkovska, A.; Wallace, J. U.; Chen, S. H. *Chem. Mater.* **2003**, *15*, 542. (f) Jo, J.; Chi, C.; Höger, S.; Wegner, G.; Yoon, D. Y. *Chem. Eur. J.* **2004**, *10*, 2681. (g) Chi, C.; Im, C.; Enkelmann, V.; Ziegler, A.; Lieser, G.; Wegner, G. *Chem. Eur. J.* **2005**, *11*, 6833. (h) Li, J.; Li, M.; Bo, Z. *Chem. Eur. J.* **2005**, *11*, 6930. (i) Chi, C.; Wegner, G.

Macromol. Rapid Commun. **2005**, *26*, 1532. (j) Li, Z. H.; Wong, M. S. *Org. Lett.* **2006**, *8*, 1499.

(9) (a) Geng, Y.; Trajkovska, A.; Culligan, S. W.; Ou, J. J.; Chen, H. M. P.; Katsis, D.; Chen, S. H. *J. Am. Chem. Soc.* **2003**, *125*, 14032. (b) Geng, Y.; Chen, A. C. A.; Ou, J. J.; Chen, S. H. *Chem. Mater.* **2003**, *15*, 4352. (c) Li, Z. H.; Wong, M. S.; Tao, Y.; Lu, J. *Chem. Eur. J.* **2005**, *11*, 3285.

(10) (a) Wong, K.-T.; Chien, Y.-Y.; Chen, R.-T.; Wang, C.-F.; Lin, Y.-T.; Chiang, H.-H.; Hsieh, P.-Y.; Wu, C.-C.; Chou, C. H.; Su, Y. O.; Lee, G.-H.; Peng, S.-M. *J. Am. Chem. Soc.* **2002**, *124*, 11576. (b) Culligan, S. W.; Geng, Y.; Chen, S. H.; Klubek, K.; Vaeth, K. M.; Tang, C. W. *Adv. Mater.* **2003**, *15*, 1176. (c) Wong, K.-T.; Liao, Y.-L.; Lin, Y.-T.; Su, H.-C.; Wu, C.-C. *Org. Lett.* **2005**, *7*, 5131. (d) Chen, A. C.-A.; Wallace, J. U.; Wei, S. K.-H.; Zeng, L.; Chen, S. H. *Chem. Mater.* **2006,** *18*, 204.

(11) Lupton, J. M.; Craig, M. R.; Meijer, E. W. *Appl. Phys. Lett*. **2002**, *80*, 4489.

(12) (a) List, E. J. W.; Guentner, R.; Scanducci de Freitas, P.; Scherf, U. *Adv. Mater*. **2002**, *14*, 374. (b) Gaal, M.; List, E. J. W.; Scherf, U. *Macromolecules* **2003**, *36*, 4236. (c) Gong, X.; Iyer, P. K.; Moses, D.; Bazan, G. C.; Heeger, A. J.; Xiao, S. S. *Adv. Funct. Mater.* **2003**, *13*, 325. (d) Romaner, L.; Pogantsch, A.; Scandiucci de Freitas, P.; Scherf, U.; Gaal, M.; Zojer, E.; List, E. J. W. *Adv. Funct. Mater.* **2003**, *13*, 597. (e) Gamerith, S.; Gadermaier, C.; Scherf, U.; List, E. J. W. *Phys. Stat. Sol. (a)* **2004**, *201*, 1132. (f) Sims, M.; Bradley, D. D. C.; Ariu, M.; Koeberg, M.; Asimakis, A.; Grell, M.; Lidzey, D. G. *Adv. Funct. Mater.* **2004**, *14*, 765.

(13) Faulkner, L. R.; *J. Electrochem. Soc.* **1997**, *124*, 1724.

(14) Noffsinger, J. B.; Danielson, N. D. *Anal. Chem.* **1987**, *59*, 865.

(15) Zu, Y.; Bard, A. J. *Anal. Chem*. **2000**, *72*, 3223.

(16) Miao, W.; Choi, J.-P.; Bard, A. J. *J. Am. Chem. Soc*. **2002**, *124*, 14478.

(17) Chang, M.-M.; Saji, T.; Bard, A. J. *J. Am. Chem. Soc*. **1977**, *99*, 5399.

(18) Rubinstein, I.; Bard, A. J. *J. Am. Chem. Soc*. **1981**, *103*, 512.

(19) White, H. S.; Bard, A. J. *J. Am. Chem. Soc*. **1982**, *104*, 6891.

(20) Choi, J.-P.; Wong, K.-T.; Chen,Y.-M.;Yu, J.-K.; Chou, P.-T.; Bard, A. J. *J. Phys. Chem. B* **2003**, *107*, 14407.

(21) Wu, C.; Malinin, S. V.; Tretiak, S.; Chernyak, V. Y. *Nature Physics* **2006**, *2*, 631.

(22) (a) Zhou, X.-H.; Yan, J.-C.; Pei, J. *Org. Lett.*, **2003**, *5*, 3543. (b) Li, B.; Li, J.; Fu, Y.; Bo, Z. *J. Am. Chem. Soc.* **2004**, *126*, 3430. (c) Li, B.; Xu, X.; Sun, M.; Fu, Y.; Yu, G.; Liu, Y.; Bo, Z. *Macromolecules* **2006**, *39,* 456. (d) Montes, V. A.; Pérez-Bolívar, C.; Agarwal, N.; Shinar, J.; Anzenbacher, Jr., P. *J. Am. Chem. Soc.* **2006**, *128*, 12436. (e) Lai, W.-Y.; Zhu, R.; Fan, Q.-L.; Hou, L.-T.; Cao, Y.; Huang, W. *Macromolecules* **2006**, *39,* 3707.

(23) Kanibolotsky, A. L.; Berridge, R.; Skabara, P. J.; Perepichka, I. F.; Bradley, D. D. C.; Koeberg, M. *J. Am. Chem. Soc*. **2004**, *126*, 13696.

(24) (a) Geng, Y.; Fechtenkötter, A.; Müllen, K. *J. Mater. Chem.*, **2001**, *11*, 1634. (b) Ponomarenko, S. A.; Kirchmeyer, S.; Elschner, A.; Huisman, B.-H.; Karbach, A.; Drechsler D. *Adv. Funct. Mater.* **2003**, *13*, 591. (c) Pei, J.; Wang, J.-L.; Cao, X.-Y.; Zhou, X.-H.; Zhang, W.-B. *J. Am. Chem. Soc.* **2003**, *125*, 9944. (d) Nicolas, Y.; Blanchard, P.; Levillain, E.; Allain, M.; Mercier, N.; Roncali, J. *Org. Lett.*, **2004**, *6*, 273. (e) Sun, Y.; Xiao, K.; Liu, Y.; Wang, J.; Pei, J.; Zhu, D. *Adv. Funct. Mater.* **2005**, *15*, 818. (f) Cravino, A.; Roquet, S.; Alévêque, O.; Leriche, P.; Frère, P.; Roncali, J. *Chem. Mater.* **2006,** *18,* 2584. (g) Cremer, J.; Bäuerle, P. *J. Mater. Chem.* **2006**, *16*, 874.

(25) (a) Holst, H. C.; Oehlhof, A. *Eur. J. Org. Chem.* **2003**, 4173. (b) Fratiloiu, S.; Senthilkumar, K.; Grozema, F. C.; Christian-Pandya, H.; Niazimbetova, Z. I.; Bhandari, Y. J.; Galvin, M. E.; Siebbeles, L. D. A. *Chem. Mater.* **2006,** *18,* 2118. (c) Brunel, J.; Mongin, O.; Jutand, A.; Ledoux, I.; Zyss, J.; Blanchard-Desce, M. *Chem. Mater.* **2003**, *15,* 4139.

(26) (a) Rodríguez, J. G.; Esquivias, J.; Lafuente, A.; Díaz, C. *J. Org. Chem.* **2003**, *68*, 8120. (b) Yamaguchi, Y.; Ochi, T.; Miyamura, S.; Tanaka, T.; Kobayashi, S.; Wakamiya, T.; Matsubara, Y.; Yoshida, Z.-I. *J. Am. Chem. Soc.* **2006**, *128*, 4504.

(27) (a) Wang, Y.; He, G. S.; Prasad, P. N.; Goodson III, T. *J. Am. Chem. Soc.* **2005**, *127*, 10128. (b) Yan, Y.-X.; Tao, X.-T.; Sun, Y.-H.; Wang, C.-K.; Xu, G.-B.; Yang, J.-X.; Ren, Y.; Zhao, X.; Wu, Y.-Z.; Yua, X.-Q.; Jiang, M.-H. *J . Mater. Chem.* **2004**, *14* , 2995.

(28) McCord, P.; Bard, A. J. *J. Electroanal. Chem*. **1991**, *318*, 91.

(29) (a) Rudolf, M. *J. Electroanal. Chem.* **2003**, *543*, 23. (b) Ruldolf, M. *J. Electroanal. Chem.* **2004**, *571*, 289. (c) Rudolf, M. *J. Electroanal. Chem.* **2003**, *558*, 171. (d) Rudolf, M. *J. Comput. Chem.* **2005**, *26*, 619. (e) Rudolf, M. *J. Comput. Chem.* **2005**, *26*, 633. (f) Rudolf, M. *J. Comput. Chem.* **2005**, *26*, 1193.

(30) Denuault, G.; Mirkin, M. V.; Bard, A. J. *J. Electroanal. Chem.* **1991**, *308*, 27.

(31) Hapiot, P.; Lagrost, C.; Le Floch, F.; Raoult, E.; Rault-Berthelot, J. *Chem. Mater.* **2005,** *17,* 2003.

(32) Santa Cruz, T. D.; Akins, D. L.; Birke, R. L. *J. Am. Chem. Soc*. **1976**, *98*, 1677.

(33) Lai, R. Y.; Fleming, J. J.; Merner, B. L.; Vermeij, R. J.; Bodwell, G. J.; Bard, A. J. *J. Phys. Chem. A* **2004,** *108,* 376.

(34) Prieto, I.; Teetsov, J.; Fox, M. A.; Vanden Bout, D. A.; Bard, A. J. *J. Phys. Chem. A* **2001,** *105,* 520.

Chapter 6

(1) Reviews of ECL, see (a) *Electrogenerated chemiluminescence*; Bard, A. J.; Ed; Marcel Dekker, INC.; New York, 2004. (b) Miao, W.; *Chem. Rev.* **2008,** *108,* 2506 (c) Richter, M. M. *Chem. Rev*. **2004**, 104, 3003. (d) Knight, A. W.; Greenway, G. M. *Analyst* **1994**, *119*, 879 (e) Bard, A. J.; Debad, J. D.; Leland, J. K.; Sigal, G. B; Wilbur,J . L.; Wohlstadter, J. N. In Encyclopedia of Analytical Chemistry: Applications, Theory and Instrumentation; Meyers, R.A., Ed.; John Wiley & Sons: New York, 2000; vol 11, p.9842.

(2) (a) Mori , J.; Miyashita, Y.; Oliveira,D.; Kasai, H.; Oikawa, H.; Nakanishi, H. *Journal of Crystal Growth* ,**2009**, *311*, 553 (b) Wu, C.; Peng, H.; Jiang,Y.; McNeill**, J.**

J. Phys. Chem. B **2006,** *110,* 14148 (c) Kaneko, K.; Shimada, S.; Onodera, T.; Kimura, T.; Matsuda, H.; Okada S.; Kasa, H.; Oikawa, H.; Kakudate, Y.; Nakanishi, H, *Jpn. J. Appl. Phys*, **2007**, *46*, 6893, (d) Kasai, H.; Nalwa, H. S.; Oikawa, H.; Okada, S.; Matsuda, H.; Minami, N.; Kakuta, A.; Ono, K.; Mukoh,A.; Nakanishi, H.; *Jpn. J. Appl. Phys*, **1992**, *31*, 1132 (e) Kasai, H.; Oikawa, H.; Okada, S.; and Nakanishi, H.; *Bull.chem. Soc. Jpn*, **1998**, *71*, 2597.

(3) An, B.-K.; Kown, S.-K.; Jung, S.-D.; Park, S.-Y. *J. Am. Chem. Soc.* **2002**, *124*, 14410.

(4) (a) Ding, Z.; Quinn, B. M.; Haram, S. K.; Pell, L. E.; Korgel, B. A.; Bard, A. J. *Science*, **2002**, *296*, 1293. (b) Bard, A. J.; Ding, Z; Myung, N.; *Structure and Bonding*, **2005**, *118*, 1. (c) Myung, N.; Lu, X.; Johnston, K. P.; Bard, A. J. *Nano Letters*, **2004**, *4*, 183. (d) Myung, N.; Lu, X.; Ding, Z.; Bard, A. J. *Nano Letters*, **2004**, *2*,1315. (e) Ren, T.; Xu, J.-Z.; Tu, Y.-F.; Xu, S.; Zhu, J.-J. *Electrochemistry communications*, **2005**, *7*, 5.

(5) Fu, H.; Loo, H.; Xiao, D.; Xie, R.; Ji, X.; Yao, J.; Zhang, B.; Zhang, L. *Angew. Chem. Int. Ed*. **2002**, *41*, 962

(6) Horn, D.; Rieger, J.; *Angew Chem. Int. Ed*. **2001**, *40*, 4330

(7) Al-Kaysi, R. O.; Muller, A. M.; Bardeen, C. J. *J. Am. Chem. Soc*. **2006**, *128*, 15938.

(8) Zhang, X.; Yuan, G.; Li, Q.; Wang, B.; Zhanh, X.; Zhang, R.; Chang, J.C.; Lee, C-S.; Lee, S-T. *Chem. Mater*. **2008**, *20*, 6945

(9) Kim, H. Y.; Bjoklund, S. - H. Lim.; Bardeen, C. J. *Langmuir*, **2003**, *19*, 3941

(10) Lai, R.Y.; Bard, A. J. *J. Phys. Chem* A. **2003**, *107*, 3335.

(11) (a) Miao, W.; Choi, J-P.; Bard, A.J. *J. Am. Chem. Soc* . **2002**, *124*, 14478. (b) Zu, Y.; Bard, A. J. *Anal. Chem*. **2000**, *72*, 3223. (c) Leland, J. K.; Powell, M. J. *J. Electrochem.Soc*. **1990**, *137*, 3127. (d) Kanoufi, F.; Zu, Y.; Bard, A. J. *J. Phys. Chem B* **2001,** *105*, 210.

(12) Myung, N.; Bae, Y.; Bard, A.J. *Nano Lett*. **2003**, *3*, 1053

(13) Chung, H.-R.; Kown, E.; Oikawa, H.; Kasai, H.; Nakanishi, H. *Journal of Crystal Growth*, **2006**, *294*, 459.

Vita

Khalid Mohammad Omer was born in the Sulaimani Governorate in the Kurdistan region in Iraq. He received his high school degree in Sulaimani city, and obtained a Bachelor of Science (B.S.) in chemistry in 1996 from the University of Salahadin-Erbil, in Erbil city, and then he pursued a Masters degree (M.S.) in Analytical Chemistry under the supervision of Professor Azad T. Faizullah at the same university in fall 1999. He went to work at the University of Sulaimani as an Assistant lecturer from Dec. 1999 to 2006, while at the same time working with Professor Fadhil M. Najib. In the fall of 2006, he joined the graduate school at the University of Texas at Austin and joined the Laboratory of Professor Allen J. Bard. He has published six peer-reviewed articles with Professor Allen J. Bard, which is listed below, and some other publications are in process (not listed). Khalid also filed one patent on "Syntheses and Characterization of Organic or Ionic Luminescent Nanoparticles for Electrogenerated Chemiluminescence".

Publications (*peer-reviewed articles*):

1. **Khalid M. Omer**, Sung-Yu Ku, Ken-Tsung Wong, and Allen J. Bard. *Angew. Chem. Int. Ed*. **2009,** *48*, in press.
2. **Khalid M. Omer**, Sung-Yu Ku, Ken-Tsung Wong, and Allen J. Bard. *J. Am. Chem. Soc.* **2009**, *131*, 10733.
3. **Khalid M. Omer** and Allen J. Bard. *J. Phys. Chem. C* **2009**, *113*, 11575.

4. Anahita Izadyar, **Khalid M. Omer**, Yunqi Liu, Shiyan Chen, Xinjun Xu, and Allen J. Bard. *J. Phys. Chem. C* **2008,** *112*, 20027.
5. Jiaguo Yu, Fu-Ren F. Fan, Shanlin Pan, Vincent M. Lynch, **Khalid M. Omer**, Allen J. Bard. *J. Am. Chem. Soc*. **2008**, *130*, 7196.
6. **Khalid M. Omer**, Alexander L. Kanibolotsky, Peter J. Skabara, Igor F. Perepichka and Allen J. Bard. *J. Phys. Chem. B* **2007**, *111*, 6612.
7. **Khalid M. Omer**. *Kurdistan Academician Journal* **2006**, *1*, 4A, 147.
8. **Khalid M. Omer**.; Fadhil M. Najib.; Aumed I Haider. *Kurdistan Academician Journal* 2006, 1, 4A, 137.
9. **Khalid M. Omer.** *Ibn Al-Haitham J. for pure & appl. sci* 2005. 18(3).

Patent *(filed)*

Allen. J Bard, Fu-Ren F. Fan, **Khalid M. Omer**, Jiaguo Yu.

PCT Int. Appl. (2009), WO 2009137002.

Permanent address: Kurdi 47 St, #15,
Al-Sulaymanyiah,
Kurdistan region, Iraq.

This dissertation was typed by the author.